universität wien

DISSERTATION / DOCTORAL THESIS

Titel der Dissertation /Title of the Doctoral Thesis

„The gut microbiota-immune-brain axis in extremely premature infants“

verfasst von / submitted by

Filip David Seki MSc

angestrebter akademischer Grad / in partial fulfilment of the requirements for the degree of

Doctor of Philosophy (PhD)

Wien, 2021/ Vienna 2021

Studienkennzahl lt. Studienblatt / degree programme code as it appears on the student record sheet:	UA 794 685 490
Dissertationsgebiet lt. Studienblatt / field of study as it appears on the student record sheet:	Molekulare Biologie
Betreut von / Supervisor:	Univ.-Prof Dr. David Berry

“Well, here we are, Mr. Pilgrim, trapped in the amber of this moment. There is no why.”

Kurt Vonnegut

Acknowledgements

I would like to express my gratitude to my parents Suzana Seki and Oliver Seki. I love you both a lot. Then I want to thank all the parents who participated in this study. For you, premature delivery was devastatingly stressful and often sad. In a bizarre way, this inspired me the most, as it pushed me to do more and to do better. It made me realize, that much of the things people tell you, really are not that important. Your participation has helped us to gain better understanding of the development of brain injury in prematurely delivered infants. It frustrates me that these types of morbidities still occur, and it hurts to think that infant mortality still exists. I hope that with this work, I can give something back.

I thank my mentor David Berry. Your guidance was indispensable for this project. You have an incredible eye for how to express yourself precisely, without losing ornamental language, showing that you have a vision of a greater picture. I am happy that we often shared similar visions, but I still look up to how effective yet brilliant you convert these into scientific stories. Thank you for taking the time to really understand my sometimes-chaotic brain. I have learned a lot from you.

I thank my colleagues and supervisors from the Medical University of Vienna. Lukas Wigrill, Vito Giordano, Katrin Klebermaß-Schrehof, Katharina Göral, and Angelika Berger. I came in as a microbial ecologist and you trusted me to work in a clinical neo-intensive care environment. I am thankful for the broad range of neurophysiological and immunological methods that you taught me, and I want to express that my time there was among the more inspired years so far.

I thank my colleagues from the University of Vienna. Margareta Mayer, Bela Hausmann, Petra Pjevac, Craig Herbold, Franziska Bauchinger, Patrick Arthofer, Stephan Köstlbacher, Michael Lukumbuzya, Anna Müller, Johanna Wiesinger, Julius Simonis. Thank you for working on projects with me, talking science with me, or partying with me. I like you a lot.

Contents

Summary

Severe brain damage is prevalent among extremely premature infants and their gut microbiota are implicated as critical factors for its pathogenesis, due to their potential to orchestrate the development of its enteric habitat, thereby involving immunological and neurological aspects of its host. Bacterial colonization of the gastrointestinal tract (GIT) is necessary for the establishment of homeostatic conditions that favor host health, as commensal bacteria induce the promotion of regulatory T cell development via signaling over dendritic cells housed in mesenteric lymph nodes. However, distortions of gut microbiome development have been observed to precede systemic inflammation, which as a consequence contributes to poor neurodevelopmental outcome.

Despite its importance, the physiology and ecology of the neonatal microbiome remain poorly understood. Therefore, the present study was initiated with the intention to gain holistic understanding of the gut microbiota, immune system, and neurophysiological development during hospitalization of 60 extremely premature infants. We conducted 16S rRNA gene amplicon sequencing in combination with qPCR for quantitative microbiome profiling, flow cytometry for T cell phenotyping, multiplex cytokine and chemokine quantification, fecal metabolite analysis, neurophysiological measurements, and neuroimaging to gain a holistic understanding of the developing gut microbiota-immune-brain-axis in early-life.

We found that brain injury is preceded by a delayed onset of electrocortical maturation that is accompanied by increased instability in cranial oxygen saturation during the first month post-delivery. We observed that this pathological state is associated with the proinflammatory priming of T lymphocytes and an impaired production of neuroprotective agents during a critical phase of neurophysiological maturation. Furthermore, we identified *Klebsiella* overgrowth in the gut as highly predictive for brain damage, and key for driving the assembly of a distinctive and stable microbiome, observed exclusively in infants with multifarious pathologies.

Zusammenfassung

Schwere Hirnschäden sind bei extremen Frühchen weit verbreitet. Es wird angenommen, dass Darmmikrobiota eine wichtige Rolle für eben jenen Krankheitsverlauf haben. Diese können nämlich Einfluss auf ihr Habitat ausüben, und folglich Einfluss auf immunologische und neurologische Aspekte ihres Wirts ausüben.

Die bakterielle Besiedelung des Magen-Darm-Trakts (MDT) ist wichtig für den Aufbau eines sich im Gleichgewicht befindlichen Systems, was wiederum positive Folgen für menschliche Gesundheit mit sich bringt. Einige dendritische Zellen halten sich in mesenterialen Lymphknoten auf. Wenn sich der Darm im Gleichgewicht befindet, so regen jene über anti-inflammatorische Signal die Entwicklung von regulatorischen T Zellen an. Es wurde jedoch beobachtet, dass drastische Abweichungen in der Entwicklung der Darmmikrobiota systemischen Entzündungen vorausgehen, die im weiteren Verlauf schwere neurophysiologische Komplikationen mit sich bringen.

Trotz seiner immensen Bedeutung ist die Physiologie und Ökologie des neonatalen Mikrobioms schlecht erfasst. Daher wurde die vorliegende Studie mit der Absicht initiiert unser Verständnis über Darmmikrobiota, des Immunsystems und der neurophysiologischen Entwicklung von 60 extremen Frühchen zu verbessern. Wir führten 16S-rRNA-Gen-Amplikon-Sequenzierung in Kombination mit qPCR für quantitatives Mikrobiom-Profiling durch, nutzten Durchflusszytometrie für T-Zell-Phänotypisierung, Multiplex-Technologie um Zytokine und Chemokine zu erfassen, analysierten Metabolite in Stuhlproben, führten neurophysiologische Messungen und bildgebende Verfahren durch, um ein letztlich ganzheitliches Verständnis über die sich entwickelnden Darmmikrobiota-Immun-Hirn-Achse zu erhalten.

Wir fanden heraus, dass Hirnverletzungen ein verzögerter Beginn electrocorticaler Reifung vorausgeht, welche mit einer erhöhten Instabilität cranialer Sauerstoffsättigung während des ersten Monats nach Entbindung einher geht. Wir beobachteten, dass dieser pathologische Zustand mit einer proinflammatorischen Prägung von T-Lymphozyten und einer beeinträchtigten Produktion von neuroprotektiven Wirkstoffen während einer kritischen Phase der neurophysiologischen

Reifung verbunden ist. Darüber hinaus identifizierten wir das übermäßige Wachstum von *Klebsiella* im Darm als hoch prädiktiv für Hirnschäden, und als Schlüssel für den Aufbau eines charakteristischen und stabilen Mikrobioms, das ausschließlich bei Säuglingen mit vielfältigen Pathologien beobachtet wurde.

Introduction

The gut microbiota-immune-brain axis

Mammals have evolved in intimate relation with microbiota and will continue to do so. In humans, the gastrointestinal tract (GIT) represents the largest reservoir for host-associated microbiota, wherein approximately 300 to 500 bacterial species, with a staggering estimated genetic repertoire of 2 million microbial genes (Guarner & Malagelada, 2003). While some microbiota are just passing through as hitchhikers with diet, others are core inhabitants of our GIT, with crucial implications for the functioning of our immune system (Olin et al., 2018), metabolism (Winter et al., 2013), and cognition (Sarkar et al., 2018). It is believed that the human body exerts strong top-down control on its microbial symbionts, by continuously avoiding overgrowth via peristaltic, and monitoring intestinal microbial activities via cooperative immunological and nervous system functioning. These actions are largely coordinated by the enteric nervous system (ENS), which is a crucial part of the autonomic peripheral nervous system, that establishes bi-directional communication between the GIT and the central nervous system (Cryan et al., 2019), including neuronal (Bonaz, Bazin and Pellissier, 2018), endocrine (Mihajlovic et al., 2021), and immunological pathways (Mazmanian, Round and Kasper, 2008). Importantly however, increasing evidence suggests that microorganisms do not simply succumb to a strong top-down control, but rather strongly participate, and even modulate the bi-directional communication between enteric nerves and the brain (Rao et al., 2017).

The developing gut microbiota-immune-brain axis in premature infants

The third trimester of pregnancy is a critical period for the establishment, refinement, and maturation of brain connectivity, which determines subsequent cognitive potential (Matthews et al., 2017). Recent MRI studies have shown that early uterine brain development is patterned. By the 22nd week of pregnancy, interhemispheric fissures, the callosal sulcus, the parieto-occipital, as well as the hippocampal fissures become present in all infants. Between 28 and 34 weeks of gestation, individual variation increases drastically between infants, as observed in rapid maturation in sulcal development (Garel et al., 2001). During that time, functional connectivity was observed to drastically increase, as thalamocortical and callosal fibers extend to cortical

regions (Krsnik et al., 2017), and intrahemispheric associations manifest over greater ranges (Ceschin et al., 2015). It is believed that microglia play an essential role in surveying embryonic brain development with key functions regarding homeostatic maintenance (Hickman et al., 2013). Cxcr4 was found to be an important cytokine receptor to regulate microglial colonization of the neocortex (Matcovitch-Natan et al., 2016). Maternal immune activation during pregnancy is known to enhance pro-inflammatory microglia priming, which disrupts proper microglial arrangement, translating into pathological central nervous system (CNS) development (Lombardo et al., 2017). Interestingly, it was shown recently that maternal microbiota influences fetal microglia development, and that complete depletion of microbiota in germ-free mice severely influences microglia transcriptomic profiles in a sex-specific matter, suggesting that under natural conditions, maternal microbiota prime fetal microglia for extra-uterine life (Thion et al., 2018).

Extremely premature infants however, are born on the verge of the third trimester, and their neural circuitry is therefore established in the face of manifold environmental cues and insults associated with preterm extra-uterine life (Stoecklein et al., 2020). It is believed, that with the maturation of thalamocortical afferentation, beginning approximately after 24 weeks of gestation, more complex electrical signals emerge in infant brains, whereby it was shown that premature infants begin to respond to nociceptive signals, such as light, speech, or sound (Hatfield, 2014). In order for neurons to properly mature, migrate, and establish connections, a homeostatic immunological tone is favorable. It is widely accepted nowadays, that infection and associated inflammation during premature infancy are involved in the pathophysiology of perinatal white matter injury in premature infants (Niño et al., 2018). Recent studies have shown that aberrant development of gut microbiota precedes severe septical conditions (Madan et al., 2012). Given that the intestine is such a great reservoir of immunologically competent cells shortly post-delivery (Torow et al., 2017), it is argued that pro-inflammatory cascades initiated in the gut will translate to negatively affect brain development, resulting in lifelong morbidities such as cognitive motor delay, cerebral palsy, neurosensory impairments, and behavioral abnormalities such as attention deficit hyperactivity disorder and learning disabilities (Seki et al., 2021). The variety of potential molecular mechanisms that could trigger aberrant gut microbiota-immune-brain development remain poorly understood.

Figure 1 provides an overview of the neonatal gut-brain axis as summarized in work from Sherman, Zaghouani, and Niklas (2015). This review of scientific literature offers an extensive description of the developing gut-brain axis in infants.

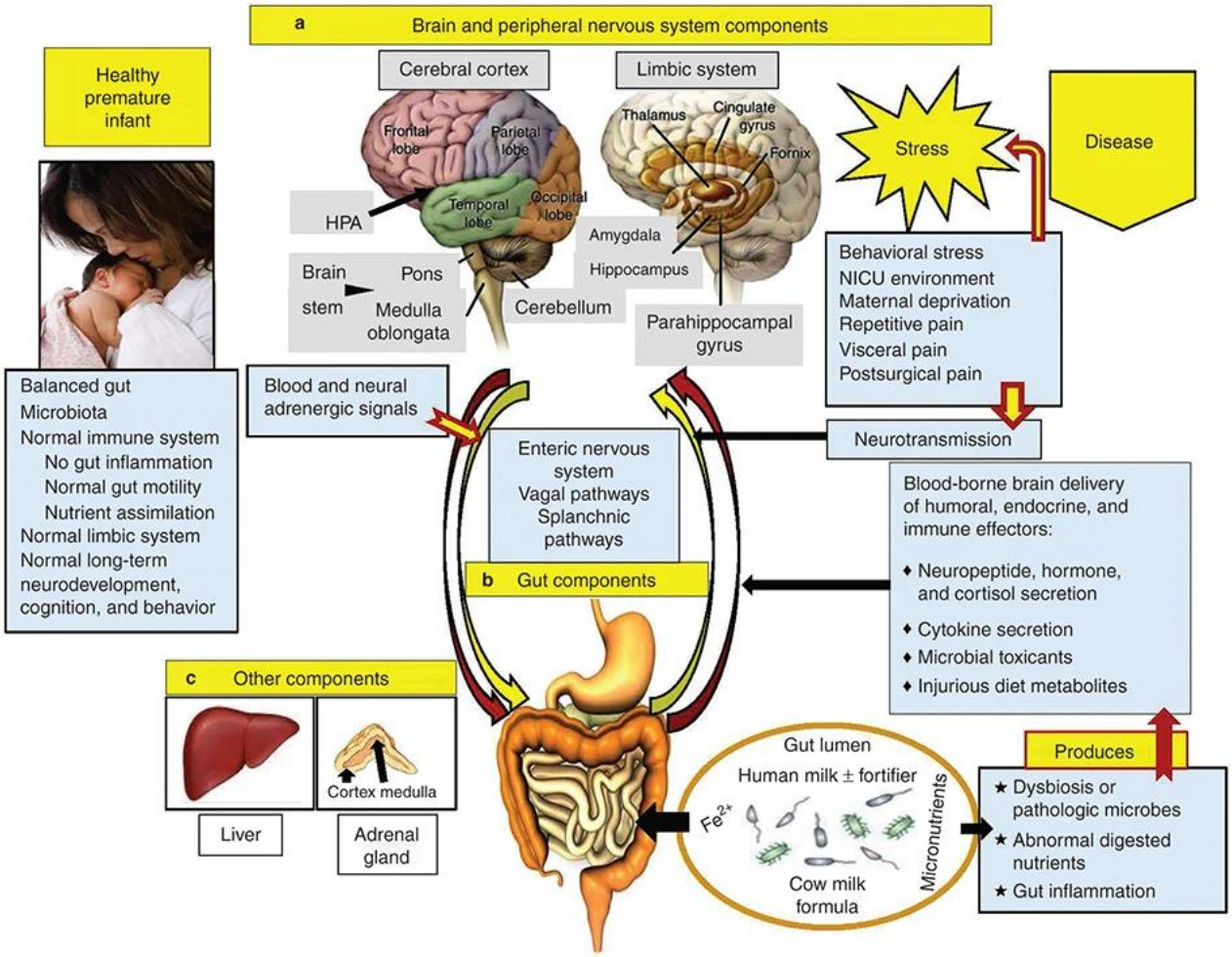

Figure 1. (Image taken from Sherman, Zaghouani, and Niklas, 2015) "The gut-brain axis". (doi:10.1038/pr.2014.161)

Primary succession of human gut microbiota

It is believed that the development of gut microbiota in neonates is predictable, as scientists very often observe a similarly ordered succession of gut-colonizing microorganisms. Generally, early-life gut microbiota assembly is characterized by an initial prevalence of typically skin-associated bacteria in the gut (e.g. *Staphylococcus*), a subsequent bloom of facultative anaerobic bacteria, and

an increase of strictly anaerobic bacteria (e.g. *Clostridia, Veillonella*) in later periods for premature infants (Seki et al., 2021), as well as for term-born infants (Stewart et al., 2018). The interactions of bacteria between each other during succession have important implications for assembly, which can furthermore translate into adverse health outcomes for premature infants (Rao et al., 2021). However, there seems to be a great inter-individual variability concerning the timing of developmental milestones and dynamics of microbiota between infants, but the forces that shape these dynamics of microbiota assembly remain poorly understood. After initial assembly, a stable infant gut community could be comprehended as a local microbial community in a large pool of microbial communities, a so-called meta-community (Miller, Svanbäck, and Bohannan, 2018). Local communities differ from each other as a result of species sorting caused by differences in combination and magnitude of selection, dispersal, and drift, provided that a certain degree of dispersal exists between communities (Figure 2; Dini-Andreote et al., 2015). Importantly, these forces drive differentiation between local communities. Therefore, these are the underlying mechanisms of individuality in developing gut microbiota of humans. As illustrated in Figure 2 (Dini-Andreote et al., 2015), initial community assembly is believed to be stochastic, as many empty ecological niches exist and could potentially be colonized. If afterwards selective filters remain weak, then established microbiota continue to diversify between local communities due to neutral drift (stochasticity). However, if selective filters are very strong, deterministic forces underlie further progression of microbial succession instead. This can either be due to i) local environments being very different from each other, whereby variable selection (VS) leads to diversification of microbiota between local communities, ii) or local environments providing very similar habitats, whereby homogenizing selection (HS) leads to very similar microbial compositions between local communities. Understanding and quantifying these processes, that ultimately define the structure and amount of turnover in community composition in meta-communities, should therefore be an important step towards explaining the progression of microbial composition during early life in humans.

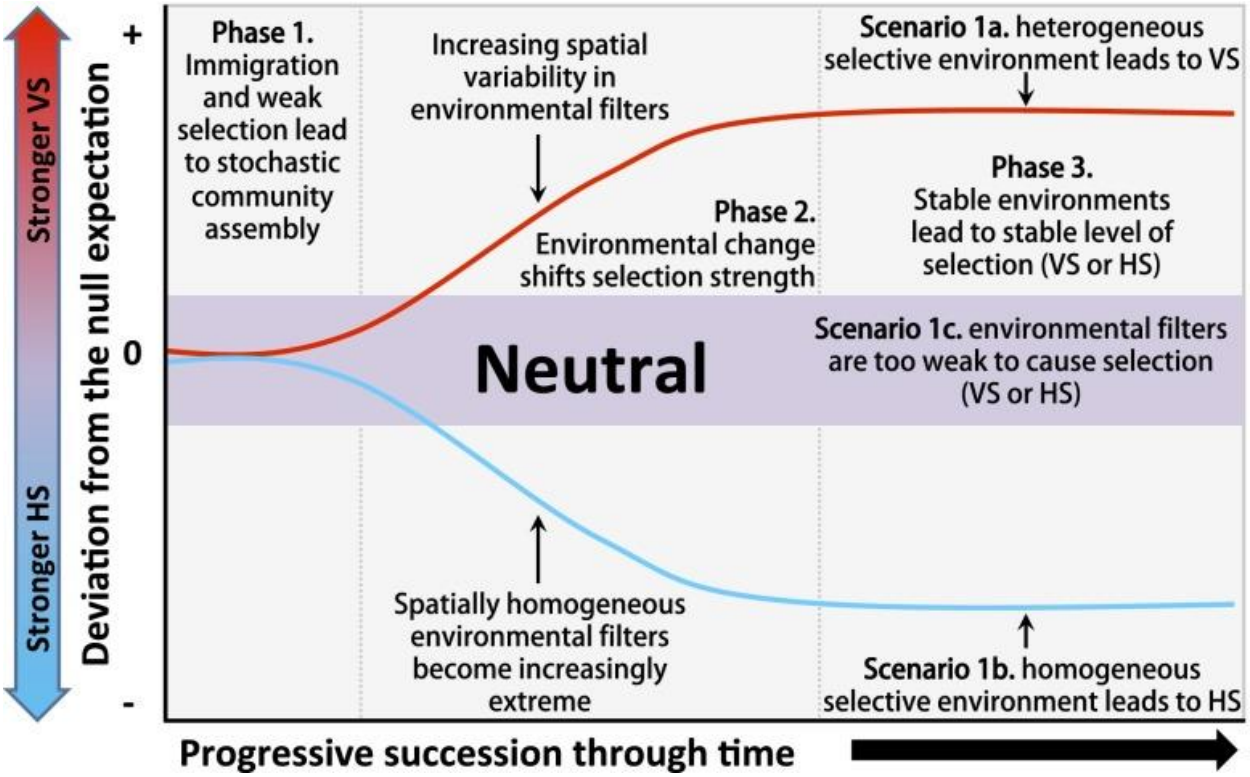

Figure 2. (Image taken from Dini-Andreote et al., 2015) "Three-phase conceptual model composed of alternative hypotheses related to changes in the strength and type of ecological selection during primary succession.". (doi:10.1073/pnas.1414261112)

Gut-brain communication via the vagus nerve

The vagus nerve is a part of the parasympathetic branch of the autonomous nervous system, connecting visceral organs to the brain and exerting bi-directional influence. In the gut, sensory neurons end in the muscle layer as well as in the mucosa of the small and large intestine (Bonaz, Bazin, and Pellissier, 2018). In the muscle layer, they are involved in the functioning of gut epithelial muscles, and also interact with the enteric nervous system by forming synapse connections between vagal endings and enteric neurons (Hansen, 2003). Mucosal afferents however, detect chemicals absorbed across the epithelial layer or released by epithelial cells in response to luminal stimuli. Two different types of mucosal vagal afferents have been described in both the small and big intestine: i) vagal villii afferents, which terminate in the apical part of a villus, close to the epithelial layer, and ii) vagal crypt afferents, which reach into the luminal end

of intestinal crypts (Fülling, Dinan, and Cryan, 2019). Unsurprisingly, these vagal afferent endings can detect luminal stimuli directly as well, thereby constituting a major terminal for direct contact with microbially produced neuroactive end-products, such as short-chain-fatty acids and other metabolites. Thereby, the vagus nerve continuously screens the GIT and provides information to the brain, which in return induces vagal activity upon visceral organs, thereby constituting the "vagal tone"– that is the strength of parasympathetic activation via the vagus nerve in the context of dynamic interaction with sympathetic branches of the autonomous nervous system (Bonaz, Bazin, and Pellissier, 2018). Alterations of gut microbiota have been shown to induce changes of vagal tone with consequences for brain and behavior, and reciprocal peripheral consequences. Anatomically, this is explained due to the fact that the vagus nerve innervates the brain-stem, specifically the nucleus tractus solitarii, from where GIT-related information is projected to various forebrain regions and beyond, that involve means for regulation of stress response and reward circuitries (Goehler et al., 2005). It was recently shown that gastro-intestinal administration of *Lactobacillus reuteri* can alleviate symptoms of autism spectrum disorder in a mouse model, by increasing oxytocin levels in the paraventricular nucleus (PVN) via interaction with the vagus nerve, thereby rescuing dopaminergic neurons in the ventral tegmental area (VTA) (Sgritta et al., 2019). This is one among many examples of gut microbiota-vagal interactions, however, concerning extremely premature infants, it should be regarded as a highly relevant one. It is speculated that severe inflammation during early-life underlies the development of behavioral abnormalities during childhood (Bale et al., 2010). To counteract aberrant development of gut microbiota in premature infants, probiotics containing *Lactobacillus* and *Bifidobacterium spp.* are widely employed, but successful colonization of probiotics in the premature GIT seems to be hampered in many cases (Alcon-Giner et al., 2020) and the underlying reasons remain unknown.

The influence of microbial metabolites on colonocyte metabolism

Colonocytes are exposed to luminal metabolites originating from inhabiting microorganisms. Human gut microbes primarily gain energy via various forms of anaerobic transformation of complex carbohydrates within human diet to a variety of fermentation end-products, so-called short-chain-fatty acids (SCFAs). Acetate, propionate, and butyrate, are the most abundant SCFAs in the adult human body, present in an adult colon in an approximate molar ratio of 60:20:20, respectively (Shah et al., 2021). In the infant and premature infant gut, we find that large

proportions of acetate likely stem from enterobacterial mixed acid fermentation, while propionate and butyrate largely originate from obligate anaerobic bacterial taxa such as *Clostridiales* and *Veilonella*. Furthermore, lactate is also present in the infant and premature infant gut due to the activity of *Bifidobacteria* and *Lactobacilli* (Seki et al., 2021).

Following their production, SCFAs are absorbed by colonocytes, mainly via monocarboxylate transporter (MCT) mediated transfer. Within colonocytes, they are consumed for mitochondrial ATP generation via the citric-acid cycle. This interplay constitutes a highly relevant eco-systematic condition, as constant supply of SCFAs forces colonocytes into a C2-skewed metabolic state, which is characterized by high oxygen consumption, thereby maintaining epithelial hypoxia and minimizing diffusion of oxygen into the gut lumen (Litvak, Byndloss, and Bäumler, 2018). Un-metabolized SCFAs are furthermore transported as substrate to hepatocytes, and consequently only a minor fraction reaches systemic circulation (Den Besten et al., 2013). These however, seem highly relevant for mechanisms underlying gut-brain axis functioning, given that they can cross the blood-brain-barrier (Silva, Bernardi, and Frozza, 2020) and given the presence of MCTs, free fatty acid receptors (FFARs), G protein-coupled receptors (GPR), and olfactory receptors (OR) on a variety of neurons and glia cells across the central and peripheral nervous system (Priyadarshini et al., 2018). FFAR3 signaling in particular is implicated in inducing intestinal glucogenesis via brain to gut circuitries (De Vadder et al., 2014), suggesting that in absence of this neurological signal, colonocytes would metabolically reorient towards a C1-skewed metabolism that is characterized by elevated anaerobic glycolysis, involving less consumption of oxygen and higher release of lactate, oxygen, and nitric oxide into the lumen, despite the availability of intracellular oxygen and glucose.

The development of premature infant gut microbiota is often disrupted due to the widespread administration of broad-spectrum antibiotics (Zwittink et al., 2017), which alters of microbiota and their fermentation end-product composition (Zarrinpar et al., 2018). As a consequence, C1-skewed colonocyte metabolisms are favored, and in response, freely available oxygen and nitrogenous sources become available in the gut lumen, providing electron acceptors that drive the expansion of facultative anaerobic bacteria (Litvak, Byndloss, and Bäumler, 2018). In the premature infant gut these mainly consist of *Enterobacteria sp.*, out of which many genera are considered opportunistic pathogens (e.g. *Klebsiella* sp.) (Wisgrill et al., 2019).

Immunological homeostasis in the developing gastrointestinal tract

T cells are an important link between the gut microbiome and the brain, but their ontogenesis during early-life, and their association with brain development post-delivery remains poorly understood. After initial contact, a mutualistic loop is expected to be formed between host and microbiota, that requires the prevention of aberrant inflammation despite constant antigen presentation in mucosal layers, so that commensal microbiota are able to colonize the GIT and co-exist (Mazmanian, Round and Kasper, 2008). It is believed that dendritic cells are key in deciding whether tolerance is sustained, or whether adaptive immune responses are about to be initiated. Under tolerating conditions, commensal antigen is presented to T cells via semi-mature dendritic cells that reside in mesenteric lymph nodes. This results in IgA production which prevents bacterial overgrowth, yet enables co-existence by favoring an anti-inflammatory enteric environment (Tezuka and Ohteki, 2019). IL-10 producing T regulatory cells are crucially involved in mediating this homeostasis . However, once these regulatory processes break down, due to invasion of pathogenic microorganisms for example, local dendritic cells become fully activated and initiate differentiation of naive T cells into effector T cells in mesenteric lymph nodes , which drive protective inflammatory processes that are vital for survival, but can also have dire consequences for developing organs such as the brain. Neonates produce very little amounts of IgA initially post-delivery, thus the main source of IgA derives from maternal colostrum (Buffet-Bataillon et al., 2021). Colostrum furthermore contains many epidermal growth factors and a mix of pro-inflammatory (IL6-, IL-8, TNFα) and anti-inflammatory cytokines (IL-10, IL-13) to support the maturation of mucosal immunity early post-delivery. It was shown that the colostrum of mothers that delivered very premature infants (born before 30 weeks of gestation) had lower concentrations of immunological factors as compared to term-delivering women (Castellote et al., 2011). Coherently, extremely premature infants often express stronger inflammatory responses to colonizing microbiota than term-born neonates (Olin et al., 2018).

$\gamma\delta$ T cells constitute a comparably small population of the human T cell repertoire, however, they were shown to be highly abundant as intraepithelial lymphocytes in gut mucosa (Ferreira, 2013) and do not require prior antigen processing and major-histocompatibility-complex (MHC) presentation of peptide epitopes. Due to these properties, $\gamma\delta$ T cells can rapidly respond to colonizing microbiota and have the potential to drive aberrant pro-inflammatory cascades via IL-17 production and chemotactic stimulation of neutrophils and monocytes (Gelderblom,

Priyadharshini and Magnus, 2014), once the homeostatic suppression of IL-10-secreting T regulatory cells diminishes. Furthermore, they have also been detected in brain lesions of premature infants with white matter injury (Albertsson et al., 2018), suggesting that they may be important mediators of gut-brain axis communication. Indeed, it was shown in an ischemic-stroke mouse model that IL-17+ γδ T cells accumulate in the meninges after stroke events. Depletion of the microbiome with antibiotics led to a reduction of IL-17+ γδ T cells due to the re-establishment of IL-10+ T regulatory cells, which in turn reduces trafficking of effector T cells from the gut to the meninges, resulting in reduced brain damage (Benakis et al., 2016)

Research objectives and approaches

Neonatal infection and inflammation have been identified as major risk factors of neonatal brain injury. Recent reports show that distortions of microbiota occur prior to sepsis and necrotizing enterocolitis (Madan et al., 2012; Pammi et al., 2017). Also, it is speculated that microbiota influence brain maturation as well as long-term neurodevelopmental outcomes. However, most mechanisms underlying gut microbiota-immune-brain axis development remain poorly understood. Therefore, the overarching aim of the present study was to elucidate the role of the gut-immune-brain axis on neonatal brain injury and its impact neurophysiological outcome of extremely premature infants.

Chapter one of the present thesis reports on a systems-level analysis of the gut microbiota, immune system, and neurophysiological development during hospitalization of 60 extremely premature infants. Infants were cohorted from 2017 to 2019 at the General Hospital of Vienna and monitored during hospitalization. The following methodologies were employed: i) 16S rRNA gene amplicon sequencing in combination with qPCR for quantitative microbiome profiling, ii) flow cytometry for T cell phenotyping, iii) multiplex cytokine and chemokine quantification, iv) fecal metabolite analysis, v) neurophysiological measurements (aEEG and NIRS), vi) and neuroimaging via cranial MRI to gain a holistic understanding of the developing gut microbiota-immune-brain-axis in early-life.

Furthermore, scientists have found that the establishing infant gut microbiota is highly personalized, varying substantially between individuals (De Muinck and Trosvik, 2018). The resulting individuality impedes the development of universally applicable therapeutic interventions, a dilemma that is luckily driving the progression of precision medicine. However, the factors that originate microbiota individuality in human gut microbiota remain poorly understood. These factors involve ecological forces that govern assembly and succession in the GIT of extremely premature infants.

Chapter two of the present thesis reports on ecological processes underlying microbial community assembly in the same cohort of 60 extremely premature infants (Seki et al., 2021), such as for a publicly available dataset comprising 32 healthy term-born infants (Janzon et al., 2019). Therefore, we compared phylogenetic observations to ecological null models to determine the contributions of selection, dispersal, and drift to the observed community turnover of premature infant gut microbiota.

Chapter 1

Aberrant gut microbiota-immune-brain axis development in premature neonates with brain damage

David Seki, Margareta Mayer, Bela Hausmann, Petra Pjevac, Vito Giordano, Katharina Goeral, Lukas Unterasinger, Katrin Klebermaß-Schrehof, Kim De Paepe, Tom Van de Wiele, Andreas Spittler, Gregor Kasprian, Benedikt Warth, Angelika Berger, David Berry, Lukas Wisgrill

Cell Host & Microbe: https://doi.org/10.1016/j.chom.2021.08.004

Supplementary information available at: https://doi.org/10.1016/j.chom.2021.08.004

Author contributions

Conceptualization: L.W., D.B., D.S.

Methodology: D.S. M.M., B.W., B.H., P.P., V.G., K.G., K.K-S., K.D.P., G.K.

Software: D.S., B.H., L.U., V.G.

Investigation: D.S.

Writing - Original Draft: D.S., D.B.

Writing - Review & Editing: D.S., D.B, L.W., K.D.P.

Resources: P.P., A.B., B.W., D.B., T.V.D.W., A.S.

Supervision: D.B.

Funding Acquisition: D.B., L.W., A.B.

Cell Host & Microbe

Aberrant gut-microbiota-immune-brain axis development in premature neonates with brain damage

Graphical abstract

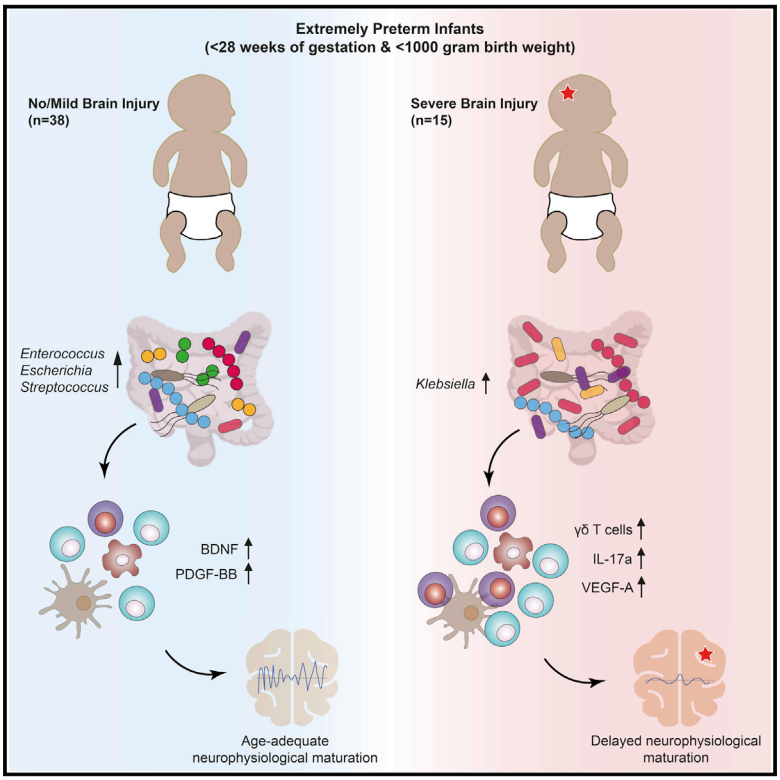

Highlights

- Microbiota, immune, and neurophysiological profile of 60 extremely premature infants
- Pro-inflammatory T cell response correlates with suppressed electrocortical maturation
- γδ T cells have central implications for the pathogenesis of brain injury
- *Klebsiella* overgrowth in the gastrointestinal tract is predictive for brain damage

Authors

David Seki, Margareta Mayer, Bela Hausmann, ..., Angelika Berger, David Berry, Lukas Wisgrill

Correspondence

david.berry@univie.ac.at (D.B.), lukas.wisgrill@meduniwien.ac.at (L.W.)

In brief

Seki et al. performed a comprehensive, time-resolved analysis of the gut microbiota-immune-brain axis in extremely premature infants. This analysis links early-life microbiome establishment to immunological and neurological development, identifying candidate biomarkers of perinatal brain injury and promising targets for personalized treatments to alleviate, or even prevent, life-long neurological morbidities.

Seki et al., 2021, Cell Host & Microbe *29*, 1–15
October 13, 2021
https://doi.org/10.1016/j.chom.2021.08.004

CellPress

Cell Host & Microbe

CellPress
OPEN ACCESS

Clinical and Translational Report

Aberrant gut-microbiota-immune-brain axis development in premature neonates with brain damage

David Seki,[1,2] Margareta Mayer,[1] Bela Hausmann,[3,4] Petra Pjevac,[1,3] Vito Giordano,[2] Katharina Goeral,[2] Lukas Unterasinger,[2] Katrin Klebermaß-Schrehof,[2] Kim De Paepe,[5] Tom Van de Wiele,[5] Andreas Spittler,[6] Gregor Kasprian,[7] Benedikt Warth,[8] Angelika Berger,[2] David Berry,[1,3,9,*] and Lukas Wisgrill[2,9,10,*]

[1]Centre for Microbiology and Environmental Systems Science, Department of Microbiology and Ecosystem Science, Division of Microbial Ecology, University of Vienna, 1090 Vienna, Austria
[2]Department of Pediatrics and Adolescent Medicine, Division of Neonatology, Pediatric Intensive Care and Neuropediatrics, Comprehensive Center for Pediatrics, Medical University of Vienna, 1090 Vienna, Austria
[3]Joint Microbiome Facility of the Medical University of Vienna and the University of Vienna, 1090 Vienna, Austria
[4]Department of Laboratory Medicine, Medical University of Vienna, 1090 Vienna, Austria
[5]Department of Biotechnology, Faculty of Bioscience Engineering, Center for Microbial Ecology and Technology, Ghent University, 9000 Ghent, Belgium
[6]Core Facility Flow Cytometry & Department of Surgery, Research Lab, Medical University of Vienna, 1090 Vienna, Austria
[7]Division of Neuroradiology and Musculoskeletal Radiology, Department of Radiology, Medical University of Vienna, 1090 Vienna, Austria
[8]Department of Food Chemistry and Toxicology, University of Vienna, 1090 Vienna, Austria
[9]These authors contributed equally
[10]Lead contact
*Correspondence: david.berry@univie.ac.at (D.B.), lukas.wisgrill@meduniwien.ac.at (L.W.)
https://doi.org/10.1016/j.chom.2021.08.004

SUMMARY

Premature infants are at substantial risk for suffering from perinatal white matter injury. Though the gut microbiota has been implicated in early-life development, a detailed understanding of the gut-microbiota-immune-brain axis in premature neonates is lacking. Here, we profiled the gut microbiota, immunological, and neurophysiological development of 60 extremely premature infants, which received standard hospital care including antibiotics and probiotics. We found that maturation of electrocortical activity is suppressed in infants with severe brain damage. This is accompanied by elevated γδ T cell levels and increased T cell secretion of vascular endothelial growth factor and reduced secretion of neuroprotectants. Notably, *Klebsiella* overgrowth in the gut is highly predictive for brain damage and is associated with a pro-inflammatory immunological tone. These results suggest that aberrant development of the gut-microbiota-immune-brain axis may drive or exacerbate brain injury in extremely premature neonates and represents a promising target for novel intervention strategies.

INTRODUCTION

The incidence of premature birth has been rising worldwide and is one of the leading causes of perinatal morbidity and mortality (Tommiska et al., 2007). Although recent advances in neonatal intensive care have increased the survival of extremely premature infants (gestational age < 28 weeks), the number of survivors with severe morbidity and life-long neurodevelopmental impairment remains high (Adams-Chapman et al., 2018). The third trimester of pregnancy is a critical period for the establishment, refinement, and maturation of human brain connectivity, which determines subsequent cognitive potential (Matthews et al., 2018). Extremely premature infants are born on the verge of the third trimester and their neural circuitry is therefore established in the face of manifold environmental cues and insults associated with preterm extra-uterine life (Stoecklein et al., 2020).

One inevitable environmental cue is the immediate post-natal colonization of the body by microorganisms. The establishing gut microbiota is in contact with a plurality of neurons of the enteric nervous system (Cryan et al., 2019). Increasing evidence suggests that during the period of early-life, enteric microorganisms participate in bidirectional signaling between the gastrointestinal tract (GIT) and the brain (Warner, 2019). This reciprocal communication between prokaryotes and the human central nervous system (CNS) is established via the gut-brain axis, whereby parasympathetic fibers from the vagus nerve are directly exposed to bacteria and their metabolites (Bonaz et al., 2018), while the immune (Rooks and Garret, 2017) and endocrine system mediate indirect crosstalk (Keunen et al.,

Please cite this article in press as: Seki et al., Aberrant gut-microbiota-immune-brain axis development in premature neonates with brain damage, Cell Host & Microbe (2021), https://doi.org/10.1016/j.chom.2021.08.004

2015). The developing brain of premature infants is at especially high risk of suffering from perinatal white matter injury (PWMI), which can manifest as intraventricular hemorrhage (IVH), periventricular leukomalacia (PVL), or diffuse white matter injury (DWMI) (Volpe, 2009). It is now widely accepted that perinatal infection and associated inflammation are involved in the pathophysiology of PWMI and can worsen the outcome of brain injuries (Niño et al., 2018), resulting in life-long morbidities such as cognitive and motor delay, cerebral palsy, neurosensory impairments, and behavioral abnormalities such as attention deficit hyperactivity disorder and learning disabilities (Woodward et al., 2006).

A balanced relationship between the developing immune system and gut microbiota is crucial to prevent excessive inflammation (Mazmanian et al., 2008). However, the establishment of a mutualistic relationship between the gut microbiota and its host seems to be impaired in extremely premature infants, despite daily administration of probiotics in many neo-intensive care units (NICUs) (Alcon-Giner et al., 2020). It remains unclear if this impairment in early-life development is due to the intensive medical care give to this vulnerable patient cohort, or if certain expected and required immunological cues are missing. T lymphocytes are key mediators of sepsis-induced brain injury (Benakis et al., 2016). $\gamma\delta$ T cells, in particular, are abundant in the neonatal gut and are unique among T cells due to the flexibility of their receptor chains (Ferreira, 2013). This flexibility allows them to respond directly to antigens without requiring prior antigen-processing and major-histocompatibility-complex presentation for their activation. They have also been detected in brain lesions of premature infants with white matter injury (Albertsson et al., 2018), suggesting that they may be important mediators of gut-brain axis communication.

Here, we report a systems-level analysis of the gut microbiota, immune system, and neurophysiological development during hospitalization of 60 extremely premature infants. We conducted 16S rRNA gene amplicon sequencing in combination with qPCR for quantitative microbiome profiling, flow cytometry for T cell phenotyping, multiplex cytokine and chemokine quantification, fecal metabolite analysis, neurophysiological measurements, and neuroimaging to gain a holistic understanding of the developing gut microbiota-immune-brain-axis in early life. We found that brain development in extremely premature infants is comprised three major phases: (1) an initial quiescent phase, (2) a period of neurophysiological maturation, and (3) a term-equivalent phase. We identified features of the microbiota and immune system in the quiescent phase that may initiate an inflammatory cascade that extends through the neurophysiological maturation phase and ultimately aggravates brain injury.

RESULTS

White matter injury is preceded by distinct neurophysiological signatures

Sixty extremely premature infants were enrolled between September 2017 and June 2019 at the Medical University of Vienna. Characteristics of the study cohort can be found in Tables 1 and S1. Over the course of hospitalization, neurophysiological development was monitored, stool samples were collected, and blood was drawn at multiple time points (Figure 1A). Brain injuries were identified by combined assessment of ultrasound imaging at multiple time points during hospitalization as well as by magnetic resonance imaging (MRI) at term-equivalent age. Out of the 60 infants, seven died, 38 displayed age-adequate MRIs or only mild brain injuries, and 15 infants were diagnosed with severe pathological brain injuries. Observed injuries included periventricular hemorrhagic infarctions (n = 5), intraventricular hemorrhages (IVH grade > 2, n = 13), cerebellar hemorrhages (n = 7), and periventricular leukomalacia (PVL, n = 4). Many of these pathologies were accompanied by a reduction of brain volume and an enlargement of the subarachnoid spaces. Representative MRI images for IVH and PVL are shown in Figure 1B. In order to quantify brain injury, the Kidokoro score was used as a standardized MRI assessment tool of the nature and extent of brain injury as well as impaired brain growth (Kidokoro et al., 2013). As expected, the Kidokoro score was significantly higher in infants with severe brain injuries (Figure 1C; t test; $p = 0.0001$). Although gestational age (GA) has been suggested to be an important predictor of cerebral injury, we found no significant association between GA at birth and neuroimaging outcome (t test; $p = 0.4371$).

In order to characterize neurophysiological development in our patients, we employed the amplitude-integrated electroencephalography (aEEG) sum score (Hellstro m-Westas et al., 2006; Klebermass et al., 2011), which quantifies four distinct patterns of electrocortical activity: (1) continuous voltage (CV), (2) discontinuous voltage (DV), (3) burst suppression (BS), and (4) flat trace (FT). These patterns reflect the cortical activity of the patient at the time of measurement. We observed a consistent trend of neurophysiological maturation that was characterized by an initial quiescent phase, in which DV was the dominant aEEG background pattern (Figures 1D, S1A, and S1B). This was followed by a period of neurophysiological maturation (maturation phase) in which CV continuously increased and eventually plateaued by term-equivalent age (term-equivalent phase). Generally, infants with brain injuries experienced a delayed onset of the maturation phase, with lower CV and higher BS 2 weeks post-delivery (Wilcoxon; $p = 0.008$ and 0.028, respectively). Also, DV was significantly lower in infants with brain injuries 2 and 4 weeks post-delivery (Wilcoxon; $p = 0.038$ and 0.045, respectively) (Figure 1D). Neurophysiological maturation patterns converged by 4 weeks post-delivery, after which both groups continued to follow a similar course.

We next evaluated brain tissue oxygenation using near-infrared spectroscopy (NIRS). In order to quantify potentially harmful instabilities in brain tissue oxygenation, we calculated the prevalence of extreme fluctuations in brain tissue oxygenation (cSO_2), defined as the fraction of time for which cSO_2 was $+/-$ 10 cSO_2 from the mean value during the NIRS measurement (VAR-cSO_2). We observed that fluctuations in cSO_2 were significantly elevated during the early maturation phase (4 weeks post-delivery) in infants with severe white matter injuries (t test; $p = 0.025$; Figure 1E).

Furthermore, we evaluated the predictive potential of aEEG and NIRS signatures at each time point for neuroimaging outcome. We found that although mean cSO_2 had no predictive value for detecting brain injury, VAR-cSO_2 had some predictive power 4 weeks post-delivery (area under the curve

Please cite this article in press as: Seki et al., Aberrant gut-microbiota-immune-brain axis development in premature neonates with brain damage, Cell Host & Microbe (2021), https://doi.org/10.1016/j.chom.2021.08.004

CellPress
OPEN ACCESS

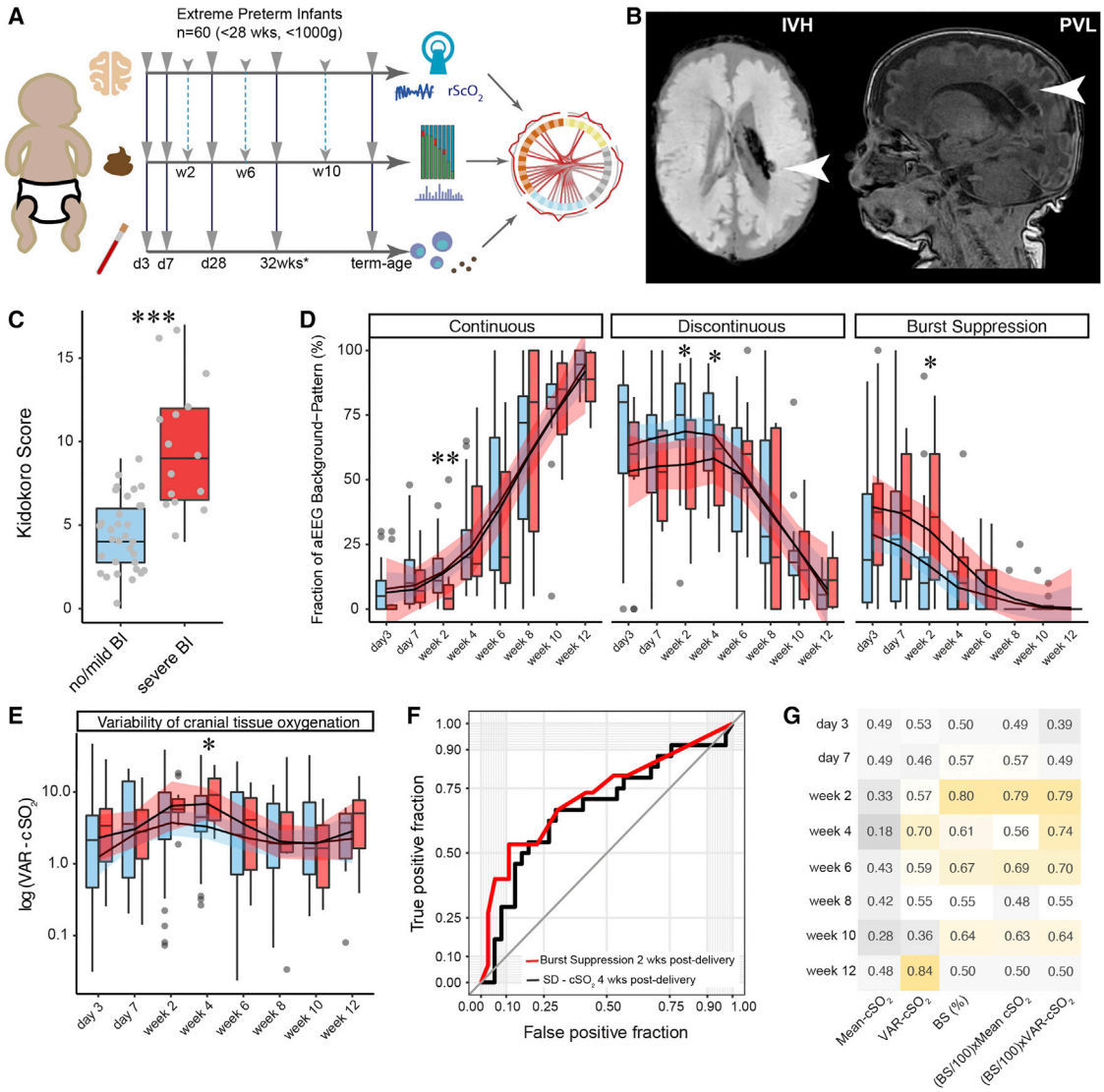

Figure 1. Neurophysiological development of extremely premature infants with and without severe brain injuries

Blue color for age-adequate cranial magnetic resonance imaging (cMRI) results or mild brain injury (BI). Red color for severe BI.

(A) Schematic illustration of study design. Solid arrows indicate sampling time points with blood drawings on day 3, day 7, day 28 post-delivery, 32 weeks gestational age, and at term-equivalent age. Dashed lines indicate time points for stool sampling and neurophysiological assessment (day 3, day 7, and day 14, followed by biweekly sampling until discharge).

(B) Representative cMRI images at term-equivalent age for IVH > 2 (left) and PVL (right).

(C) Comparison of Kidokoro scores between infants with and without severe BI.

(D) Comparison of aEEG background patterns (1) continuous voltage (CV), (2) discontinuous voltage (DV), (3) burst suppression (BS).

(E) Comparison of the variability of cranial oxygen supply (VAR-cSO_2) (fraction of deviation beyond 10% from the mean of the total NIRS measurement) between infants with and without BI.

(F) Receiver operating characteristic (ROC) curve visualizing the predictive potential of cranial oxygen fluctuation (VAR-cSO_2) 4 weeks post-delivery, and BS signatures 2 weeks post-delivery for brain damage.

(G) Summary of area under the curve (AUC) scores of neurophysiological parameters at given time points. Color gradient ranges from dark gray (low AUC score) to dark yellow (high AUC score). Box plots show group median and interquartile range. Smoothed lines result from locally estimated scatterplot smoothing (LOESS) and indicate trends of neurophysiological development. Asterisks represent p values: *p < 0.05, **p < 0.01, ***p < 0.001.

[AUC] = 0.70). The level of BS was most predictive 2 weeks post-delivery (AUC = 0.80) and by combining BS and VAR-cSO_2 (BS/100 × VAR-cSO_2), predictive potential was at AUC = 0.79 2 weeks post-delivery and increased to AUC = 0.74 2 and 4 weeks post-delivery (Figures 1F and 1G).

Therefore, we conclude that neuroimaging outcome is preceded by a delayed onset of electrocortical maturation. This transient suppression of neurophysiological development and increased instability in cranial oxygen saturation at approximately 2 to 4 weeks post-delivery is predictive for PWMI at

Please cite this article in press as: Seki et al., Aberrant gut-microbiota-immune-brain axis development in premature neonates with brain damage, Cell Host & Microbe (2021), https://doi.org/10.1016/j.chom.2021.08.004

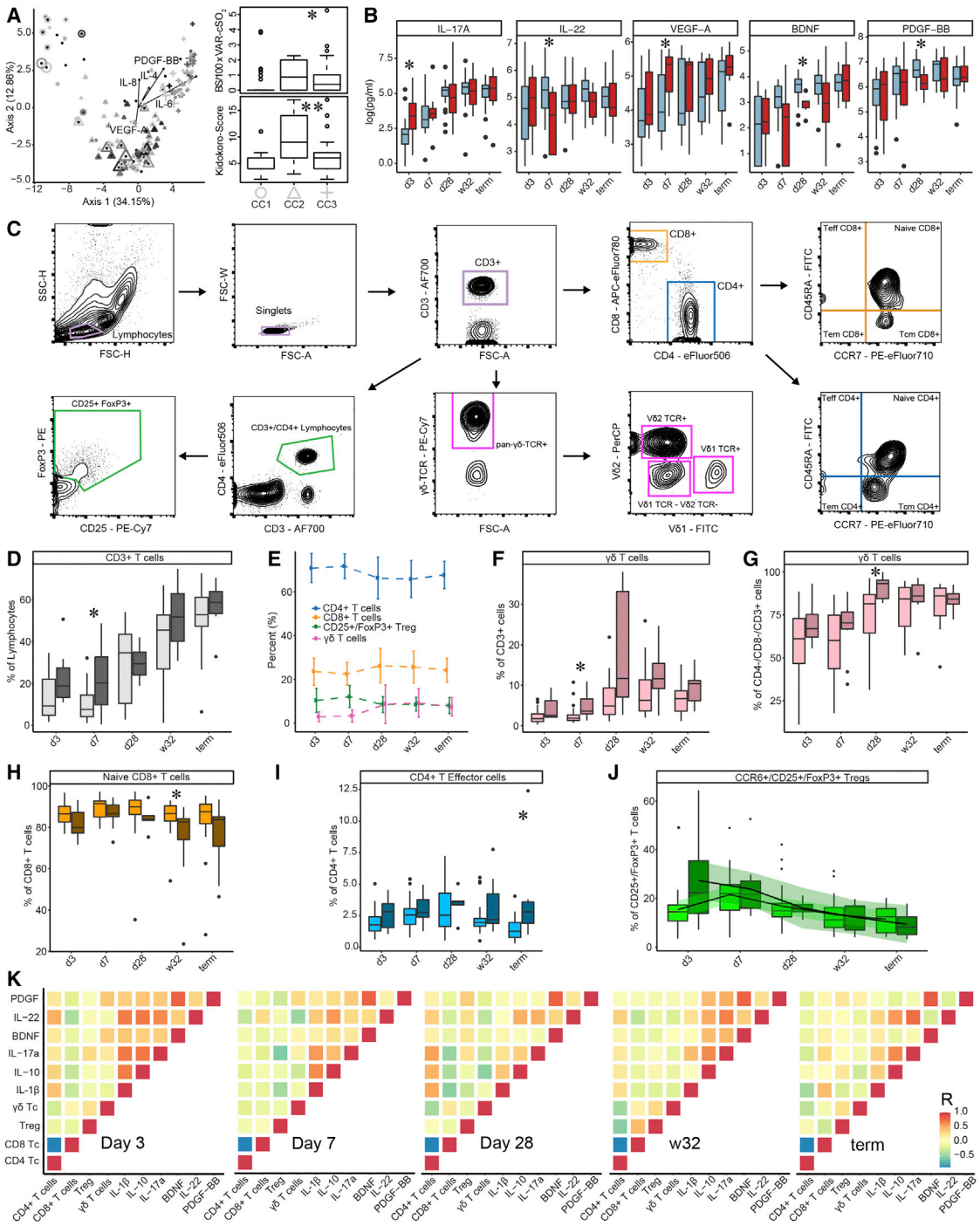

Figure 2. T cell ontogenesis in extremely premature infants with and without severe brain injury

(A) Principal coordinates analysis (PCoA)—biplot of sequestered cytokine and chemokine composition. Silhouette scoring identified 3 main cyto-Clusters (as indicated by different symbols). The shade of the symbols (gray to black) is determined by days post-delivery—the older the infant the darker the symbol. The size of the symbols is determined by the Kidokoro Score as assessed at term-equivalent age via cMRI—the higher the score the larger the symbol. Significantly correlated ($p < 0.05$) cytokines/chemokines are plotted as arrows. In addition, box plots next to PCoA show the range of combined values for burst suppression and variance of cranial oxygenation (BS/100 × VAR-cSO_2), as well as the range of Kidokoro Scores in the respective cyto-clusters (cyto-cluster 1, CC1; cyto-cluster 2, CC2; cyto-cluster 3, CC3).

(B) Blood cytokine/chemokine concentrations in infants with (red) and without (blue) severe BI (3 days post-delivery, d3; 7 days post-delivery, d7; 28 days post-delivery, d28; 32 weeks of gestational age, w32; term-equivalent age = term).

(legend continued on next page)

term-equivalent age and may have an important role in its pathology.

Neonates with brain injury display a pro-inflammatory polarized T cell response

Although T cells are an important link between the gut microbiome and the brain (Benakis et al., 2016) their ontogenesis during early life, and their association with perinatal brain damage in extremely premature infants, remains poorly understood. To investigate temporal changes in T cell dynamics in relation to perinatal brain damage, we investigated T cell subsets via fluorescence-activated cell sorting (FACS) and their corresponding cytokine response via multiplex immunoassays in blood samples from 40 extremely premature infants at 5 time points. Out of these, four died, 26 displayed age-adequate MRIs or only mild brain injuries, and ten infants were diagnosed with severe pathological brain injuries. Principal coordinates analysis (PCoA) of cytokine response revealed three distinct clusters of samples: one early-life cluster (Cyto-Cluster 1; mean days post-delivery: 17) and two clusters from later time points (Cyto-Cluster 2 and 3; mean days post-delivery: 30 and 35, respectively) (Figure 2A). Cyto-Cluster 2 was enriched in samples from infants suffering brain damage (38% in Cyto-Cluster 2 versus 10% in Cyto-Cluster 3). Strikingly, Kidokoro scores at term-equivalent age, as well as BS combined with VAR-cSO_2 (BS/100 × VAR-cSO_2) were higher in Cyto-Cluster 2 as compared with Cyto-Cluster 3 (Wilcoxon; p = 0.035 and 0.0088, respectively). Levels of interleukins 4, 6, and 8 (IL-4, IL-6, and IL-8), vascular endothelial growth factor-A (VEGF-A), and platelet-derived growth factor-BB (PDGF-BB) were significantly associated with the observed variance of the PCoA, with VEGF-A driving the formation of Cyto-Cluster 2 and the other cytokines being associated with Cyto-Cluster 3. Furthermore, we built a correlation network of secreted cytokines and chemokines to reveal connectivity within their expression. Most notably, we found that networks produced with samples from infants without severe brain injuries displayed a more central role of PDGF-BB as compared with infants with severe brain injuries, whose networks were rather centered around interleukin 17a (IL-17a) (Figures S2A–S2C). Also, by employing topographical data analysis of cytokine levels, we observed a divergence in the developmental trajectory in premature infants 1 month after birth, which converges at term age (Figure S2D).

When comparing cytokine expression between infants with and without brain injury, we observed that peripheral blood T cells in infants with brain injury had elevated production of IL-17a 3 days post-delivery (Wilcoxon; p = 0.048) and VEGF-A 7 days post-delivery (Wilcoxon; p = 0.034), accompanied by reduced interleukin 22 (IL-22) 7 days post-delivery (Wilcoxon; p = 0.044; Figure 2B). Although these differences had disappeared by 28 days post-delivery, samples from infants with brain injury 28 days post-delivery exhibited reduced production of the neuroprotectants brain-derived neurotrophic factor (BDNF) (Wilcoxon; p = 0.012) and PDGF-BB (Wilcoxon; p = 0.026) (Figure 2B). These data suggest that a pro-inflammatory T cell polarization via IL-17a early after birth underlies latter aberrant diversification, during which a dysregulated VEGF-A response is key for the pathogenesis of brain injury. Additional cytokines and chemokines that were quantified but did not show significant differences between infants with and without brain injuries are shown in Figure S2G.

We then profiled T regulatory, T helper, cytotoxic, and γδ T cells from the same samples via FACS (Figures 2D–2J). T helper cells (TH:$CD4^+$/$CD3^+$) were the most abundant $CD3^+$ lymphocytes, followed by cytotoxic T cells (TH:$CD8^+$/$CD3^+$), regulatory T cells (Treg:$CD25^+$FoxP3+/$CD3^+CD4^+$), and γδ T cells (γδPAN/$CD3^+$) (Figure 2E). Infants with brain injuries had increased levels of T cells 1 week after birth (Wilcoxon; p = 0.039; Figure 2D), which corresponded with elevated levels of γδ T cells in the $CD3^+$ population (Wilcoxon; p = 0.027; Figure 2F). The majority of γδ T cells exist as double negative (DN; CD8 and CD4) T cells. Shortly after birth, ~60% of the cells within the overall DN T cell population expressed a PAN-γδ T cell marker. 1 month after birth, DN PAN-γδ T cells increased in relative numbers and were significantly more abundant in infants with brain injuries (Wilcoxon; p = 0.031; Figure 2G). In addition, infants with severe brain injuries had fewer naive $CD8^+$ T cells at 32 weeks corrected GA (Wilcoxon; p = 0.031; Figure 2H) and more effector $CD4^+$ T cells at term-equivalent age (Wilcoxon; p = 0.014; Figure 2I). Although not statistically significant, we observed elevated numbers of migration-stimulating CCR6+ T regulatory cells (Yamazaki et al., 2008) in infants with brain injuries shortly after birth (Figure 2J). Additional T cell receptors that were quantified but did not show significant differences between infants with and without brain injuries are shown in Figure S2H.

Next, we sought to unravel the interplay of VEGF-A, interleukins, and the neuroprotectants PDGF-BB and BDNF with different T cell populations via correlation analysis (Figure 2K). The presented values are extracted from a correlation analysis of all measured cytokines and T cells. T helper cells were negatively associated with cytotoxic T cells at all time points, as well as with γδ T cells at three and 28 days post-delivery and at 32 weeks GA. 3 days post-delivery, VEGF-A was negatively associated with the neuroprotectants PDGF-BB and BDNF. Seven days post-delivery T helper cells were negatively associated with IL-10 and IL-22, while T regulatory cells were

(C) Representative images illustrating the gating strategy for FACS analysis. Differently colored gates mark gating for respective cell populations. Magenta, untargeted; blue, T helper cells; orange, cytotoxic T cells; green, T regulatory cells; pink, γδ T cells. For box plots in (D) and (F–J), darker shade represents data from infants with, and lighter shade from infants without, severe BI.

(D) Proportion of $CD3^+$ cells during hospitalization.

(E) Relative distribution of T regulatory (green), T helper (blue), γδ T (pink), and cytotoxic T cells (orange).

(F–I) Box plots showing the expression of T cell receptors relative to the given parental population throughout hospitalization.

(J) Box plots showing the expression of CCR6+/T regulatory cells with the addition of smoothed lines resulting from locally estimated scatterplot smoothing (LOESS) to indicate trends of development.

(K) Spearman correlation analysis to reveal associations between T cell populations and selected sequestered cytokines/chemokines at respective time points ($p < 0.001$). Red color indicates positive correlation, blue color indicates negative correlation. Box plots show group median and interquartile range. Asterisks represent p values: *$p < 0.05$, **$p < 0.01$, ***$p < 0.001$.

Please cite this article in press as: Seki et al., Aberrant gut-microbiota-immune-brain axis development in premature neonates with brain damage, Cell Host & Microbe (2021), https://doi.org/10.1016/j.chom.2021.08.004

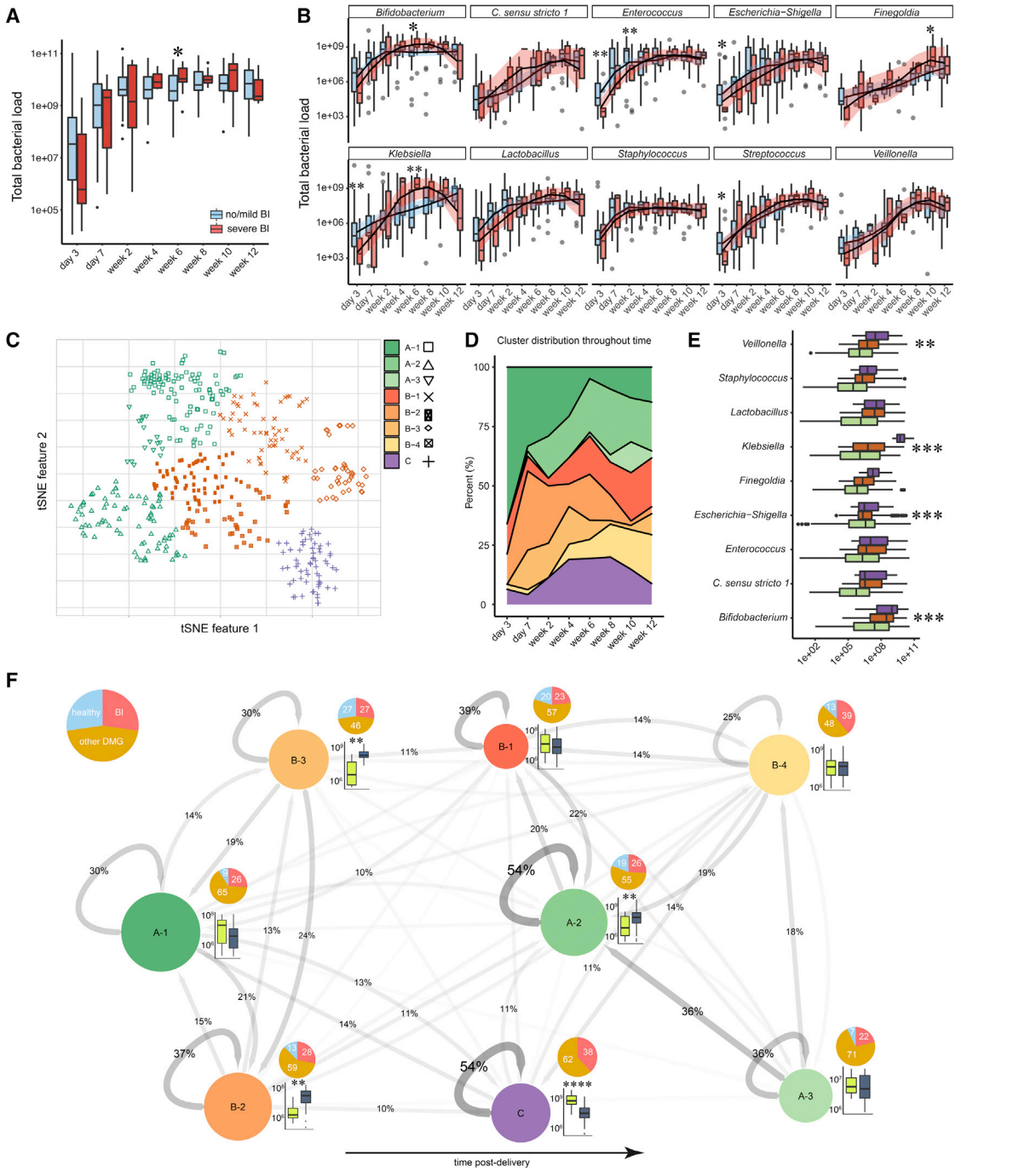

Figure 3. The microbiome of extremely premature infants and its diversification corresponding to brain injury

(A) Total bacterial cell counts per gram feces over time.

(B) Absolute abundances of the most abundant bacterial genera in infants with (red) and without (blue) severe BI.

(C) T-distributed stochastic neighbor embedding (tSNE) ordination of all 16S rRNA gene amplicon libraries corrected by absolute abundances and 16S rRNA gene copy number. Hierarchical clustering (Ward's method) identified 3 main clusters (green, orange, and purple) and 8 sub-clusters (symbols).

(D) Area plot illustrating the percentage distribution of sub-clusters throughout time.

(E) Absolute abundance of bacterial genera in respective main clusters.

(F) Network illustrating the trajectories of microbiome succession in extremely premature infants. Circles correspond to tSNE sub-clusters. Circle size indicates the number of patients found in a sub-cluster for at least one sampling time. Arrows represent transitions between clusters, whereby the thickness and shade of the arrow indicates the probability of the transition. Recursive arrows represent the percentage of consecutive observations within the same cluster. Pie charts show the distribution of patients in respective clusters diagnosed as healthy (blue, lacking any diagnosis listed in Table 1), with severe BI (red), or other

(legend continued on next page)

Please cite this article in press as: Seki et al., Aberrant gut-microbiota-immune-brain axis development in premature neonates with brain damage, Cell Host & Microbe (2021), https://doi.org/10.1016/j.chom.2021.08.004

negatively associated with IL-1beta and IL-17a. γδ T cells, however, were positively associated with IL-8 and PDGF-BB. At 28 days post-delivery, VEGF-A was associated positively with the increase of γδ T cells, but negatively with T regulatory cells. This positive association disappeared in later time points, whereas the negative association with T regulatory cells persisted. Furthermore, we assessed the influence of cytokine and chemokine secretion levels, as well as Kidokoro scores and myelination scores assessed via cMRI at term age, on the variance of given T cell populations via canonical correlation analysis (CCA). We found that the composition of T regulatory cells, T helper cells, cytotoxic T cells, and γδ T cells across all samples was significantly affected by the expression of IL-17a (p value: 0.004), IL-12P40 (p value: 0.004), PDGF-BB (p value: 0.002), and IL-4 (p value: 0.028), as well as cranial myelination at term age (p value 0.028), with a combined explanatory power of all variables of $R^2 = 0.26$. (Figure S2E).

We conclude that the increase of γδ T cells starting 7 days post-delivery may be involved in the pathogenesis of PWMI. This initial polarization correlates with IL-8, IL-17a, VEGF-A, and PDGF-BB secretion at first. Subsequently, a strong link between VEGF-A and γδ T cells persists, whereas the further secretion of neuroprotectants PDGF-BB and BDNF is suppressed in infants with severe brain damage.

Overgrowth of *Klebsiella* is associated with brain damage

The microbiota is an important instigator of immunological tolerance, as the nature and quantity of microbial antigens determine lymphocyte responses (Sekirov et al., 2010). We employed 16S rRNA gene-targeted qPCR and 16S rRNA gene amplicon sequencing to quantify total bacterial load in stool samples and for quantitative microbiome profiling of community composition. We observed an increase in bacterial load over time that plateaued by 2 weeks post-delivery, reaching a concentration of $\sim 10^9$ cells per g feces (Figure 3A). 6 weeks post-delivery, patients with brain injuries had slightly higher bacterial loads (Wilcoxon; p = 0.03), but otherwise, colonization dynamics were very similar to patients without brain injury. Overall, the gut microbiota was dominated by 10 abundant and prevalent genera (*Bifidobacterium*, *Escherichia-Shigella*, *Enterococcus*, *Lactobacillus*, *Staphylococcus*, *Streptococcus*, *Klebsiella*, *Clostridium* sensu stricto 1, *Veillonella*, and *Finegoldia*), which occurred in a minimum of 20% of samples with an abundance of at least 10^5 cells and together comprised 75% of all 16S rRNA amplicon sequence variants (ASVs; Figure S3A). We observed that strictly anaerobic core bacteria (*Clostridia*, *Finegoldia*, and *Veillonella*) occurred sparsely early post-delivery and increased in abundance in later periods (Figure 3B; Pearson correlation, R = 0.53, 0.62, and 0.48, respectively, p < 0.001; Figure S3C). Strikingly, *Klebsiella* was on average 1.7-fold more abundant 4 weeks post-delivery (Wilcoxon; p = 0.0049), but less abundant shortly post-delivery in infants with severe brain injury (Wilcoxon; p = 0.0066; Figure 3B). Consistent with this observation, there was a statistically significant association of *Klebsiella pneumoniae* ASV_c07_vnh_xuf with severe brain injury (edgeR differential abundance test; p = 0.0467). This strain was isolated from stool of a premature infant suffering from severe brain injury, and its genome features several potential virulence factors as well as genes allowing it to colonize in the inflamed gut, including biofilm formation potential, a repertoire of antibiotic resistance genes, iron-scavenging siderophores, and the genes for dissimilatory nitrate reduction to ammonium (Tables S2 and S3). Furthermore, we observed increased *Bifidobacterium* sp. 6 weeks post-delivery, and *Finegoldia* sp. shortly before discharge, in infants with severe brain injuries (Wilcoxon; p = 0.0455 and 0.033, respectively). However, infants without severe brain injuries furthermore had elevated levels of *Enterococcus*, *Escherichia-Shigella*, and *Streptococcus* (Wilcoxon; p = 0.0083, 0.028, and 0.045, respectively) 3 days post-delivery, as well as more *Enterococcus* 2 weeks post-delivery (Wilcoxon; p = 0.0065; Figure 3B).

In order to better understand microbiome assembly and dynamics, we used T-distributed stochastic neighbor embedding (tSNE) to identify distinct microbiome states. This analysis revealed three major microbiome clusters that could be further subdivided into eight sub-clusters, as determined by silhouette score cluster optimization (Figures 3C, 3D, and S3D). Overall, the clusters had different bacterial loads (repeated measures ANOVA; p < 0.001), with cluster C having an increased load compared with clusters A and B (Tukey's post-hoc test; p = 0.0017 and 0.0003, respectively). Cluster A divided into three and cluster B into four sub-clusters, respectively, whereas cluster C did not form sub-clusters. Furthermore, the bacterial genera *Veillonella*, *Klebsiella*, *Escherichia-Shigella*, and *Bifidobacterium* had differential abundances within the clusters (repeated measures ANOVA; p = 0.002, < 0.001, < 0.001, and 0.001). Additionally, *Veillonella* was elevated in cluster C as compared with cluster A (Tukey's post-hoc test; p = 0.0012), *Klebsiella* was elevated in cluster C as compared with clusters A and B (Tukey's post-hoc test; both $p \leq 0.001$), *Escherichia-Shigella* was elevated in clusters A over cluster B (Tukey's post-hoc test; p < 0.001), and *Bifidobacterium* was elevated in cluster C as compared with clusters A and B (Tukey's post-hoc test; p = 0.036 and < 0.001, respectively; Figure 3E).

We next used the sub-clusters to examine microbiome dynamics and to determine whether the microbiome undergoes characteristic trajectories which could be indicative of deterministic succession (Figure 3F). We observed a trend in the frequency of clusters over the first 12 weeks of life, with early-life clusters A1 and B2 gradually becoming less prominent concomitant with increases in the prevalence of A2 and B1. At later time points, cluster B4 also became more frequently detected. clusters A2 and C had the highest stability, i.e., the highest probability of the microbiome staying in the same cluster at the subsequent time point. In cluster C, *Klebsiella* was the dominant genus, whereas in cluster A2 *Escherichia-Shigella* was more abundant. As no fecal samples of healthy infants were observed in cluster C, we conclude that *Klebsiella* domination and overgrowth in the gut may be key for

pathologies (other DMG, see Table 1; ochre). Sub-clusters are arranged according to the average patient age of samples in the cluster, ordered from youngest (left) to oldest (right). Box plots next to circles show the absolute abundance of *Klebsiella* (bright green) and *Escherichia-Shigella* (dark blue) in the associated sub-cluster. Box plots show group median and interquartile range. Smoothed lines result from locally estimated scatterplot smoothing (LOESS) and indicate trends of microbiome development. Asterisks represent p values: *p < 0.05, **p < 0.01, ***p < 0.001.

Please cite this article in press as: Seki et al., Aberrant gut-microbiota-immune-brain axis development in premature neonates with brain damage, Cell Host & Microbe (2021), https://doi.org/10.1016/j.chom.2021.08.004

Table 1. Subject cohort demographics

Characteristic	Extremely premature infants without or with mild brain injury	Extremely premature infants with severe brain injury	p value (t test and Fisher's exact test)
Individuals, number	38	15	
GA at birth, weeks	25.5 ± 1.2	24.8 ± 1.3	0.100
Birth weight, grams	774 ± 137	718 ± 156	0.213
Birth head circumference, cm	23.2 ± 1.4	22.7 ± 1.6	0.234
Birth length, cm	32.9 ± 2.3	32.4 ± 2.0	0.520
Female gender, %	63%	53%	0.546
Spontaneous birth, %	11%	53%	0.001
IUGR, %	8%	13%	0.614
pPROM, %	63%	33%	0.068
Received lung maturation, %	97%	93%	0.489
Apgar score at 5 min	8.4 ± 0.9	8.4 ± 1	0.874
Apgar score at 10 min	8.7 ± 0.8	8.9 ± 0.2	0.468
CSI, %	32%	47%	0.351
Culture-proven EOS, %	5%	0%	1
Clinical LOS, %	16%	33%	0.257
Culture-proven LOS, %	29%	20%	0.731
Hospitalization, days	91.82 ± 37.32	91.53 ± 24.29	0.884
NEC, %	8%	0%	1
ROP, %	47%	100%	0.0003
BPD, %	27%	20%	0.733
PDA, %	37%	60%	0.217
Antibiotic intervention, days	15.89 ± 11.5	18.00 ± 13.4	0.598
Age at discharge, weeks	39.2 ± 4.5	38.7 ± 2.0	0.693
Weight at discharge, grams	2,929 ± 956	2,788 ± 325	0.600
Length at discharge, cm	47.0 ± 5.2	46.4 ± 2.6	0.699
Head circumference at discharge, cm	33.0 ± 3.1	32.8 ± 2.0	0.855
Milk formula fortifier administered shortly before discharge	77%	77%	1

IUGR, intrauterine growth restriction; pPROM, preterm premature rupture of membranes; CSI, clinical-suspected inflammation; EOS, early-onset sepsis; LOS, late-onset sepsis; BPD, bronchopulmonary dysplasia; NEC, necrotizing enterocolitis; ROP, retinopathy of prematurity; PDA, persistent ductus arteriosus. Data are presented as mean ± SD or percentage (%).

driving the assembly of a distinctive and remarkably stable microbiome that is associated with neurological pathologies.

Furthermore, mode of delivery and heavy use of antibiotics have been discussed as potential drivers of aberrant microbial succession (Aguilar-Lopez et al., 2021) Although we observed no difference in time spent on antibiotics during hospitalization between infants with and without severe brain injuries, there was a significant association of severe brain injury with spontaneous delivery (Table 1). Neither the duration of antibiotic administration nor delivery mode, however, were significantly associated with the proportion of samples per patient classified as cluster-C microbiota (chi-square test, p = 0.792 and 0.723, respectively). This suggests that spontaneous birth involves particular risks for pathological brain development but does not imply subsequent development of cluster-C-like microbiota.

Enteral nutrition drives gut fermentation but does not control bacterial load

Though the healthy human adult gut is considered to be a largely anoxic environment, the GIT of premature infants has been reported to be partially oxic (Singer et al., 2019) and therefore must transition to anoxia in the course of post-natal development. In the absence of terminal electron acceptors such as oxygen, bacteria must gain energy via substrate-level phosphorylation, and in the gut this is typically accomplished by fermentation of dietary or host-derived compounds into short-chain fatty acids (SCFAs), which can act as neurological (Dalile et al., 2019) and immunological (Parada Venegas et al., 2019) signaling molecules. Although the major source of nutrients for the gut microbiota may well be expected to be derived from enteral nutrition, we observed that bacterial load was uncoupled from the quantity of enteral nutrition, with bacterial load plateauing several weeks before the enteral nutrition amount (Figures 3A and 4A). This may be due to the presence of alternative substrates such as meconium, mucins, or post-natal intestinal cell sloughing. Conversely, growth restricting effects could be introduced by molecules such as bile acids, maternal antibodies, and alternative limiting nutrients such as iron.

We did not observe statistically significant differences between infants with and without severe brain injuries concerning the amount of acetate, butyrate, propionate, lactate, and formate measured in stool at specific sampling time points (Figure 4B). Overall, SCFA production peaked at approximately 50 days post-delivery and, unlike bacterial load, appeared to be driven by the amount of enteral nutrition (Figure 4C). Acetate and lactate can be produced by either aerobic or anaerobic metabolism, but as bacteria transition from aerobic to anaerobic metabolism, bacteria oxidize pyruvate to acetyl-CoA and formate, rather than to acetyl-CoA, CO_2, and NADH (White, 2000). Interestingly, we observed the highest accumulations of formate 1 month post-delivery. This was followed by a gradual increase in propionate and butyrate, indicating that anaerobic fermentation activity gradually increases over time. This shift to anoxia is mirrored in the increase in the obligate anaerobic taxa (Figures 3B and 4B). Therefore, we pooled samples before and after 28 days post-delivery to reveal characteristics of an oxygen-influenced and anoxic premature infant gut. After day 28 post-delivery, *Clostridium* sensu strictu 1 correlated positively with butyrate production, and *Veillonella* correlated with acetate and propionate (Pearson correlation; R = 0.5, 0.3, and 0.4, respectively, $p < 0.001$; Figure 4E), consistent with its ability to produce acetate and propionate via fermentation (Ng and Hamilton, 1971). However, as we detect small amounts of butyrate and propionate early post-delivery as well, we conclude that although aerobic metabolism might be dominant early after birth, fermentation can exist in parallel, presumably in anaerobic microniches. To test if either early or late fermentation processes

Please cite this article in press as: Seki et al., Aberrant gut-microbiota-immune-brain axis development in premature neonates with brain damage, Cell Host & Microbe (2021), https://doi.org/10.1016/j.chom.2021.08.004

CellPress
OPEN ACCESS

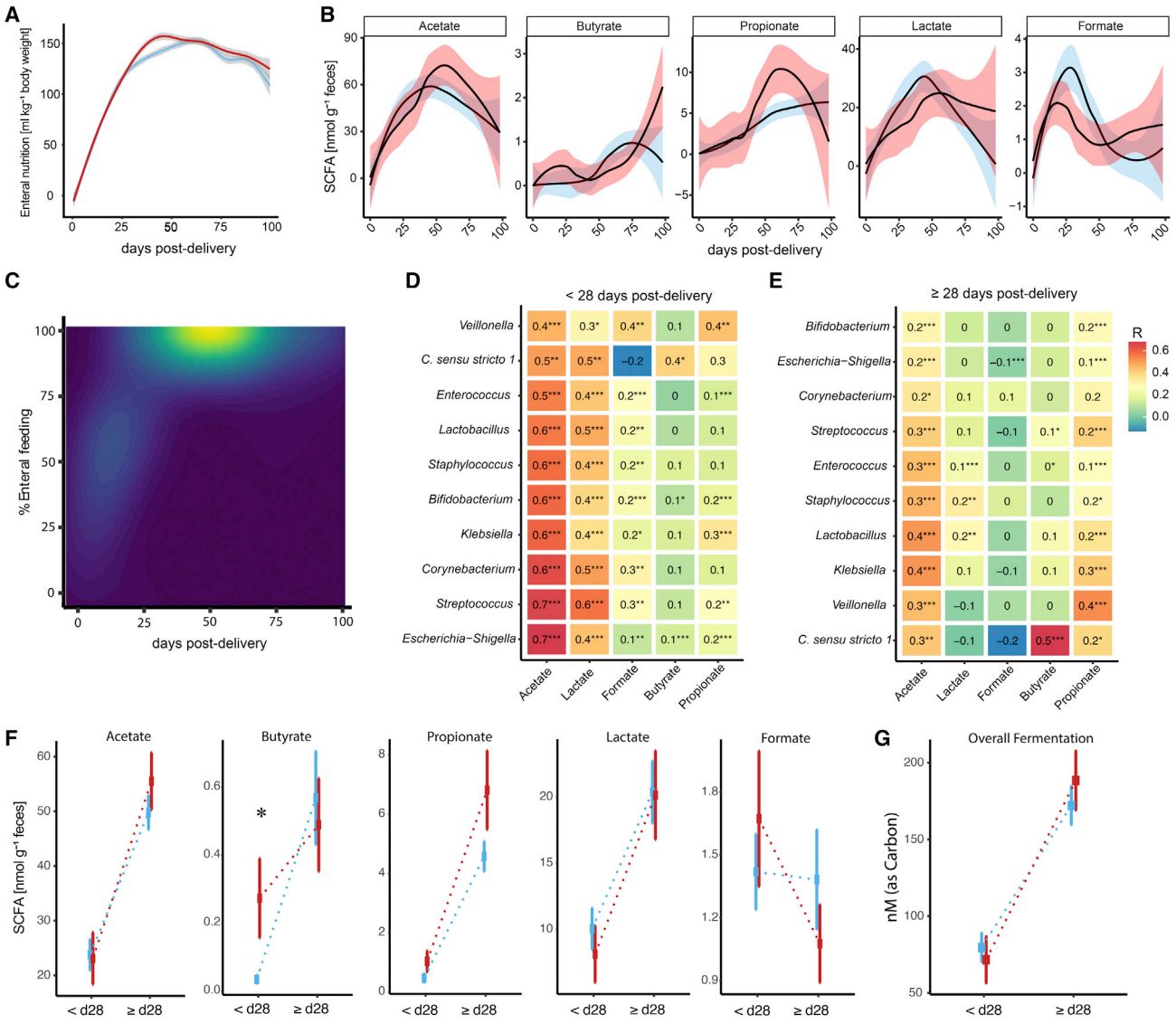

Figure 4. SCFAs in stool of extremely premature infants

(A) Enteral feeding over time for infants with (red) and without severe BI (blue).

(B) Fecal SCFAs in nmol g^{-1} feces throughout hospitalization of premature infants with (red) and without (blue) severe BI.

(C) Weighted contour plot showing the association of SCFAs with percentage of enteral feeding and days post-delivery. Brighter color indicates higher SCFA concentrations.

(D–F) (D) Heatmap of Pearson correlations of bacterial genus abundance with SCFA levels [nmol] before 28 days post-delivery and (E) at or after 28 days post-delivery (F) SCFA concentrations in infants with brain injuries (red) and infants without (blue) before 28 days post-delivery (< d28) and at or after (> d28).

(G) Differences in overall fermentation measured as nM per Carbon (nM_C) between infants with (red) and without severe BI (blue) before 28 days post-delivery (< d28) and at after (> d28). Squares show group median, error bars show standard deviation. Smoothed lines result from LOESS and indicate trends of microbiome development. Asterisks represent p values: *p < 0.05, **p < 0.01, ***p < 0.001.

have implications for brain damage, we evaluated the association of SCFAs with severe brain injury. Therefore, we calculated a mean value per patient within pools of samples before and after 28 days post-delivery (Figures 4F and 4G). We found that at early time points patients with brain damage had significantly elevated levels of butyrate and slightly elevated levels of propionate (Wilcoxon; p = 0.005 and 0.068, respectively), but that there was no significant difference at later time points, suggesting that an early transition to gut anoxia may be associated with brain injury.

Biomarkers of the gut-microbiota-immune-brain axis predict PWMI

In order to identify robust biomarkers of brain damage in our dataset, we employed an integrative analysis of microbiome, metabolome, clinical, immunological, and neurophysiological data (Singh et al., 2019). The strongest indicators for white matter injury were elevated *Klebsiella* levels, peripheral blood C-reactive protein (CRP), specific T cell populations (effector memory T cells TH:Tem $CD4^+/CD4^+$, $CCR6^+$ T cell receptor and γδ T cells), and

Please cite this article in press as: Seki et al., Aberrant gut-microbiota-immune-brain axis development in premature neonates with brain damage, Cell Host & Microbe (2021), https://doi.org/10.1016/j.chom.2021.08.004

Figure 5. The gut-microbiota-immune-brain axis of extremely premature infants and biomarkers of brain injury

(A) Data integration analysis for biomarker discovery using Latent variable approaches (Diablo). Integration of microbiome (yellow), metabolite (pink), T cell (gray), cytokine and chemokine secretion (orange), and neurophysiological/clinical (blue) data (n = 84). Lines within the circle represent positive correlations in green, and negative correlations in black (canonical correlation cut-off: +/− 0.65). Lines outside of the circle indicate the predictive potential of corresponding variables for age-adequate or mild (blue) or severe (red) BI.

(B) Correlation circle plot showing associations between variables as measured via canonical correlations. Neighboring of variables indicates correlations between variables.

increased T cell production of several cytokines and chemokines (IL-2, LAG-3, VEGF-A, IL1-beta, and IL-17a) (Figure 5A). Next, we evaluated correlations across different data types (Figure 5B). We observed an association of *Klebsiella* levels with γδ T cells, VEGF-A secretion, $CD4^+$ T effector memory cells, and CCR6+ T regulatory cells. Concomitantly, *Klebsiella* levels are inversely associated with the secretion of many other cytokines/chemokines including the neuroprotectants PDGF-BB and BDNF.

In summary, we have identified several features suggestive of an aberrant gut-microbiota-immune-brain axis development. Infants with severe brain injuries displayed a pro-inflammatory T cell polarization, which was marked by the expansion of γδ T cells in peripheral blood and driven by elevated IL-17a and VEGF-A secretion shortly post-delivery. Subsequently, the onset of neurophysiological maturation was delayed in these infants and was characterized by a suppression of electrocortical potential, an increased instability in cranial oxygen saturation, as well as a lack in secretion of neuroprotectants PDGF-BB and BDNF. *Klebsiella* overgrowth in the gut was key for driving the assembly of a distinctive and remarkably stable microbiome that associated with severe brain injury. Therefore, we conclude that *Klebsiella* spp. are involved in the dysregulation of the gut microbiota-immune-brain axis and may exacerbate PWMI.

DISCUSSION

Our study addresses the development of the gut-microbiota-immune-brain axis in extremely premature infants. We observed a characteristic trajectory of extra-uterine brain maturation that can be divided into three major phases: a neurodevelopmental quiescent phase, neurophysiological maturation phase, and a term-equivalent state. Using systems-biology approaches, we identified *Klebsiella* overgrowth in the gut as highly predictive for brain damage (Figure 5). Microbiome cluster analysis revealed that *Klebsiella*-dominated gut communities were remarkably stable and observed exclusively in infants with pathologies (Figure 3). This potentially pathological community state is associated with pro-inflammatory and T cell migratory cues during the quiescent phase and an impaired production of neuroprotective agents accompanied by an expansion of γδ T cells during the neurophysiological maturation phase (Figure 2).

1 week post-delivery, we observed elevated levels of $CCR6^+$ T regulatory cells in all infants (Figure 2J) indicating an onset of migratory events in immunological development, which may be triggered in part by the increase in bacterial numbers in the GIT (Figure 3A). Infants with brain injuries had higher levels of $CCR6^+$ T regulatory cells 3 days post-delivery (Figure 2J), as well as elevated peripheral blood levels of the migration stimulant VEGF-A 7 days post-delivery (Figure 2B). VEGF-A plays a key role in the pathogenesis of retinopathy of prematurity (ROP) by promoting abnormal branching of blood vessels emanating from the retina (Kandasamy et al., 2017). Interestingly, all infants with brain injuries were also diagnosed with ROP (Table 1). Infants with ROP but without severe brain damage displayed similar levels of VEGF-A in peripheral blood. However, infants unaffected by ROP or brain injury showed significant reduction of VEGF-A levels 7 days post-delivery as compared with infants with severe brain injury (Wilcoxon; $p = 0.0091$) and infants with ROP but without severe brain damage (Wilcoxon; $p = 0.032$). This suggests that increased VEGF-A

secretion early post-delivery associated with both ROP and brain injury and that notably severe brain injury includes ROP, but not vice versa.

Furthermore, we observed an increase of γδ T cells in peripheral blood in infants with severe brain injuries at 7 and 28 days post-delivery (Figures 2F and 2G). γδ T cells are important early-life immune cells as they can respond to innate-derived cytokines (Ferreira, 2013; Xu et al., 2020), and gut-resident γδ T cells have been shown to sense microbial colonization and support immunological tolerance and barrier function (Nielsen et al., 2017). During pro-inflammatory conditions, γδ T cells partially disappear from GIT tissue and abandon their intraepithelial support function (Weitkamp et al., 2014). IL-17a is an important signal for γδ T cells to migrate to the CNS, where they aggravate brain injuries (Benakis et al., 2016; Albertsson et al., 2018). Interestingly, in our cohort we observed that infants suffering from brain injury displayed elevated IL-17a levels in peripheral blood shortly after birth (Figure 2E). These data suggest that γδ T cell proliferation and migration is at least partially driven by IL-17a and is involved in the pathogenesis of perinatal brain damage.

The gut microbiota and its metabolic products have significant immunomodulatory potential, including for example being able to drive the increase of IL-17a-producing γδ T cells (Duan et al., 2010). We observed that infants with brain injuries had elevated levels of fecal butyrate, a major microbially produced metabolite, in the first month of life (Figure 4F). Importantly, differences in fecal butyrate or other SCFA levels must not solely arise from altered microbial production but may also result from altered absorption and colonocyte utilization (Litvak et al., 2018). Although butyrate can act positively on IL-10 expression and epithelial barrier function (Zheng et al., 2017), it has also been shown to aggravate GIT barrier dysfunction in patients with active inflammation (Vancamelbeke et al., 2019). As premature infants may have compromised epithelial barrier functions (Hill et al., 2017), these could potentially underlie the elevated fecal butyrate levels in early life, which may antagonize healthy mucosal development.

In premature infants, prescription of broad-spectrum antibiotics (Zwittink et al., 2017) and mode of delivery (Aguilar-Lopez et al., 2021) have been reported to affect gut-microbiota development. Cesarean (C)-sections are generally considered to be the safer delivery method for extremely premature infants, given the increased risk for respiratory distress during spontaneous delivery which can lead to brain injuries (Humberg et al., 2017). This agrees with our observation of heightened incidence for severe brain injury in spontaneously delivered premature infants (Table 1). However, C-sections have been shown to promote the growth of facultative anaerobes such as *Enterobacteriaceae* (Shao et al., 2019), which in our cohort were predominantly represented by the genera *Escherichia-Shigella* and *Klebsiella*. Interestingly, we observed elevated numbers of both genera in infants delivered via C-section shortly post-delivery (Figure 3B), but no association of delivery mode, or duration of antibiotic treatment with the establishment of cluster-C-like microbiota, suggesting that other mechanisms underlie the development of the given pathological community state. *Enterobacteriaceae* perform mixed-acid fermentation under anaerobic GIT conditions but also thrive by aerobic metabolism when oxygen is available. We observed that infants with severe brain injuries had higher bacterial loads in general, as well as higher numbers of *Klebsiella* 6 weeks post-delivery (Figures 3A and 3B). *Klebsiella*–related 16S rRNA gene amplicon sequences, as well as genomic evidence of *Klebsiella* isolates, indicated that *Klebsiella pneumoniae* was the dominant species of this genus (Table S2). It has recently been demonstrated that *Klebsiella* is capable of exploiting pioneer communities in the premature infant gut and establishes during later periods of microbial succession (Rao et al., 2021), though the mechanisms underlying this remain unknown. *Klebsiella* has previously been associated with sepsis, necrotizing enterocolitis (NEC), and nosocomial infections in neonates (Starzyk-Łuszcz et al., 2017; Wisgrill et al., 2019). Multidrug-resistant and hyper-virulent *Klebsiella* has emerged globally and is now a major cause of severe infections, particularly in immuno-compromised patients (Lee et al., 2017). Virulent *Klebsiella* strains can possess pathogenicity factors such as adhesins (Di Martino et al., 1995), type 1 and type 3 pili (Di Martino et al., 2003), siderophores (Holden et al., 2016), a thick capsule, and altered lipopolysaccharides to evade host recognition (Evrard et al., 2010). In addition to potentially producing pro-inflammatory cell components, *K. pneumoniae* overgrowth may also be responsible for early gut luminal oxygen depletion as well as elevated early-life butyrate levels, either directly via dark fermentation (García-Depraect et al., 2021) or indirectly by facilitating the colonization of obligate anaerobes such as *Clostridia* (Figure 3B). By doing so, *Klebsiella* may drive the pro-inflammatory polarization of immune cells and be responsible for the subsequent migration of γδ T cells. It remains unclear, however, whether *Klebsiella* employs specific modifications that allow host evasion to reach overgrowth, or if certain nutritional sources, e.g., host-derived nitrate, become available under pro-inflammatory conditions (Winter et al., 2013), leading to a subsequent bloom that overwhelms gastrointestinal clearance by mechanisms such as breast-milk-derived immunoglobulins (Gopalakrishna et al., 2019). Future studies should elucidate the mechanisms by which *Klebsiella* evades clearance from the gut, as well as to reveal the diversity of *Klebsiella* strains in the premature neonate gut via methods such as shotgun metagenomics.

Furthermore, probiotics are widely discussed as a potentially protective therapy against enteric pathogens. Indeed, prescription of probiotics seems to lower the risk for sepsis and NEC but fails to completely eradicate their occurrence (van Best et al., 2020). Similarly, we find that the daily probiotic administration in our cohort did not completely protect from PWMI. More research concerning the host recognition of probiotic strains during early life, as well as interaction of these with other microbiota in the GIT, is urgently needed for the development of preemptive measures other than broad-spectrum antibiotics.

We conclude that aberrant development of the gut-microbiota-immune-brain axis may play a role in brain injury in extremely premature neonates. Specifically, our data suggest that *Klebsiella* overgrowth as well as associated alterations in the microbiome may exacerbate brain injury, perhaps by triggering changes in immunological development such as elevated γδ T cell levels. These immunological alterations, combined with the subsequent depletion of neuroprotective agents, may affect neurophysiological development and neurodevelopmental

maturation. These findings suggest that novel therapeutic measures targeting the gut-microbiota-immune-brain axis may hold potential for protecting premature infants from PWMI.

STAR★METHODS

Detailed methods are provided in the online version of this paper and include the following:

- KEY RESOURCES TABLE
- RESOURCE AVAILABILITY
  - Lead contact
  - Materials availability
  - Data and code availability
- EXPERIMENTAL MODEL, CLINICAL DEFINITIONS AND SUBJECT DETAILS
- METHOD DETAILS
  - Stool and blood sample collection
  - Assessment of neurophysiological development
  - Analysis of cytokine secretion
  - Enumeration and phenotyping of peripheral T cells
  - 16S rRNA gene amplicon sequencing and qPCR
  - Detection of short chain fatty acids in stool samples
  - *Klebsiella pneumoniae* isolation and genome sequencing
- QUANTIFICATION AND STATISTICAL ANALYSIS
  - Processing and analysis of neurological data
  - Processing and analysis of immunological data
  - 16S rRNA gene amplicon sequence analysis
  - Quantification of bacterial load, 16S rRNA gene copy number correction, and analysis
  - Basic statistical analysis and data integration
  - Data visualization
  - Additional resources

SUPPLEMENTAL INFORMATION

Supplemental information can be found online at https://doi.org/10.1016/j.chom.2021.08.004.

ACKNOWLEDGMENTS

We thank all families for their participation and all medical staff for their help with sample collection. We thank Clemens Schauberger from the University of South Denmark, Department of Biology, for his computational help and advice. This project was funded by an inter-university cluster project grant between the University of Vienna and the Medical University of Vienna ("PreMiBraIn"), the European Research Council (Starting grant: FunKeyGut 741623), and the Austrian Science Fund (FWF; P27831-B28).

AUTHOR CONTRIBUTIONS

Conceptualization, L.W., D.B., and D.S.; methodology, D.S., M.M., B.W., B.H., P.P., V.G., K.G., K.K.-S., K.D.P., and G.K.; software, D.S., B.H., L.U., and V.G.; investigation, D.S.; writing – original draft, D.S. and D.B.; writing – review & editing, D.S., D.B., L.W., and K.D.P.; resources, P.P., A.B., B.W., D.B., T.V.D.W., and A.S.; supervision, D.B.; and funding acquisition, D.B., L.W., and A.B.

DECLARATION OF INTERESTS

The authors declare no competing interests.

Received: May 3, 2021
Revised: June 30, 2021
Accepted: August 9, 2021
Published: September 3, 2021

REFERENCES

Adams-Chapman, I., Heyne, R.J., DeMauro, S.B., Duncan, A.F., Hintz, S.R., Pappas, A., Vohr, B.R., McDonald, S.A., Das, A., Newman, J.E., et al. (2018). Neurodevelopmental impairment Among extremely preterm infants in the neonatal research network. Pediatrics *141*, e20173091. https://doi.org/10.1542/peds.2017-3091.

Aguilar-Lopez, M., Dinsmoor, A.M., Ho, T.T.B., and Donovan, S.M. (2021). A systematic review of the factors influencing microbial colonization of the preterm infant gut. Gut Microbes *13*, 1–33. https://doi.org/10.1080/19490976.2021.1884514.

Albertsson, A.M., Zhang, X., Vontell, R., Bi, D., Bronson, R.T., Supramaniam, V., Baburamani, A.A., Hua, S., Nazmi, A., Cardell, S., et al. (2018). γδ T cells contribute to injury in the developing brain. Am. J. Pathol. *188*, 757–767. https://doi.org/10.1016/j.ajpath.2017.11.012.

Alcon-Giner, C., Dalby, M.J., Caim, S., Ketskemety, J., Shaw, A., Sim, K., Lawson, M.A.E., Kiu, R., Leclaire, C., Chalklen, L., et al. (2020). Microbiota supplementation with Bifidobacterium and Lactobacillus modifies the preterm infant gut microbiota and metabolome: an observational study. Cell Rep. Med. *1*, 100077. https://doi.org/10.1016/j.xcrm.2020.100077.

Antonov, N.K., Ruzal-Shapiro, C.B., Morel, K.D., Millar, W.S., Kashyap, S., Lauren, C.T., and Garzon, M.C. (2017). Feed and wrap MRI technique in infants. Clin. Pediatr. *56*, 1095–1103. https://doi.org/10.1177/0009922816677806.

Apprill, A., McNally, S., Parsons, R., and Weber, L. (2015). Minor revision to V4 region SSU rRNA 806R gene primer greatly increases detection of SAR11 bacterioplankton. Aquat. Microb. Ecol. *75*, 129–137. https://doi.org/10.3354/ame01753.

Holden, V.I., Breen, P., Houle, S., Dozois, C.M., and Bachman, M.A. (2016). Klebsiella pneumoniae Siderophores induce inflammation, bacterial dissemination, and HIF-1α stabilization during pneumonia. mBio *7*, e01397–16.

Bankevich, A., Nurk, S., Antipov, D., Gurevich, A.A., Dvorkin, M., Kulikov, A.S., Lesin, V.M., Nikolenko, S.I., Pham, S., Prjibelski, A.D., et al. (2012). SPAdes: a new genome assembly algorithm and its applications to single-cell sequencing. J. Comput. Biol. *19*, 455–477. https://doi.org/10.1089/cmb.2012.0021.

Benakis, C., Brea, D., Caballero, S., Faraco, G., Moore, J., Murphy, M., Sita, G., Racchumi, G., Ling, L., Pamer, E.G., et al. (2016). Commensal microbiota affects ischemic stroke outcome by regulating intestinal γδ T cells. Nat. Med. *22*, 516–523. https://doi.org/10.1038/nm.4068.

Bonaz, B., Bazin, T., and Pellissier, S. (2018). The vagus nerve at the interface of the microbiota-gut-brain axis. Front. Neurosci. *12*, 49. https://doi.org/10.3389/fnins.2018.00049.

Burdjalov, V.F., Baumgart, S., and Spitzer, A.R. (2003). Cerebral function monitoring: a new scoring system for the evaluation of brain maturation in neonates. Pediatrics *112*, 855–861. https://doi.org/10.1542/peds.112.4.855.

Callahan, B.J., Sankaran, K., Fukuyama, J.A., McMurdie, P.J., and Holmes, S.P. (2016). Bioconductor workflow for microbiome data analysis: from raw reads to community analyses. F1000Res *5*, 1492. https://doi.org/10.12688/f1000research.8986.2.

Cryan, J.F., O'Riordan, K.J., Cowan, C.S.M., Sandhu, K.V., Bastiaanssen, T.F.S., Boehme, M., Codagnone, M.G., Cussotto, S., Fulling, C., Golubeva, A.V., et al. (2019). The microbiota-gut-brain axis. Physiol. Rev. *99*, 1877–2013. https://doi.org/10.1152/physrev.00018.2018.

Dalile, B., Van Oudenhove, L., Vervliet, B., and Verbeke, K. (2019). The role of short-chain fatty acids in microbiota–gut–brain communication. Nat. Rev. Gastroenterol. Hepatol. *16*, 461–478. https://doi.org/10.1038/s41575-019-0157-3.

Davis, N.M., Proctor, D.M., Holmes, S.P., Relman, D.A., and Callahan, B.J. (2018). Simple statistical identification and removal of contaminant sequences

in marker-gene and metagenomics data. Microbiome *6*, 226. https://doi.org/10.1186/s40168-018-0605-2.

de Vries, L.S., Eken, P., and Dubowitz, L.M.S. (1992). The spectrum of leukomalacia using cranial ultrasound. Behav. Brain Res. *49*, 1–6. https://doi.org/10.1016/S0166-4328(05)80189-5.

Di Martino, P., Bertin, Y., Girardeau, J.P., Livrelli, V., Joly, B., and Darfeuille-Michaud, A. (1995). Molecular characterization and adhesive properties of CF29K, an adhesin of Klebsiella pneumoniae strains involved in nosocomial infections. Infect. Immun. *63*, 4336–4344. https://doi.org/10.1128/iai.63.11.4336-4344.1995.

Di Martino, P., Cafferini, N., Joly, B., and Darfeuille-Michaud, A. (2003). Klebsiella pneumoniae type 3 pili facilitate adherence and biofilm formation on abiotic surfaces. Res. Microbiol. *154*, 9–16. https://doi.org/10.1016/S0923-2508(02)00004-9.

Duan, J., Chung, H., Troy, E., and Kasper, D.L. (2010). Microbial colonization drives expansion of IL-1 receptor 1-expressing and IL-17-producing gamma/delta T cells. Cell Host Microbe *7*, 140–150. https://doi.org/10.1016/j.chom.2010.01.005.

Edgar, R.C. (2010). Search and clustering orders of magnitude faster than BLAST. Bioinformatics *26*, 2460–2461. https://doi.org/10.1093/bioinformatics/btq461.

Epskamp, S., Cramer, A.O.J., Waldorp, L.J., Schmittmann, V.D., and Borsboom, D. (2012). Qgraph: network visualizations of relationships in psychometric data. J. Stat. Soft. *48*. https://doi.org/10.18637/jss.v048.i04.

Evrard, B., Balestrino, D., Dosgilbert, A., Bouya-Gachancard, J.L., Charbonnel, N., Forestier, C., and Tridon, A. (2010). Roles of capsule and lipopolysaccharide O antigen in interactions of human monocyte-derived dendritic cells and Klebsiella pneumoniae. Infect. Immun. *78*, 210–219. https://doi.org/10.1128/IAI.00864-09.

Fasy, B.T., Kim, J., Lecci, F., and Maria, C. (2015). Introduction to the R package TDA. https://hal.inria.fr/hal-01113028/document.

Ferreira, L.M.R. (2013). Gammadelta T cells: innately adaptive immune cells? Int. Rev. Immunol. *32*, 223–248. https://doi.org/10.3109/08830185.2013.783831.

BD. (2019). FlowJo™. software version 6.1. https://flowjo.com/.

García-Depraect, O., Muñoz, R., Rodríguez, E., Rene, E.R., and León-Becerril, E. (2021). Microbial ecology of a lactate-driven dark fermentation process producing hydrogen under carbohydrate-limiting conditions. Int. J. Hydr. Energy *46*, 11284–11296. https://doi.org/10.1016/j.ijhydene.2020.08.209.

Gastmeier, P., Geffers, C., Schwab, F., Fitzner, J., Obladen, M., and Rüden, H. (2004). Development of a surveillance system for nosocomial infections: the component for neonatal intensive care units in Germany. J. Hosp. Infect. *57*, 126–131. https://doi.org/10.1016/j.jhin.2003.12.038.

Gopalakrishna, K.P., Macadangdang, B.R., Rogers, M.B., Tometich, J.T., Firek, B.A., Baker, R., Ji, J., Burr, A.H.P., Ma, C., Good, M., et al. (2019). Maternal IgA protects against the development of necrotizing enterocolitis in preterm infants. Nat. Med. *25*, 1110–1115. https://doi.org/10.1038/s41591-019-0480-9.

Hellstro m-Westas, L., Rosen, I., de Vries, L.S., and Greisen, G. (2006). Amplitude-integrated EEG classification and interpretation in preterm and term infants. NeoReviews *7*, e76–e87. https://doi.org/10.1542/neo.7-2-e76.

Herbold, C.W., Pelikan, C., Kuzyk, O., Hausmann, B., Angel, R., Berry, D., and Loy, A. (2015). A flexible and economical barcoding approach for highly multiplexed amplicon sequencing of diverse target genes. Front. Microbiol. *6*, 731. https://doi.org/10.3389/fmicb.2015.00731.

Higgins, R.D., Jobe, A.H., Koso-Thomas, M., Bancalari, E., Viscardi, R.M., Hartert, T.V., Ryan, R.M., Kallapur, S.G., Steinhorn, R.H., Konduri, G.G., et al. (2018). Bronchopulmonary dysplasia: executive summary of a workshop. J. Pediatr. *197*, 300–308. https://doi.org/10.1016/j.jpeds.2018.01.043.

Hill, D.R., Huang, S., Nagy, M.S., Yadagiri, V.K., Fields, C., Mukherjee, D., Bons, B., Dedhia, P.H., Chin, A.M., Tsai, Y.-H., et al. (2017). Bacterial colonization stimulates a complex physiological response in the immature human intestinal epithelium. eLife *6*, e29132. https://doi.org/10.7554/eLife.29132.

Humberg, A., Härtel, C., Paul, P., Hanke, K., Bossung, V., Hartz, A., Fasel, L., Rausch, T.K., Rody, A., Herting, E., et al. (2017). Delivery mode and intraventricular hemorrhage risk in very-low-birth-weight infants: observational data of the German Neonatal Network. Eur. J. Obstet. Gynecol. Reprod. Biol. *212*, 144–149. https://doi.org/10.1016/j.ejogrb.2017.03.032.

International Committee for the Classification of Retinopathy of Prematurity (2005). The international classification of retinopathy of prematurity revisited. Arch. Ophthalmol. *123*, 991–999. https://doi.org/10.1001/archopht.123.7.991.

Justin Donaldson, M. (2016). Package "tsne" Title T-Distributed Stochastic Neighbor Embedding for R (t-SNE), pp. 2–5. https://cran.r-project.org/web/packages/tsne/tsne.pdf.

Kandasamy, Y., Hartley, L., Rudd, D., and Smith, R. (2017). The association between systemic vascular endothelial growth factor and retinopathy of prematurity in premature infants: a systematic review. Br. J. Ophthalmol. *101*, 21–24. https://doi.org/10.1136/bjophthalmol-2016-308828.

Keunen, K., van Elburg, R.M., van Bel, F., and Benders, M.J. (2015). Impact of nutrition on brain development and its neuroprotective implications following preterm birth. Pediatr. Res. *77*, 148–155. https://doi.org/10.1038/pr.2014.171.

Kidokoro, H., Niel, J.J., and Inder, T.E. (2013). New MR imaging assessment tool to define brain abnormalities in very preterm infants at term. AJNR Am. J. Neuroradiol. *34*, 2208–2214. https://doi.org/10.3174/ajnr.A3521.

Klebermass, K., Olischar, M., Waldhoer, T., Fuiko, R., Pollak, A., and Weninger, M. (2011). Amplitude-integrated EEG pattern predicts further outcome in preterm infants. Pediatr. Res. *70*, 102–108. https://doi.org/10.1203/PDR.0b013e31821ba200.

Lee, C.R., Lee, J.H., Park, K.S., Jeon, J.H., Kim, Y.B., Cha, C.J., Jeong, B.C., and Lee, S.H. (2017). Antimicrobial resistance of hypervirulent Klebsiella pneumoniae: epidemiology, hypervirulence-associated determinants, and resistance mechanisms. Front. Cell. Infect. Microbiol. *7*, 483. https://doi.org/10.3389/fcimb.2017.00483.

Legendre, P., and Gallagher, E.D. (2001). Ecologically meaningful transformations for ordination of species data. Oecologia *129*, 271–280. https://doi.org/10.1007/s004420100716.

Litvak, Y., Byndloss, M.X., and Bäumler, A.J. (2018). Colonocyte metabolism shapes the gut microbiota. Science *362*. https://doi.org/10.1126/science.aat9076.

Matthews, L.G., Walsh, B.H., Knutsen, C., Neil, J.J., Smyser, C.D., Rogers, C.E., and Inder, T.E. (2018). Brain growth in the NICU: critical periods of tissue-specific expansion. Pediatr. Res. *83*, 976–981. https://doi.org/10.1038/pr.2018.4.

Mazmanian, S.K., Round, J.L., and Kasper, D.L. (2008). A microbial symbiosis factor prevents intestinal inflammatory disease. Nature *453*, 620–625. https://doi.org/10.1038/nature07008.

Movafagh, A., Heydary, H., Mortazavi-Tabatabaei, S.A., and Azargashb, E. (2011). The significance application of indigenous phytohemagglutinin (PHA) mitogen on metaphase and cell culture procedure. Iran. J. Pharm. Res. *10*, 895–903.

Ng, S.K., and Hamilton, I.R. (1971). Lactate metabolism by Veillonella parvula. J. Bacteriol. *105*, 999–1005. https://doi.org/10.1128/jb.105.3.999-1005.1971.

Nielsen, M.M., Witherden, D.A., and Havran, W.L. (2017). γδ T cells in homeostasis and host defence of epithelial barrier tissues. Nat. Rev. Immunol. *17*, 733–745. https://doi.org/10.1038/nri.2017.101.

Niño, D.F., Zhou, Q., Yamaguchi, Y., Martin, L.Y., Wang, S., Fulton, W.B., Jia, H., Lu, P., Prindle, T., Zhang, F., et al. (2018). Cognitive impairments induced by necrotizing enterocolitis can be prevented by inhibiting microglial activation in mouse brain. Sci. Transl. Med. *10*. https://doi.org/10.1126/scitranslmed.aan0237.

Oksanen, J., Blanchet, F.G., Kindt, R., Legendre, P., Minchin, P.R., O'hara, R.B., Simpson, G.L., Solymos, P., Stevens, M.H.H., Wagner, H., and Oksanen, M.J. (2013). Package 'vegan'. *Community ecology package*. version *2*, 1–295.

Papile, L.A., Burstein, J., Burstein, R., and Koffler, H. (1978). Incidence and evolution of subependymal and intraventricular hemorrhage: a study of infants

with birth weights less than 1,500 gm. J. Pediatr. *92*, 529–534. https://doi.org/10.1016/S0022-3476(78)80282-0.

Parada Venegas, D.P., De la Fuente, M.K., Landskron, G., González, M.J., Quera, R., Dijkstra, G., Harmsen, H.J.M., Faber, K.N., and Hermoso, M.A. (2019). Short chain fatty acids (SCFAs)-mediated gut epithelial and immune regulation and its relevance for inflammatory bowel diseases. Front. Immunol. *10*, 277. https://doi.org/10.3389/fimmu.2019.00277.

Parada, A.E., Needham, D.M., and Fuhrman, J.A. (2016). Every base matters: assessing small subunit rRNA primers for marine microbiomes with mock communities, time series and global field samples. Environ. Microbiol. *18*, 1403–1414. https://doi.org/10.1111/1462-2920.13023.

Parks, D.H., Imelfort, M., Skennerton, C.T., Hugenholtz, P., and Tyson, G.W. (2015). CheckM: assessing the quality of microbial genomes recovered from isolates, single cells, and metagenomes. Genome Res. *25*, 1043–1055. https://doi.org/10.1101/gr.186072.114.

Pérez-Brocal, V., Magne, F., Ruiz-Ruiz, S., Ponce, C.A., Bustamante, R., San Martin, V., Gutierrez, M., Gatti, G., Vargas, S.L., and Moya, A. (2020). Optimized DNA extraction and purification method for characterization of bacterial and fungal communities in lung tissue samples. Scientific Rep *10* (1), 1–15. https://doi.org/10.1038/s41598-020-74137-2.

Pjevac, P., Hausmann, B., Schwarz, J., Kohl, G., Herbold, C.W., Loy, A., and Berry, D. (2021). An economical and flexible dual barcoding, two-step PCR approach for highly multiplexed amplicon sequencing. Front Microbiol *12*, 669776. https://doi.org/10.3389/fmicb.2021.669776.

Pruesse, E., Peplies, J., and Glöckner, F.O. (2012). SINA: accurate high-throughput multiple sequence alignment of ribosomal RNA genes. Bioinformatics *28*, 1823–1829. https://doi.org/10.1093/bioinformatics/bts252.

Quast, C., Pruesse, E., Yilmaz, P., Gerken, J., Schweer, T., Yarza, P., Peplies, J., and Glöckner, F.O. (2013). The SILVA ribosomal RNA gene database project: improved data processing and web-based tools. Nucleic Acids Res. *41*, D590–D596. https://doi.org/10.1093/nar/gks1219.

R Core Team (2017). R: A language and environment for statistical computing. (R Foundation for Statistical Computing). https://www.R-project.org/.

Rao, C., Coyte, K.Z., Bainter, W., Geha, R.S., Martin, C.R., and Rakoff-Nahoum, S. (2021). Multi-kingdom ecological drivers of microbiota assembly in preterm infants. Nature *591*, 633–638. https://doi.org/10.1038/s41586-021-03241-8.

Rooks, M.G., and Garrett, W.S. (2016). Gut microbiota, metabolites and host immunity. Nat. Rev. Immunol. *16*, 341–352. https://doi.org/10.1038/nri.2016.42.

Sachs, M.C. (2017). Plotroc: A tool for plotting ROC curves. J. Stat. Softw. *79*. https://doi.org/10.18637/jss.v079.c02.

Sekirov, I., Russell, S.L., Antunes, L.C., and Finlay, B.B. (2010). Gut microbiota in health and disease. Physiol. Rev. *90*, 859–904. https://doi.org/10.1152/physrev.00045.2009.

Shannon, P., Markiel, A., Ozier, O., Baliga, N.S., Wang, J.T., Ramage, D., Amin, N., Schwikowski, B., and Ideker, T. (2003). Cytoscape: a software environment for integrated models of biomolecular interaction networks. Genome Res. *13*, 2498–2504. https://doi.org/10.1101/gr.1239303.

Shao, Y., Forster, S.C., Tsaliki, E., Vervier, K., Strang, A., Simpson, N., Kumar, N., Stares, M.D., Rodger, A., Brocklehurst, P., et al. (2019). Stunted microbiota and opportunistic pathogen colonization in caesarean-section birth. Nature *574*, 117–121. https://doi.org/10.1038/s41586-019-1560-1.

Singer, J.R., Blosser, E.G., Zindl, C.L., Silberger, D.J., Conlan, S., Laufer, V.A., DiToro, D., Deming, C., Kumar, R., Morrow, C.D., et al. (2019). Preventing dysbiosis of the neonatal mouse intestinal microbiome protects against late-onset sepsis. Nat. Med. *25*, 1772–1782. https://doi.org/10.1038/s41591-019-0640-y.

Singh, A., Shannon, C.P., Gautier, B., Rohart, F., Vacher, M., Tebbutt, S.J., and Lê Cao, K.A. (2019). Diablo: an integrative approach for identifying key molecular drivers from multi-omics assays. Bioinformatics *35*, 3055–3062. https://doi.org/10.1093/bioinformatics/bty1054.

Starzyk-Łuszcz, K., Zielonka, T.M., Jakubik, J., and Życińska, K. (2017). Mortality due to nosocomial infection with Klebsiella pneumoniae ESBL<sup/>. Adv. Exp. Med. Biol. *1022*, 19–26. https://doi.org/10.1007/5584_2017_38.

Stoddard, S.F., Smith, B.J., Hein, R., Roller, B.R., and Schmidt, T.M. (2015). rrnDB: improved tools for interpreting rRNA gene abundance in bacteria and archaea and a new foundation for future development. Nucleic Acids Res. *43*, D593–D598. https://doi.org/10.1093/nar/gku1201.

Stoecklein, S., Hilgendorff, A., Li, M., Förster, K., Flemmer, A.W., Galiè, F., Wunderlich, S., Wang, D., Stein, S., Ehrhardt, H., et al. (2020). Variable functional connectivity architecture of the preterm human brain: impact of developmental cortical expansion and maturation. Proc. Natl. Acad. Sci. USA *117*, 1201–1206. https://doi.org/10.1073/pnas.1907892117.

Tenenhaus, A., and Tenenhaus, M. (2011). Regularized generalized canonical correlation analysis. Psychometrika *76*, 257–284. https://doi.org/10.1007/s11336-011-9206-8.

Tettamanti Boshier, F.A., Srinivasan, S., Lopez, A., Hoffman, N.G., Proll, S., Fredricks, D.N., and Schiffer, J.T. (2020). Complementing 16S rRNA gene amplicon sequencing with total bacterial load to infer absolute species concentrations in the vaginal microbiome. mSystems *5*. e00777–19. https://doi.org/10.1128/mSystems.00777-19.

Tommiska, V., Heinonen, K., Lehtonen, L., Renlund, M., Saarela, T., Tammela, O., Virtanen, M., and Fellman, V. (2007). No improvement in outcome of nationwide extremely low birth weight infant populations between 1996–1997 and 1999–2000. Pediatrics *119*, 29–36. https://doi.org/10.1542/peds.2006-1472.

van Best, N., Trepels-Kottek, S., Savelkoul, P., Orlikowsky, T., Hornef, M.W., and Penders, J. (2020). Influence of probiotic supplementation on the developing microbiota in human preterm neonates. Gut Microbes *12*, 1–16. https://doi.org/10.1080/19490976.2020.1826747.

Vancamelbeke, M., Laeremans, T., Vanhove, W., Arnauts, K., Ramalho, A.S., Farré, R., Cleynen, I., Ferrante, M., and Vermeire, S. (2019). Butyrate does not protect against inflammation-induced loss of epithelial barrier function and cytokine production in primary cell monolayers from patients with ulcerative colitis. J. Crohns Colitis *13*, 1351–1361. https://doi.org/10.1093/ecco-jcc/jjz064.

Volpe, J.J. (2009). Brain injury in premature infants: a complex amalgam of destructive and developmental disturbances. Lancet Neurol. *8*, 110–124. https://doi.org/10.1016/S1474-4422(08)70294-1.

Warner, B.B. (2019). The contribution of the gut microbiome to neurodevelopment and neuropsychiatric disorders. Pediatr. Res. *85*, 216–224. https://doi.org/10.1038/s41390-018-0191-9.

Wei, T., and Simko, V. (2021). R package 'corrplot': visualization of a correlation matrix, (0.90 Version). https://github.com/taiyun/corrplot.

Weitkamp, J.H., Rosen, M.J., Zhao, Z., Koyama, T., Geem, D., Denning, T.L., Rock, M.T., Moore, D.J., Halpern, M.D., Matta, P., et al. (2014). Small intestinal intraepithelial TCRγδ+ T lymphocytes are present in the premature intestine but selectively reduced in surgical necrotizing enterocolitis. PLoS One *9*, e99042. https://doi.org/10.1371/journal.pone.0099042.

Wells, C.J. (1928). Preparation of the patient. Anesthesia & Analgesia *7*, 257–262. https://doi.org/10.1213/00000539-192801000-00096.

White, D. (2000). Physiology and Biochemistry of Prokaryotes (Oxford University Press).

Wickham, H. (2011). Ggplot2. WIREs. Comp. Stat. *3*, 180–185. https://doi.org/10.1002/wics.147.

Winter, S.E., Winter, M.G., Xavier, M.N., Thiennimitr, P., Poon, V., Keestra, A.M., Laughlin, R.C., Gomez, G., Wu, J., Lawhon, S.D., et al. (2013). Host-derived nitrate boosts growth of E. coli in the inflamed gut. Science *339*, 708–711. https://doi.org/10.1126/science.1232467.

Wisgrill, L., Lepuschitz, S., Blaschitz, M., Rittenschober-Böhm, J., Diab-El Schahawi, M., Schubert, S., Indra, A., and Berger, A. (2019). Outbreak of yersiniabactin-producing *Klebsiella pneumoniae* in a neonatal intensive care unit. Pediatr. Infect. Dis. J. *38*, 638–642. https://doi.org/10.1097/INF.0000000000002258.

Wistuba-Hamprecht, K., Pawelec, G., and Derhovanessian, E. (2014). OMIP-020: phenotypic characterization of human γδ T-cells by multicolor flow cytometry. Cytometry A *85*, 522–524. https://doi.org/10.1002/cyto.a.22470.

Woodward, L.J., Anderson, P.J., Austin, N.C., Howard, K., and Inder, T.E. (2006). Neonatal MRI to predict neurodevelopmental outcomes in preterm infants. N. Engl. J. Med. *355*, 685–694. 1018. https://doi.org/10.1056/NEJMoa053792.

Xu, W., Lau, Z.W.X., Fulop, T., and Larbi, A. (2020). The aging of γδ T cells. Cells *9*, 1–18. https://doi.org/10.3390/cells9051181.

Yamazaki, T., Yang, X.O., Chung, Y., Fukunaga, A., Nurieva, R., Pappu, B., Martin-Orozco, N., Kang, H.S., Ma, L., Panopoulos, A.D., et al. (2008). CCR6 regulates the migration of inflammatory and regulatory T cells. J. Immunol. *181*, 8391–8401. https://doi.org/10.4049/jimmunol.181.12.8391.

Zheng, L., Kelly, C.J., Battista, K.D., Schaefer, R., Lanis, J.M., Alexeev, E.E., Wang, R.X., Onyiah, J.C., Kominsky, D.J., and Colgan, S.P. (2017). Microbial-derived butyrate promotes epithelial barrier function through IL-10 receptor–dependent repression of Claudin-2. J. Immunol. *199*, 2976–2984. https://doi.org/10.4049/jimmunol.1700105.

Zwittink, R.D., van Zoeren-Grobben, D., Martin, R., van Lingen, R.A., Groot Jebbink, L.J., Boeren, S., Renes, I.B., van Elburg, R.M., Belzer, C., and Knol, J. (2017). Metaproteomics reveals functional differences in intestinal microbiota development of preterm infants. Mol. Cell. Proteomics *16*, 1610–1620. https://doi.org/10.1074/mcp.RA117.000102.

Please cite this article in press as: Seki et al., Aberrant gut-microbiota-immune-brain axis development in premature neonates with brain damage, Cell Host & Microbe (2021), https://doi.org/10.1016/j.chom.2021.08.004

STAR★METHODS

KEY RESOURCES TABLE

REAGENT or RESOURCE	SOURCE	IDENTIFIER
Antibodies		
CD3 (UCHT-1)	Thermo Fisher	Cat# 56-0038; RRID:AB_10597906
CD4 (RPA-T4)	Thermo Fisher	Cat# 69-0049; RRID:AB_2637466
CD8 (SK1)	Thermo Fisher	Cat# 47-0087; RRID:AB_2016684
CD27 (O323)	Thermo Fisher	Cat# 17-0279;RRID:AB_10671130
CD28 (CD28.6)	Thermo Fisher	Cat# 16-0288-81; RRID:AB_468924
CD45RA (HI100)	Thermo Fisher	Cat# 48-0458; RRID:AB_1272059
γδ-TCR (IMMU510)	Beckman Coulter	Cat# B10247
Vd1-TCR (TS8.2)	Thermo Fisher	Cat# TCR2730; RRID:AB_223624
Vd2-TCR (B6)	BioLegend	Cat# 331410; RRID:AB_1877263
CXCR3 (1C6)	BD Biosciences	Cat# 741005; RRID:AB_2740628
CCR4 (D8SEE)	Thermo Fisher	Cat# 12-1949; RRID:AB_2572591
CXCR5 (MU5UBEE)	Thermo Fisher	Cat# 25-9185; RRID:AB_2573540
CCR10 (1B8)	BD Biosciences	Cat# 564770; RRID:AB_2738942
CCR6 (R6H1)	Thermo Fisher	Cat# 17-1969; RRID:AB_10733388
CD25 (BC96)	Thermo Fisher	Cat# 12-0259-80; RRID:AB_657722
CCR7 (4B12)	Thermo Fisher	Cat# 47-1971; RRID:AB_2573974
CD39 (eBioA1)	BD Biosciences	Cat# 11-0399; RRID:AB_11151149
CD49d (9F10)	BD Biosciences	Cat# 744587; RRID:AB_2742336
Helios (22F6)	BD Biosciences	Cat# 563951; RRID:AB_2738506
CCR5 (3A9)	BD Biosciences	Cat# 741005; RRID:AB_396312
CTLA-4 (BNI3)	BD Biosciences	Cat# 562743; RRID:AB_2737762
Biological samples		
Peripheral blood samples from extremely premature infants	General Hospital of Vienna	N/A
Fecal samples from extremely premature infants	General Hospital of Vienna	N/A
Chemicals, peptides, and recombinant proteins		
Phenol/Chloroform/Isoamylalcohol	Sigma Aldrich	Cat# P3803
Brilliant III Ultra-Fast SYBR Green Master Mix	Agilent Technologies	Cat# 600882
Nuclease free water	Thermo Fisher	Cat# 10977015
Milli-Q water	Merck Millipore	Cat# C205110
AIM V	Thermo Fisher	Cat# 12055091
Phytohemagglutinin-L	Thermo Fisher	Cat# 00-4977-93
VersaLyse Red blood cell lysis solution	Beckman Coulter	Cat# A09777
Fixative Solution IOTest 3 10x concentrate	Beckman Coulter	Cat# A07800
1% Staining Buffer (PBS w/o Ca2+/Mg2+ + 1% FCS)	Thermo Fisher	Cat# 16140071
Critical commercial assays		
Procartaplex 23 Cytokines	Thermo Fisher	N/A
PerFix-nc kit	Beckman Coulter	Cat# 16140071
SequalPrep™ Normalization Plate Kit	Thermo Fisher	Cat# A1051001
Quant-iT PicoGreen dsDNA Assay	Thermo Fisher	Cat# P7589
Deposited data		
16S rRNA gene amplicon sequencing data	NCBI	PRJNA715072
Klebsiella pneumoniae genome	NCBI	PRJNA715072

(*Continued on next page*)

Please cite this article in press as: Seki et al., Aberrant gut-microbiota-immune-brain axis development in premature neonates with brain damage, Cell Host & Microbe (2021), https://doi.org/10.1016/j.chom.2021.08.004

CellPress
OPEN ACCESS

Continued

REAGENT or RESOURCE	SOURCE	IDENTIFIER
Oligonucleotides		
Forward primer rRNA sequencing and qPCR (515F): 5'-GTG YCA GCM GCC GCG GTA A-3'	(Parada et al., 2016)	N/A
Reverse primer rRNA sequencing and qPCR (806R): 5'-GGA CTA CNV GGG TWT CTA AT-3'	(Apprill et al., 2015)	N/A
Head sequence of forward primer for barcoding (H1): 5'-GCT ATG CGC GAG CTG C-3'	(Herbold et al., 2015)	N/A
Head sequence of reverse primer for barcoding (H2): 5'-TAG CGC ACA CCT GGT A-3'	(Pjevac et al., 2021)	N/A
Software and algorithms		
R 4.0	(R Core Team, 2017)	https://www.r-project.org/
FlowJo™ Software	(BD, 2019)	https://flowjo.com/
Cytoscape	(Shannon et al., 2003)	https://doi.org/10.1101/gr.1239303
FASTA/FASTQ demultiplexer	Laros JFJ	github.com/jfjlaros/demultiplex
DADA2	(Callahan et al., 2016)	https://doi.org/10.12688/F1000RESEARCH.8986.1
SILVA database	(Quast et al., 2013)	https://doi.org/10.1093/nar/gks1219
decontam	(Davis et al., 2018)	https://doi.org/10.1186/s40168-018-0605-2
usearch	(Edgar, 2010)	https://doi.org/10.1093/bioinformatics/btq461
CFX Manager Software	Bio-Rad Laboratories	#1845000
R package "Corrplot"	(Wei and Simko, 2021)	https://github.com/taiyun/corrplot
R package "qgraph"	(Epskamp et al., 2012)	https://doi.org/10.18637/jss.v048.i04
R package "TDA"	(Fasy et al., 2015)	https://doi.org/hal-01113028
R package "Vegan"	(Oksanen et al., 2013)	https://cran.r-project.org, https://github.com/vegandevs/vegan
R package "tSNE"	(Justin Donaldson, 2016)	https://cran.r-project.org/web/packages/tsne/tsne.pdf.
R package "ggplot2"	(Wickham, 2011)	https://doi.org/10.1002/wics.147
R package "plotROC"	(Sachs, 2017)	https://doi.org/10.18637/jss.v079.c02
R package "mixomics"	(Singh et al., 2019)	https://doi.org/10.1093/bioinformatics/bty1054

RESOURCE AVAILABILITY

Lead contact

Further information and requests for resources and reagents should be directed to and will be fulfilled by the Lead Contact David Berry (david.berry@univie.ac.at).

Materials availability

16S rRNA gene amplicon sequencing data and the *Klebsiella pneumoniae* genome were deposited under the BioProject accession number PRJNA715072.

Data and code availability

Any additional information required to reanalyze the data reported in this paper is available from the lead contact upon request.

EXPERIMENTAL MODEL, CLINICAL DEFINITIONS AND SUBJECT DETAILS

This study was approved by the ethics committee of the Medical University of Vienna (Ethics number 1348/2017). 60 extremely premature infants were enrolled between September 2017 and June 2019 at the Medical University of Vienna as part of the PreMiBraIn study. Inclusion criteria were birth before the 28th week of gestation with less than 1000 g birth weight. Infants with congenital malformations, chromosomal aberrations, maternally transmitted infectious diseases (e.g. HIV, hepatitis A/B/C, etc.) and inborn errors of metabolism were excluded. Clinical parameters of each patient were prospectively monitored by the clinical staff during hospitalization and recorded within the hospitals' electronic database ICIP (Philips Healthcare Systems). Intrauterine growth restriction was defined as birth weight under the 10th percentile. Culture-proven early-onset sepsis was defined as infection with elevated inflammatory parameters (C-reactive protein; CRP > 0.5 mg dl^{-1} or IL-6 > 150 pg ml^{-1}) and positive blood culture. Since the detection

rate of blood cultures directly after birth was very low in our cohort, we defined the term "clinical-suspected inflammation" for infants with elevated inflammatory markers after birth (CRP > 0.5 mg dl^{-1} or IL-6 > 150 pg ml^{-1}). Late-onset sepsis (LOS) was defined according to the NEO-KISS protocol for nosocomial infection surveillance for preterm infants (Gastmeier et al., 2004). Clinical LOS as well as LOS with coagulase negative *Staphylococcus* (CoNS) were defined as an episode with the following characteristics: > 72 hours post-delivery, empiric antibiotic therapy $\geq$ 5 days, no apparent infection at another body site, and additionally fulfilling any two of the following criteria: temperature > 38°C or < 36.5°C, temperature instability, tachycardia, bradycardia, apnoea, hypotension, hyperglycaemia, metabolic acidosis, prolonged recapillarization time or positive blood infection parameter (CRP > 2 mg dl^{-1} or IL-6 > 50 pg ml^{-1}). Culture-positive LOS was defined as a clinical infection as described above with the additional growth of a pathogen in the corresponding blood culture. Bronchopulmonary dysplasia (BPD) was defined as supplemental oxygen treatment or oxygen plus respiratory support at 36 weeks postmenstrual age (Higgins et al., 2018). Retinopathy of prematurity (ROP) was diagnosed and staged according to the international consensus guidelines (International Committee for the Classification of Retinopathy of Prematurity, 2005).

Furthermore, every infant received, starting from the first day of life, the probiotic preparation Infloran® (*Bifidobacterium bifidum* and *Lactobacillus acidophilus*) until the corrected age of 34 weeks of gestational age (GA). The enteral feeding regimen included the infant's own pasteurized mother's milk or pasteurized human donor milk. When 100 ml kg^{-1} enteral feeding was achieved, the milk was fortified with 4% bovine milk fortifier until term-equivalent age.

Over the course of hospitalization, neurophysiological development was monitored, stool samples were collected, and blood was drawn at intended time points as described in Figure 1A. In total we collected 547 stool samples, 162 blood samples, and obtained and assessed 335 amplitude integrated electroencephalography (aEEG) and 423 near-infrared spectroscopy (NIRS) spectra. Brain injuries were identified and assessed by combined assessment of magnetic resonance imaging (MRI) at term-equivalent age (Kidokoro et al., 2013) and routine ultrasound imaging (Papile et al., 1978; de Vries *et al.*, 1992).

METHOD DETAILS

Stool and blood sample collection

Stool samples from all 60 extremely premature infants were collected from diapers via collection tubes during patient care routines, without the addition of any type of preservation buffer, and stored at -80° until further analysis. Samples were kept on dry ice while aliquoting for the extraction of nucleic acids and analysis of SCFAs respectively. For the isolation of bacteria, additional stool was sampled randomly, and stored in 40% (v:v) glycerol at -80°C. Blood samples were drawn from premature infants at intended time points via arterial catheter or peripheral venous puncture. Sampling of blood was only conducted if combined with clinical routine sampling to minimize stressing the patients. 300 μL blood was sampled into Lithium Heparin S-Monovettes and stored at 4°C for a maximum of 4 hours before further analysis. For each sampling time point, except for "day 3" samples (Figure 1A), we allowed for a +/- 2-day time window for sample collection. "Day 3" samples were collected +1/-2-day time window for sample collection.

Assessment of neurophysiological development

Neurophysiological characteristics from premature infants were assessed at intended time points (Figure 1A). aEEG was used for monitoring of cerebral activity. A total of 5 gold cup electrodes were applied in combination with skin preparation and electrode contact gels. To ensure conduct, a tissue wetted with NaCl 0.9 % solution was placed upon the prepared electrode. The reference electrode was placed either frontal or dorsal of the infants' head, the remaining were placed on C3, P3, C4 and P4, according to the 10-20 system (Wells, 1928). Electrodes were fixed by either using a bandage wrapped around the infants' head, or by placing a CPAP hat above. Electrodes were connected to a CFM Olympic Brainz Monitor device (OBM, Natus) and the measurement lasted for at least 3 hours.

For assessment of cerebral oxygenation, NIRS (INVOS, Medtronic) was employed. A cerebral oximetry infant-neonatal sensor was placed on the left side of the forehead with detector placement towards a lateral position below the gold cup electrodes. The probe was connected to a cerebral oximeter and the measurement lasted in parallel to the aEEG measurement, for at least 3 hours. Cranial magnetic resonance imaging (cMRI) images was performed at term-equivalent age (between 36 and 40 weeks of GA), using a standard neonatal MR protocol (Antonov et al., 2017) at 1.5 Tesla.

Analysis of cytokine secretion

25 μL of peripheral whole blood was used for analysis of T cell-specific cytokine production from patients 1-40 after incubation of whole blood with 250 μL AIM V and 20μL phytohemagglutinin-L (PHA-L end concentration: 1.25 μg ml^{-1}) for 72 hours (Movafagh et al., 2011). All incubations were conducted in 96-well plates on 37°C. Afterwards, samples were centrifuged at 1,000 *g* for 5 minutes and the supernatants were collected and stored at -80°C for subsequent analysis. Cytokines within supernatants were assessed via customized ProcartaPlex immunoassays, following the protocol of each respective assay. Upon completion of each multiplex assay, the amounts of respective cytokines were analyzed via Luminex.

Enumeration and phenotyping of peripheral T cells

50 μL of peripheral whole blood was used for analysis of T helper, cytotoxic T cells, γδ T cells, and T regulatory cells respectively. This analysis was conducted with blood drawn from patients 1-40. The employed monoclonal antibodies are shown in the

key resources table. Cellular staining of γδ T, cytotoxic T cells and T helper cells was conducted as described elsewhere (Wistuba-Hamprecht *et al.*, 2014). Staining of T regulatory cells was conducted according to protocol, employing a PerFix-nc kit in combination with Brilliant Violet Staining Buffer for enhanced surface staining, and 100% fetal calf serum (FCS) as a buffer during fixation for subsequent intracellular staining. Stained cells were resuspended in 50 μL staining buffer (1x PBS without Ca^{2+}/Mg^{2+} + 1% FCS) and analyzed within 4 hours via fluorescence activated cell sorting (FACS).

16S rRNA gene amplicon sequencing and qPCR

547 stool samples of 60 preterm infants were weighed in (20–30 mg) for phenol-chloroform extraction of total nucleic acids (TNA) (Pérez-Brocal et al., 2020), with the inclusion of one bead-beating step, and an additional extraction of one negative control per extraction-batch, consisting of nuclease-free water to allow for the assessment of contamination. TNA were eluted in 40 μl nuclease free water and stored at -20°C until further analysis. Extracted TNA concentration was measured using Quant-iT PicoGreen dsDNA Assay (Thermo Fisher). Extracts served as templates for qPCR amplification of bacterial 16S rRNA genes, as well as for 16S rRNA gene amplicon sequencing.

For the enumeration of gene copy numbers, the primer pair 515F (Parada et al., 2016) and 806R (Apprill et al., 2015), modified with a linker sequence (Herbold et al., 2015), were used for qPCR amplification of 16S rRNA genes using a CFX96 Real-Time System. The concentration of each sample was adjusted to a concentration between 1-20 ng μl^{-1}. PCR assay mixtures consisted of 10 μl Brilliant III Ultra-Fast SYBR Green Master Mix already containing a SureStart Taq DNA polymerase, $MgCl_2$ at a concentration of 2.5 mM, two times 0.8 μl primer solution (400 nM), 7.4 μl sterile nuclease-free water, and 1 μl template DNA solution or adjusted 6.4 μl sterile nuclease-free water and 2 μl template DNA. The PCR amplification program encompassed an initial denaturation step at 95°C for 3 min followed by 40 two-step cycles at 95°C for 10 s and at 55°C for 30 s. In each run a no-template (without TNA) control was included. Genomic DNA of *Escherichia coli* DH5alpha was used as a standard (highest concentration 25 ng μl^{-1} following a four-times 1:10 dilution series).

16S rRNA gene amplification and amplicon sequencing was performed at the Joint Microbiome Facility of the Medical University of Vienna and the University of Vienna. The V4 region of the bacterial and archaeal 16S rRNA gene was amplified (30 cycles) from the DNA using the mentioned modified primer pair and barcoded (8 cycles) in a unique dual barcoding setup (UDB-H12). Thereafter, barcoded samples were purified and normalized over a SequalPrep™ Normalization Plate Kit using a Biomek® NXP Span-8 pipetting robot (Beckman Coulter), and pooled and concentrated on columns (Analytik Jena). Indexed sequencing libraries were prepared with the Illumina TruSeq Nano Kit as described previously (Herbold et al., 2015), and sequenced in paired-end mode (600 cycles; V3 chemistry) on an Illumina MiSeq following the manufacturer's instructions. The workflow systematically included four negative controls (PCR blanks, i.e., PCR-grade water as template) for each 90 samples sequenced. Also, a ZYMObiomics mock community was sequenced and analyzed at the sequencing facility as part of their established quality control routine (Pjevac et al., 2021)

Detection of short chain fatty acids in stool samples

The fecal samples (0.026 ± 0.012 g) were suspended in 1.5 ml milli-Q water by vortexing for 10 minutes at maximum speed. The supernatant after centrifuging samples for 10 minutes at 10,000*g*, was filtered through a 0.2 μm membrane filter. Filtered samples were 1:2 diluted with milliQ water and analyzed on a 930 Compact IC Flex instrument equipped with an 858 Professional Sample Processor with extended MiPuT (Micro Metrohm intelligent Partial Loop Injection Technique), a Metrohm CO_2 Suppressor for inline bicarbonate removal, a Metrosep Organic acids 250/7.8 column, a Metrosep Organic acids Guard/4.6 guard column and an 850 IC conductivity detector (Metrohm, Herisau, Switzerland).

Klebsiella pneumoniae isolation and genome sequencing

Klebsiella pneumoniae was isolated from stool anaerobically on peptone yeast glucose (PYG) agar plates. Colonies were re-streaked multiple times to ensure clonality. After identifying *Klebsiella pneumoniae* by 16S rRNA gene-targeted PCR, the culture was grown in PYG medium and DNA was isolated via phenol-chloroform extraction as described above. Illumina sequencing libraries were prepared using the NEBNext Ultra II FS DNA Library Prep Kit, and sequencing was performed with an Illumina Miseq (v3 kit, 600 cycles). Sequencing data was quality-trimmed at a phred score of 15 using bbmap (https://sourceforge.net/projects/bbmap/), and assembled with SPAdes 3.11.1 (Bankevich et al., 2012). Contigs shorter than 1000 bp were removed from the assembly, and the quality of the genome draft was assessed with CheckM (Parks et al., 2015) and annotated with RAST.

QUANTIFICATION AND STATISTICAL ANALYSIS

Processing and analysis of neurological data

Resulting aEEGs were analyzed by visual assessment of Burdjalov total maturational scores (Burdjalov et al., 2003) and percentages of background patterns (Hellstro m-Westas et al., 2006; Klebermass et al., 2011). Routine cranial ultrasound screenings and cMRIs were assessed for brain damage via established scores (Kidokoro et al., 2013), as well as expert radiologist knowledge. Near-infrared spectra (NIRS) were examined individually. Artifacts (e.g., probe fell off forehead) were removed. Variability of cranial oxygen supply was calculated as a percentage of the fraction of time spent with an oxygen supply deviating beyond 10% from the mean of the total measurement. To calculate and visualize receiver operating characteristics (ROC) curves we employed the R package plotROC (Sachs, 2017).

Processing and analysis of immunological data

Ordinations of T cell populations were performed via canonical correlation analysis (CCA) with the cca() function from the R package vegan version 2.5 (Oksanen et al., 2013). The function ordistep() was then used in forward model selection to define the adjusted R^2 value for significant cytokines. Subsequently, the respective CCAs were rerun with significant cytokines solely. Missing values for the Multiplex (*in vitro* Cytokines) and FACS dataset (*in vivo* T cell ontogenesis) were interpolated using mean value interpolation. Principal Coordinate Analysis (PCoA was conducted based on the abundance-based canberra dissimilarity matrix and visualized with ggplot(). Silhouette Clustering (Oksanen et al., 2012) was employed to identify the optimal number of clusters (Figure S2F). Weighted averages of cytokine and chemokine concentrations were added *a posteriori* to the ordination plot by computing the covariance of variables with all axes. Afterwards, only positive eigenvalues were selected and the value of covariance was standardized as described in (Legendre and Gallagher, 2001). Furthermore, topographical data analysis (TDA) was employed on cytokine and chemokine data via the TDAmapper R function (https://cran.r-project.org/web/packages/TDAmapper/index.html). TDA was calculated with five intervals, allowing for 70% overlap, and ten clustering bins.

16S rRNA gene amplicon sequence analysis

Amplicon pools were extracted from the raw sequencing data using the FASTQ workflow in BaseSpace (Illumina) with default parameters. Demultiplexing was performed with the python package demultiplex allowing one mismatch for barcodes and two mismatches for linkers and primers. Amplicon sequence variants (ASVs) were inferred using the DADA2 R package version 1.14.1, applying the recommended workflow (Callahan et al., 2016). FASTQ reads were trimmed at 150nt with allowed expected errors of 2. ASV sequences were subsequently merged and classified using SINA version 1.6.0 (Pruesse et al., 2012) and the SILVA database SSU Ref NR 99 release 138 using default parameters (Quast et al., 2013).

Quantification of bacterial load, 16S rRNA gene copy number correction, and analysis

All qPCR reactions were performed in triplicates. All reactions with a standard deviation greater than 25% were repeated. The quality of each qPCR run was assessed via Bio-Rad CFX Manager Software. A standard curve was constructed by plotting the known log-transformed starting quantity against the cycle threshold (Ct–value). The whole *E.coli* DH5alpha genome was searched via NCBI Reference database and the molecular weight was calculated using an oligonucleotide properties calculator. The molecular weight was needed for the calculation of genome copies μl^{-1} via Dalton's equation. Multiplication of the genome copies μl^{-1} with the 16S rRNA gene copies per genome (7) leads to the correct 16S rRNA gene copy numbers μl^{-1}. The standard amount of 16S rRNA gene copy numbers μl^{-1} of *E. coli* DH5alpha was 3.7×10^7. This value of the standard was used to calculate back to 16S rRNA gene copy numbers (g^{-1} of faeces) taking into account the dilution factor for each sample (samples were initially diluted to a starting concentration of < 20ng μl^{-1}).

16S rRNA gene counts were normalized via rarefying to even minimal sampling depth (4,000 reads per sample). Subsequently, a filter was applied to exclude ASVs that occurred in less than three samples overall. Rarefied and filtered counts were multiplied by the qPCR total cell counts, and ASV counts at genus level or above were corrected for the number of 16S rRNA operons (Stoddard et al., 2015). As this method has been shown to be susceptible to errors in quantification of relatively underrepresented ASVs in a sample (Tettamanti Boshier et al., 2020), abundances of rarer taxa should be treated as approximations. Filtered abundance-corrected data was used to conduct a cluster analysis via T-distributed stochastic neighbor embedding (tSNE) of ASVs with 10,000 iterations and a perplexity of 30, employing the R package "Rtsne" (Justin Donaldson, 2016). Silhouette Clustering (Oksanen et al., 2012) was employed to identify the optimal number of microbiome clusters in the dataset (hierarchical clustering; Ward's method). Furthermore, EdgeR was used to identify count-based differential expression of ASVs between infants with and without brain injuries, using the microbiome analyst platform as described on the developer's website (www.microbiomeanalyst.ca). To define the extremely premature infant core microbiota, an additional filter was applied to identify ASVs that occurred in a minimum of 20% of samples with an abundance of $>10^5$ cells g^{-1}.

Basic statistical analysis and data integration

Basic statistical analysis (Student's T-test, ANOVA, repeated measures ANOVA, Wilcoxon Test, and chi-square test, Fisher's exact test) was performed via R version 4.0 and the R package rstatix version 0.7.0. All p-values were adjusted using Bonferroni's method for Unpaired T Test and Wilcoxon Rank Sum Test, as well as Tukey post-hoc test for ANOVA.

Data Integration Analysis for Biomarker discovery using Latent variable approaches for Omics studies (DIABLO) was used to integrate complementary microbiome, immunological, metabolic, and neurophysiological data. DIABLO analysis was performed using the "Mixomics" R package (Singh et al., 2019). The DIABLO framework builds on Generalized Canonical Correlation Analysis (Tenenhaus and Tenenhaus, 2011) to generalize partial least squares (PLS) for multiple matching data sets. In total we picked the maximum of 80 matching samples to combine our datasets. Only highly prevalent ASVs (occurrence in at least 20% of all samples with an absolute abundance > 10^5) were included in the analysis. Two components were used (centroid distance and overall error rate) to fine tune the model selection as described on the developer's website (www.mixomics.org). As a result, we interpreted a correlation value of each feature to its corresponding feature in another dataset (e.g. *Klebsiella* [microbiome] to effector $CD4^+$ [T cells].

Please cite this article in press as: Seki et al., Aberrant gut-microbiota-immune-brain axis development in premature neonates with brain damage, Cell Host & Microbe (2021), https://doi.org/10.1016/j.chom.2021.08.004

Data visualization

Data was visualized via R version 4.0 and R package ggplot2 version 3.3.3 (Wickham, 2011). Transitions throughout tSNE clusters were modelled via Cytoscape (https://cytoscape.org). For FACS gating the FlowJo™ Software was used.

Additional resources

This study was registered at ClinicalTrials.gov under the number NCT03213275.

Chapter 2

Individuality of the neonatal gut microbiota is driven by ecological drift

David Seki, Clemens Schauberger, Bela Hausmann, Angelika Berger, Lukas Wisgrill, David Berry

Submitted

Author contributions

Conceptualization: D.S., C.S.

Methodology: D.S., C.S., B.H.

Software: D.S., C.S.

Investigation: D.S., D.B.

Writing - Original Draft: D.S.

Writing - Review & Editing: D.S., D.B.

Resources: D.B., L.W.

Supervision: D.B.

Funding Acquisition: D.B., A.B.

Individuality of the neonatal gut microbiota is driven by ecological drift

David Seki[1,2], Clemens Schauberger[3], Bela Hausmann[4,5], Angelika Berger[2], Lukas Wisgrill[2], David Berry[1,4,*]

[1]Centre for Microbiology and Environmental Systems Science, Department of Microbiology and Ecosystem Science, Division of Microbial Ecology, University of Vienna, 1090 Vienna, Austria

[2]Department of Pediatrics and Adolescent Medicine, Division of Neonatology, Pediatric Intensive Care and Neuropediatrics, Comprehensive Center for Pediatrics. Medical University of Vienna, 1090 Vienna, Austria

[3]Hadal & Nordcee, Department of Biology, University of Southern Denmark, 5000 Odense, Denmark

[4]Joint Microbiome Facility of the Medical University of Vienna and the University of Vienna, Vienna, Austria

[5]Department of Laboratory Medicine, Medical University of Vienna, Vienna, Austria

*Corresponding author: david.berry@univie.ac.at

Abstract

The initial contact between humans and their colonizing gut microbiota after birth is thought to have expansive and long-lasting consequences for physiology and health. Premature infants are at high risk of suffering from life-long impairments, due in part to aberrant development of gut microbiota that can contribute to early-life infections and inflammation. Despite its importance to health, the ecological assembly and succession processes governing gut microbiome composition in premature infants remained incompletely understood. Here, we quantified these ecological processes in a spatiotemporally-resolved 16S rRNA gene amplicon sequencing dataset of 60 extremely premature neonates using an established mathematical framework. We found that gut colonization during the first months of life is predominantly stochastic, whereby inter-individual diversification of microbiota is driven by ecological drift. Dispersal limitations are initially small but have increasing influence at later stages of succession. Furthermore, we find similar trends in a cohort of 32 healthy term-born infants. These results suggest that the uniqueness of individual neonatal gut microbiota is the result of stochastic assembly.

Introduction

The human gut microbiota performs a variety of functions essential for the survival of its host. Adults harbor gut microbiota that are generally resistant to perturbation, and which maintain a stable composition over years and even decades[1]. Human-associated microbial lineages are also globally distributed and estimated to have much higher dispersal rates between continents compared to other terrestrial bacteria[2]. However, the human gut microbiota is highly personalized, varying substantially between individuals[3]. With birth, the gut microbiota begins assembling *de novo* and eventually stabilizes into a complex community, and it is thought that the initial assembly and succession of the early-life microbiota heavily impacts the composition of the resulting stable community[4]. However, despite the importance of early-life microorganisms for host health and development, the ecological processes underlying early-life gut microbiota assembly remain poorly understood.

Primary succession begins post-delivery with the arrival of pioneer communities, which shape subsequent steps of succession[5]. Over the course of this process, the human host exerts a strong top-down control on colonizing bacteria. Factors such as intestinal transit time[6], diet[7], geographic location[8], host genetics[9], medication use[10], and endocrine[11] and neurological function[12] partially explain inter-individual microbiome variation. These factors exert deterministic influence, by which species are selected for or expelled from the environment due to differences in their ecological fitness[13]. In addition to a variety of deterministic processes driven by the host or interactions within the microbiota (e.g., niche construction), neutral processes can also play a role in shaping ecological systems[14]. Stochastic events include the dynamics of passive dispersal[15] and ecological drift[16]. For a variety of environments in non-equilibrium states, it is believed that stochasticity dominates initial community assembly, given the general assumption that a broad range of organisms can grow successfully in an uncolonized environment[17].

The gut microbiota of an individual infant can be viewed as a local part of a larger pool of communities found in the infant population, or a so-called metacommunity[18]. Local communities differ from each other as a result of species sorting, which can be caused by differences in the combination and magnitude of selection, dispersal, and drift[19]. Quantification of the processes that ultimately define the structure and amount of turnover in and between local microbial communities is an important step towards understanding the assembly and succession of the early life gut microbiota in humans. This understanding is particularly

important for the health of premature infants, as aberrant gut microbiota development can contribute to early-life inflammation and adverse outcomes[20]. Premature infancy has been rising in incidence worldwide, and is one of the leading causes of perinatal morbidity and mortality[21]. Identifying features that impose aberrant development of microbiota assembly is a crucial task towards improving the overall health outcome for premature infants.

In this study, we quantified the ecological processes underlying microbial community assembly in 60 extremely premature infants (born before 28 weeks of gestation with less than 1 kg), based on data obtained in a previously published study[20]. We compared our phylogenetic observations to ecological null models to determine the contributions of selection, dispersal, and drift to the observed community turnover[22] in the premature infant gut microbiota. As a comparison, we evaluated a publicly-available dataset describing the succession of microorganisms in 32 healthy infants born at term-age[23]. We found that the early-life gut microbiota is initially unstable and low in diversity. However, as succession proceeded both stability and diversity increased. This progression was driven largely by ecological drift, with a small contribution of deterministic factors and increasing importance of dispersal limitation over time.

Results

Indications for deterministic assembly and succession of gut microbiota in extremely premature infants

Data was obtained from a previously published study of a cohort of 60 extremely premature infants (gestational age <28 weeks and birth weight 1kg[20]). Stool was sampled from each individual at three, seven, and 14 days post-delivery, and then bi-weekly until discharge from the hospital. 16S rRNA gene-targeted amplicon sequencing and qPCR was employed to characterize microbial composition and quantify total bacterial load, allowing for quantitative microbiome profiling of community composition.

We first examined the abundances of the dominant taxa over time, averaged across the patient cohort. *Staphylococcus* was abundant three and seven days post-delivery, but subsequently decreased as total bacterial load plateaued by two weeks post-delivery (Wilcoxon; $p < 0.001$; Comparison: *Staphylococcus* abundance at day 7 and at week 4) following an expansion of *Escherichia-Shigella* (Wilcoxon; $p < 0.001$; Comparison: *Escherichia-Shigella* abundance at day 7 and at week 2). Interestingly, by analyzing the relative proportions of ASV reads without a correction for total bacterial load we found that the increase of *Staphylococcus* during the first week post-delivery was overestimated by the relative abundance data, whereas the subsequent expansion of *Escherichia-Shigella* was underestimated as compared to the quantitative profile (Figure S1). By 8-10 weeks, strictly anaerobic bacteria (*Clostridia*, *Finegoldia*, and *Veillonella*), which were detected only rarely in early time points, increased in abundance (Wilcoxon; $p = 0.006$; 0.07; 0.0002 respectively; Comparison: Clostridia, Finegoldia, and Veillonella abundances at week 6 and at week 8; Figure 1A). Their occurrence is synchronized to a significant increase of ASV richness between the adjacent time points at week 6 and week 8 (Figure 1B; T.test; $p = 0.003$), providing indications for reproducible, deterministic assembly and succession processes being involved in shaping the early-life microbiota. Furthermore, we observed a trending decrease in Bray-Curtis dissimilarity between samples at adjacent time points from the same individual (Figure 1C), suggesting that ASV turnover is initially fast and decelerates over later periods. However, Bray Curtis dissimilarities did not significantly differ between adjacent time points. Also, we found considerable temporal instability in the microbiota of individual patients, particularly during the first month post-delivery. In some cases, this was due to transient reversions to communities similar to initial (day 3) microbiomes, as indicated by outliers in Figure 1D. Lastly, we noted that the variation

in the microbiome across the cohort tended to increase with age, suggesting that the microbiomes were becoming increasingly different from one another (Figure 1E; Mantel statistic r: 0.1284; $p < 0.001$). Accordingly, inter-individual variation contributed significantly to the observed gut microbiota composition (PERMANOVA; $p = 0.03$). Together with the increased stability of the microbiome within patients, this provides indications for an increasingly individualized gut microbiome.

Ecological drift dominates assembly and succession of early life gut microbiota

To quantify the contributions of stochastic and deterministic processes in shaping the gut microbiota of this cohort, we calculated the β nearest-taxa index (βNTI) and determined the phylogenetic turnover of microbial communities relative to a null model[22], allowing only for pairwise comparisons of microbiota from different patients that are situated in the same neonatal ward at a given time point. A pairwise comparison of βNTI values indicates that two communities are phylogenetically less similar (>2) or more similar (<-2) than by random chance and are therefore likely driven by either variable or homogenizing selection. Values greater than |2| are characteristic results of either similar or divergent selective forces that deterministically structure microbiomes. Values equal to or less than |2| indicate stochastic processes being the main forces driving microbial community composition. We observed that stochastic processes are the dominant forces driving species turnover in extremely premature infants. Variable selection, which was present shortly after birth, quickly diminished over the course of hospitalization (Figure 2A), suggesting that variable selection primarily shapes microbial community structure when gastro-intestinal niches are still relatively vacant.

To further analyze the stochastic processes affecting microbiota turnover, we used the modification of Raup-Crick (RC_{Bray}) dissimilarity[22]. A deviation of RC_{Bray} greater than |0.95| as compared to the null model would indicate that communities are assembled by either homogenizing dispersal ($RC_{Bray} < -0.95$), or the combination of dispersal limitation and randomly varying birth and death rates (drift) ($RC_{Bray} > 0.95$). Homogenizing dispersal and homogenizing selection both appeared to play a minor role throughout most of the hospitalization period. Interestingly, we observed that dispersal limitation gradually increased over time, concomitant with a decrease in drift acting alone (Figure 2B). This trend was also reflected in the pairwise comparison of all samples to early post-delivery samples, which showed that dispersal limitation between developed and founder microbiota remained below 10% during the first month post-delivery but increased afterwards (Figure 2C). Accordingly,

149 RC_{Bray} values differed significantly between the time points “day 3 to day 3” and “day 3 to
150 week 10” (T.test; p = 0.008).

151 We conclude that the succession of the extremely premature infant gut microbiota is
152 predominantly stochastic. Species turnover is dominated by drift once the microbiota has
153 reached the carrying capacity of the premature infant gastrointestinal tract (GIT) approximately
154 two weeks post-delivery. Throughout hospitalization, dispersal limitation acts in concert with
155 drift and becomes increasingly important over time. This suggests that stochasticity underlies
156 diversification of the microbiota, allowing exchange of microbes between infants and their
157 environment. Only shortly before discharge dispersal limitation begins to act in concert with
158 drift. However, the presence of variable selection shortly post-delivery raises the possibility
159 that varying priority effects manifest in different infants, a legacy that might translate into
160 diversification during later periods.

161 Differences in gestational age at birth underlie early-life variable 162 selection

163 Next, we evaluated which factors underlie the observed variable selection immediately post-
164 delivery. βNTI values > 2 were extracted out of all pairwise community comparisons from
165 samples obtained during the first three days of life. Regression analysis was then performed
166 using this subset of βNTI values and measured clinical variables to reveal factors associated
167 with variable selection.

168 Notably, we found that differences in gestational age at birth, measured as days post-
169 conception, was significantly associated with elevated βNTI values ($R = 0.32$, $p < 0.0001$;
170 Figure 3A). Other factors, such as the influence of infection (CRP), weight, mechanical
171 ventilation (FiO_2), and the amount of enteral nutrition showed no such association ($p > 0.05$;
172 Figure S2). In order to better understand initial microbiome assembly, we used principal
173 component analysis (PCA) on all fecal samples obtained during the first week post-delivery.
174 We observed three different microbiome clusters which seem to be driven by dominance of
175 *Bifidobacterium*, *Escherichia-Shigella*, and a combination of *Staphylococcus* and *Klebsiella*
176 respectively (Figure 3B). However, none of these genera associated significantly with
177 gestational age at birth. We conclude that differences of gestational age at birth influence initial
178 microbial assembly, presumably as infants with very low gestational age (GA) at birth have
179 underdeveloped gastro-intestinal tissues compared to infants born with a higher GA.

Drift causes divergence of underlying ecological processes between neonatal wards

Neonatal wards have been implicated as an important source of bacteria that are transferred between occupants and the room[24]. Our cohort was hospitalized in four different clinical wards that are physically separated from each other, and therefore can be thought of as regional meta-communities that may have different dispersal limitations due to the physical proximity of co-housed infants. However, these regional metacommunities are also connected to each other due to the directional transfer of infants between wards. All patients were initially hospitalized in neo-intensive care unit 1 (NICU-1) and when clinically stable were then transferred to an intermediate-care unit (IMCU-1 or IMCU-2). Transfers from NICU-1 to NICU-2 occurred when infants were not yet clinically stable but beds at NICU-1 were fully occupied (Figure 4A).

The gut microbiota of patients in IMCUs were generally more diverse (Figure S3A), whereat NICU-1 and NICU-2 are statistically different from IMCU-1 and IMCU-2 (T-test; $p < 0.0001$ respectively), while the observed richness was similar when comparing IMCU-1 to IMCU-2 (T-test; $p = 0.22$) and NICU-1 to NICU-2 (T-test; $p = 0.75$). *Staphylococcus* was most abundant in NICU1 (Figure S3B), but its association with NICU-1 was not significant (ANOVA; $p = 0.09$). In general, room was not significantly associated with the observed microbial composition (PERMANOVA; $R^2 = 0.01$; $p = 0.15$). Microbial composition could be rather explained by patient (PERMANOVA; $R^2 = 0.14$; $p = 0.015$), as well as the combined effects of patient and age (PERMANOVA; $R^2 = 0.13$; $p = 0.005$). However, to determine if ward residency affected the ecological assembly processes, we again employed the βNTI and RC Bray framework as described above. For this, βNTI values were determined across all pairwise community comparisons between samples of the same room, obtained during the same calendar week. Consistent with our previous results, we observed that drift was the dominant ecological assembly process in all hospital wards. However, there were differences between the wards, with NICU-1 having the highest occurrence of variable selection (βNTI > 2) (Figure 4B). All infants received initial care at NICU-1, and thus NICU-1 included the youngest infants. Interestingly, βNTI values of the two NICUs were not significantly different, but NICU-1 differed from IMCU-2 and NICU-2 differed to IMCU-1 (T-test, $p = 0.014$ and $p = 0.01$, respectively; Figure 4C). βNTI values between IMCU-1 and IMCU-2 were also significant (Wilcoxon test, $p < 0.001$). Direct transfers of infants from NICU-1 to IMCU-1 occurred more frequently than from NICU-1 to IMCU-2 (21% versus 12%), which might explain the slight

increase of βNTI values beyond |2| in IMCU-1 compared to IMCU-2. We next evaluated inter-ward dispersal limitation (Figure 4D). We find that as most transfers occurred from NICU-1 to NICU-2, these wards also seem the least restricted by dispersal limitation (7%). However, as the fewest transfers occurred from NICU-1 to IMCU-2, dispersal limitation is higher between those wards (14%). Accordingly, RC_{Bray} values differed significantly in a comparison between "NICU-1 ←→ NICU-2" and "NICU-1 ←→ IMCU-2" (T.test; $p < 0.001$). Generally, however, dispersal limitation was lower between NICUs or IMCUs, but higher in comparison between the different types of neonatal ward.

We conclude that the observed diversification of premature infant microbiomes is a matter of time post-delivery rather than to ward residency. Interestingly however, there seems to be an increase of dispersal based on the flow of the infants between neonatal wards, suggesting that as infants come from the same environment, they are more likely to share microbiota in a new environment. However, the general lack of homogenizing dispersal additionally suggests that although there is ongoing dispersal, we do not capture its homogenizing effects due to rapid turnover of microbiota during early succession.

Gut microbiome assembly in healthy term-born neonates

To compare how GIT microbial community assembly progresses in extremely premature infants compares healthy term-age infants (>38 weeks of gestation), we analyzed a publicly-available dataset consisting of 16S rRNA gene sequences from fecal samples of infants that were sampled over the first 18 months of life[23]. Similarly to premature infants, drift dominated microbial assembly and succession (Figure 5). Interestingly, dispersal limitation in combination with drift increased over time, but at a much later time point than for premature infants, becoming the dominant assembly process only after one year post-delivery. Variable selection remained minor but present throughout the whole early life period, varying between 3% and 14%.

Discussion

Our study addresses the ecological processes underlying assembly of microbes in the GIT of extremely premature infants. Initially, the gut microbiota had a very low diversity. With time, the phylogenetic and functional complexity of the microbiota increased, as demonstrated by the late arrival of strictly anaerobic bacteria (Figure 1). Our analysis suggests that this progression seems mainly driven by neutral ecological processes (Figure 2). Furthermore, the

stability of the microbiota increased with time, as marked by less frequent recursion to founder communities and increased dispersal limitation between developed and founder communities.

Stochastic processes have also been found to dominate microbial colonization during succession in other environments such as during the formation of hyper-saline microbial mats, which were initially stochastic but showed a trend towards deterministic selection in later stages of succession[4]. We did not observe the emergence of such a trend for either preterm or term infants (Figures 2B and 5). However, the gut microbiota of adults has been shown to be much more influenced by deterministic processes[8], suggesting that there may be a transition point later in childhood or puberty in which deterministic processes become more influential.

The neonatal ward environment has been implicated as an important source of microbes for the colonization of premature infant guts[24]. Although we observed associations between certain microbial taxa and NICU and IMCU environments (Figure S3), this was confounded by differences in patient age, and may also be driven in part by ward-specific clinical practices such as different antibiotic regimes. It has been shown, for example, that bifidobacteria are especially susceptible to antibiotic interventions[25], whereas many potentially-pathogenic *Enterobacteriaceae* are resistant to a variety of antibiotics[26]. Furthermore, it was recently shown that probiotically-administered bifidobacteria are less abundant in infants with very low gestational age[27]. It remains unclear whether the prematurity of the host or NICU conditions suppress bifidobacterial colonization. Interestingly, we observed that IMCU-1 was ecologically different from IMCU-2 (Figure 4B and 4C). The design of the both wards differs, with IMCU-1 having two to three bed rooms, and IMCU-2 being an open ward, which potentially contributes to the observed differences. However, they both have similar clinical practices and the average age of hospitalized infants was similar in both (IMCU1: 61 days; IMCU2: 55 days), in contrast to infants in NICU-1 (15 days) and NICU-2 (35 days). We partially explain the observed ecological differences based on the differential flow of infants between wards. IMCU-1, in contrast to IMCU-2, had a considerable influx of infants directly from NICU-1, in which variable selection was most prevalent. Correspondingly, variable selection is higher in IMCU-1 than IMCU-2, suggesting that infants not only shuttle microbiota between neonatal wards but also influence ward-level microbiota assembly processes.

During early microbiota succession, most of the observed bacteria are facultative anaerobes, with obligate anaerobes arriving only later and contributing towards an increased richness and diversity (Figure 1). This initial progression was predominantly stochastic with minimal

barriers to dispersal between infants, especially early post-delivery (Figure 2A, B). Dispersal constitutes a major ecological process with important implications for the diversity in local microbial communities[19]. Theoretically, higher rates of dispersal should result in a homogenizing increase of alpha diversity and decrease of beta diversity in local communities. However, we find no homogenizing effect despite the lack of dispersal limitations during initial assembly in premature (Figure 2B) as well as term-born infants (Figure 5). We speculate that, as all GITs are un-colonized post-delivery and any dispersing microbe could theoretically colonize successfully, initial assembly is dominated by ecological drift. However, we did observe an increase of dispersal limitation in later periods of succession (Figure 2B), especially between founder and developed communities (Figure 2C). These late phases of assembly have increased compositional stability, as characterized by fewer recursions to founder states (Figure 1C and D), suggesting that the established microbiota buffers from arrival of novel microorganisms. This colonization resistance, in concert with drift, gives rise to the observed increase in inter-individuality (Figure 1E). We observed a similar trend in term-born infants as well, whereby dispersal-limitation begins to increase six months post-delivery. Interestingly, this time frame corresponds to the typical period of introduction of novel foods beside breast milk.

Although stochastic processes appear to be the major determinant of microbiota assembly, we found that variable selection played a role shortly post-delivery, and differences in gestational age at birth partially drove initial assembly (Figure 4A). This was reflected in part by differential abundances of *Bifidobacterium*, *Escherichia-Shigella*, *Staphylococcus*, and *Klebsiella* at day 3 (Figure 3B). Especially the colonization with *Klebsiella* spp. has critical implications for health, and we recently showed that *Klebsiella* dominance underlies the formation of a potentially pathological community state, which associates with perinatal brain injury and may thereby be involved in long-lasting morbidities[20].

We conclude that gut microbiota assembly and succession in extremely premature, as well as term-born neonates, is predominantly stochastic, with increasing dispersal limitation over time. These findings reveal ecological aspects of early-life microbiome assembly in human GITs and underline the individuality of microbiota development and the need for personalized microbiome-targeted therapeutic options to ensure proper development and maturation in premature infants.

Acknowledgments

We thank all families for their participation and all medical staff, especially Vito Giordano, Katharina Göral, and Katrin Klebermaß-Schrehof from the PreMiBraIn team, for their help with sample collection. We thank Jillian Waters and Ruth Ley from the Department of Microbiome Science at the Max Planck Institute for Developmental Biology in Tübingen for providing access to healthy term-born infant data. Also, we thank Lucas Fillinger from the Department of Functional & Evolutionary Ecology for his computational advice. This project was funded by an inter-university cluster project grant between the University of Vienna and the Medical University of Vienna (‘‘PreMiBraIn’’), the European Research Council (Starting grant: FunKeyGut 741623), and the Austrian Science Fund (FWF; P27831-B28).

Author Contributions

Conceptualization, D.S. and C.S..; methodology, D.S., C.S., and B.H.; software, D.S. and C.S.; investigation, D.S., D.B; writing – original draft, D.S.; writing – review & editing, D.S. and D.B.; resources, D.B. and L.W.; supervision, D.B.; and funding acquisition, D.B. and A.B.

Declaration of Interest

The authors declare no competing interests.

Material and Methods

Experimental model and subject details

60 extremely premature infants were enrolled between September 2017 and June 2019 at the General Hospital of Vienna as part of the PreMiBraIn study, which was approved by the ethics commission of the Medical University of Vienna (Ethics number 1348/2017). Inclusion criteria were birth before the 28th week of gestation with less than 1000 g birth weight. Infants with congenital malformations, chromosomal aberrations, maternally transmitted infectious diseases (e.g. HIV, hepatitis A/B/C, etc.) and inborn errors of metabolism were excluded. Clinical parameters of each patient were prospectively monitored by the clinical staff during hospitalization and recorded within the hospitals’ electronic database ICIP (Philips Healthcare Systems). To minimize study bias, the general house-internal standard procedures for neonatal

care were obtained consistently over the whole study period, including antibiotic regimen, probiotic administration, and feeding regimen. Every infant received, starting from the first day of life, the probiotic preparation Infloran (*Bifidobacterium bifidum & Lactobacillus acidophilus*) until the corrected age of 34 weeks of gestation. The enteral feeding regimen includes the infant's own mother's milk or pasteurized human donor milk. When 100ml/kg enteral feeding was achieved, the milk was fortified with 4% bovine milk fortifier until term-equivalent age. Over the course of hospitalization, stool samples were collected three, seven, and 14 days post-delivery, and thereafter bi-weekly until discharge. In total we collected 547 stool samples, each was sampled from diapers via collection tubes during patient care routines, and immediately stored at -80°C until further analysis.

Data acquisition and analysis

16S rRNA data for term-born infants was generated as described in[23]. 16S rRNA data for extremely premature infants was generated and corrected for absolute abundance via qPCR as described in[20].

Basic statistical analysis and data visualization (e.g. Student's T-test, ANOVA, PERMANOVA and Wilcoxon Test) was performed via R version 4.0 and the R packages rstatix version 0.7.0, Ampvis 2.0[28], and ggplot2 version 3.3.3[29]. All p-values were adjusted using Bonferroni's method for Unpaired T Test and Wilcoxon Rank Sum Test, as well as Tukey post-hoc test for ANOVA. Alpha and beta diversity indices were calculated using the R package vegan version 2.5[30].

We employed a null-model analysis to compare beta Mean Nearest Taxon Index (βNTI) for pairwise comparisons between specific samples to assess whether their phylogenetic similarity is significantly higher or lower than expected by chance[22]. The picante package was used to calculate βNTI[31]. Briefly, a pairwise comparison of βNTI values indicates that two communities are phylogenetically less similar (> 2) or more similar (< -2) than by random chance and are therefore likely driven by either variable or homogenizing selection. Values greater than |2| are characteristic results of either similar or divergent selective forces that deterministically structure microbiomes. Values smaller than |2| identify stochastic processes as the main forces driving microbial community composition. To furthermore analyze ASV turnover we used the modification of Raup-Crick (RC_{Bray}) dissimilarity[22], to additionally characterize βNTI values between |2|. A significant deviation of RC_{Bray} beyond |0.95|, as compared to a null model would indicate that given communities are assembled by either

372 homogenizing dispersal (RC_{Bray} <-0.95), or the combination of dispersal limitation and
373 randomly varying birth and death rates (drift) (RC_{Bray} >0.95).

374 References

375 1. Faith, Jeremiah J., et al. "The long-term stability of the human gut microbiota." Science
376 341.6141 (2013).
377 2. Louca, Stilianos. "The rates of global bacterial and archaeal dispersal." The ISME
378 Journal (2021): 1-9.
379 3. De Muinck, Eric J., and Pål Trosvik. "Individuality and convergence of the infant gut
380 microbiota during the first year of life." Nature communications 9.1 (2018): 1-8.
381 4. Brislawn, Colin J., et al. "Forfeiting the priority effect: turnover defines biofilm
382 community succession." The ISME journal 13.7 (2019): 1865-1877.
383 5. Gilbert, Jack A., and Susan V. Lynch. "Community ecology as a framework for human
384 microbiome research." Nature medicine 25.6 (2019): 884-889.
385 6. Huizinga, Jan D., and Wim JEP Lammers. "Gut peristalsis is governed by a multitude
386 of cooperating mechanisms." American Journal of Physiology-Gastrointestinal and Liver
387 Physiology 296.1 (2009): G1-G8.
388 7. David, Lawrence A., et al. "Diet rapidly and reproducibly alters the human gut
389 microbiome." Nature 505.7484 (2014): 559-563.
390 8. Martínez, Inés, et al. "The gut microbiota of rural papua new guineans: composition,
391 diversity patterns, and ecological processes." Cell reports 11.4 (2015): 527-538.
392 9. Bonder, Marc Jan, et al. "The effect of host genetics on the gut microbiome." Nature
393 genetics 48.11 (2016): 1407-1412.
394 10. Forslund, Kristoffer, et al. "Disentangling type 2 diabetes and metformin treatment
395 signatures in the human gut microbiota." Nature 528.7581 (2015): 262-266.
396 11. Mihajlovic, Jovana, et al. "Combined hormonal contraceptives are associated with
397 minor changes in composition and diversity in gut microbiota of healthy women."
398 Environmental Microbiology (2021).
399 12. Bonaz, Bruno, Thomas Bazin, and Sonia Pellissier. "The vagus nerve at the interface
400 of the microbiota-gut-brain axis." Frontiers in neuroscience 12 (2018): 49.
401 13. Pereira, Fátima C., and David Berry. "Microbial nutrient niches in the gut."
402 Environmental microbiology 19.4 (2017): 1366-1378.
403 14. Furman, Ori, et al. "Stochasticity constrained by deterministic effects of diet and age
404 drive rumen microbiome assembly dynamics." Nature communications 11.1 (2020): 1-13.

15. Burns, Adam R., et al. "Interhost dispersal alters microbiome assembly and can overwhelm host innate immunity in an experimental zebrafish model." Proceedings of the National Academy of Sciences 114.42 (2017): 11181-11186.
16. Shafquat, Afrah, et al. "Functional and phylogenetic assembly of microbial communities in the human microbiome." Trends in microbiology 22.5 (2014): 261-266.
17. Dini-Andreote, Francisco, et al. "Disentangling mechanisms that mediate the balance between stochastic and deterministic processes in microbial succession." Proceedings of the National Academy of Sciences 112.11 (2015): E1326-E1332.
18. Miller, Elizabeth Theresa, Richard Svanbäck, and Brendan JM Bohannan. "Microbiomes as metacommunities: understanding host-associated microbes through metacommunity ecology." Trends in Ecology & Evolution 33.12 (2018): 926-935.
19. Leibold, Mathew A., et al. "The metacommunity concept: a framework for multi-scale community ecology." Ecology letters 7.7 (2004): 601-613.
20. Seki, David, et al. "Aberrant gut-microbiota-immune-brain axis development in premature neonates with brain damage." Cell Host & Microbe (2021).
21. Tommiska, Viena, et al. "No improvement in outcome of nationwide extremely low birth weight infant populations between 1996–1997 and 1999–2000." Pediatrics 119.1 (2007): 29-36.
22. Stegen, James C., et al. "Quantifying community assembly processes and identifying features that impose them." The ISME journal 7.11 (2013): 2069-2079.
23. Janzon, Anders, et al. "Interactions between the gut microbiome and mucosal immunoglobulins A, M, and G in the developing infant gut." Msystems 4.6 (2019): e00612-19.
24. Brooks, Brandon, et al. "Microbes in the neonatal intensive care unit resemble those found in the gut of premature infants." Microbiome 2.1 (2014): 1-16.
25. Zhou, J. S., et al. "Antibiotic susceptibility profiles of new probiotic Lactobacillus and Bifidobacterium strains." International journal of food microbiology 98.2 (2005): 211-217.
26. Davin-Regli, Anne, Jean-Philippe Lavigne, and Jean-Marie Pagès. "Enterobacter spp.: update on taxonomy, clinical aspects, and emerging antimicrobial resistance." Clinical microbiology reviews 32.4 (2019): e00002-19.
27. Alcon-Giner, Cristina, et al. "Microbiota supplementation with Bifidobacterium and Lactobacillus modifies the preterm infant gut microbiota and metabolome: an observational study." Cell Reports Medicine 1.5 (2020): 100077.
28. Andersen, Kasper S., Kirkegaard, Rasmus H., Karst Soren M. and Albertsen Mads. “ampvis2: an R package to analyse and visualise 16S rRNA amplicon data.” bioRxiv. (2018).

29. Wickham, Hadley. "Elegant graphics for data analysis." Media 35.211 (2009): 10-1007.
30. Oksanen, Jari, et al. "Package ‘vegan’." Community ecology package, version 2.9 (2013): 1-295
31. Kembel, Steven W., et al. "Picante: R tools for integrating phylogenies and ecology." Bioinformatics 26.11 (2010): 1463-1464.

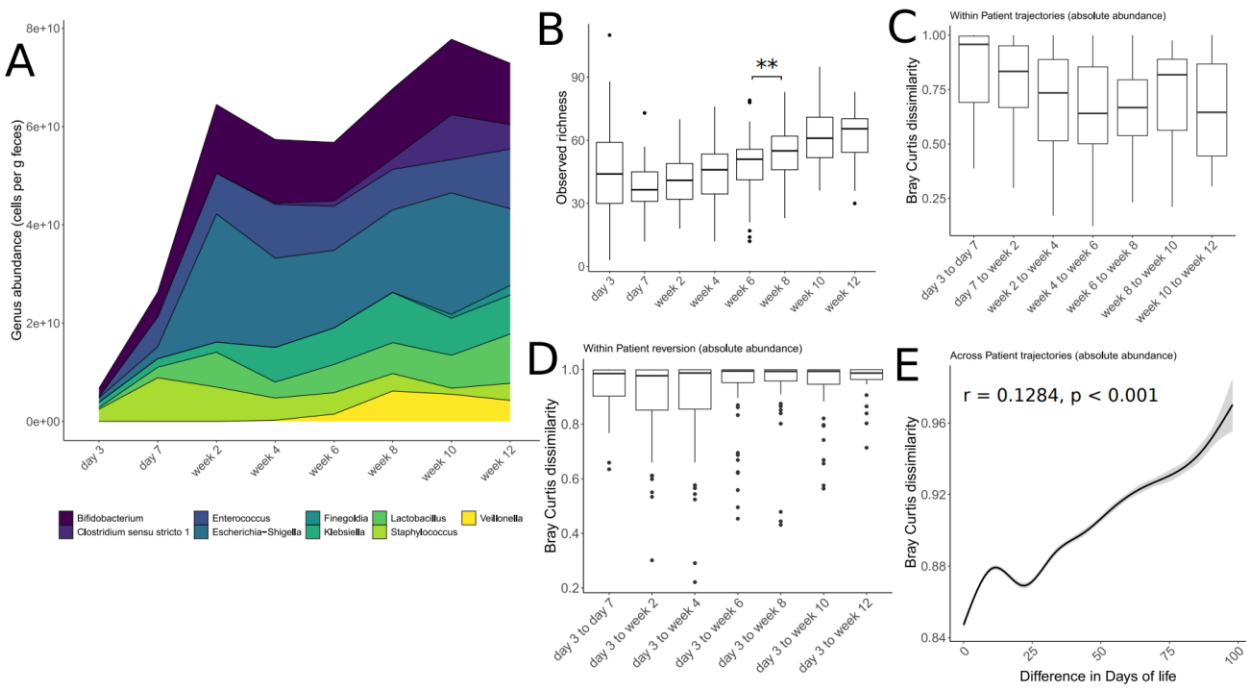

Figure 1. Succession of gut microbiota in extremely premature infants.

(A) Absolute abundances of the core genera in premature infants throughout hospitalization. (B) Observed ASV richness. (C) Calculation of Bray-Curtis dissimilarity between adjacent samples of the same individual. (D) Calculation of Bray-Curtis dissimilarity between the first sample and all following of the same individual. (E) Mantel correlogram of between-infants Bray-Curtis dissimilarities and the increase of difference in age. Box plots show group median and interquartile range. Smoothed lines result from locally estimated scatterplot smoothing (LOESS) and indicate trends of development. Asterisks represent p values: *p <

0.05, **p < 0.01, ***p < 0.001.

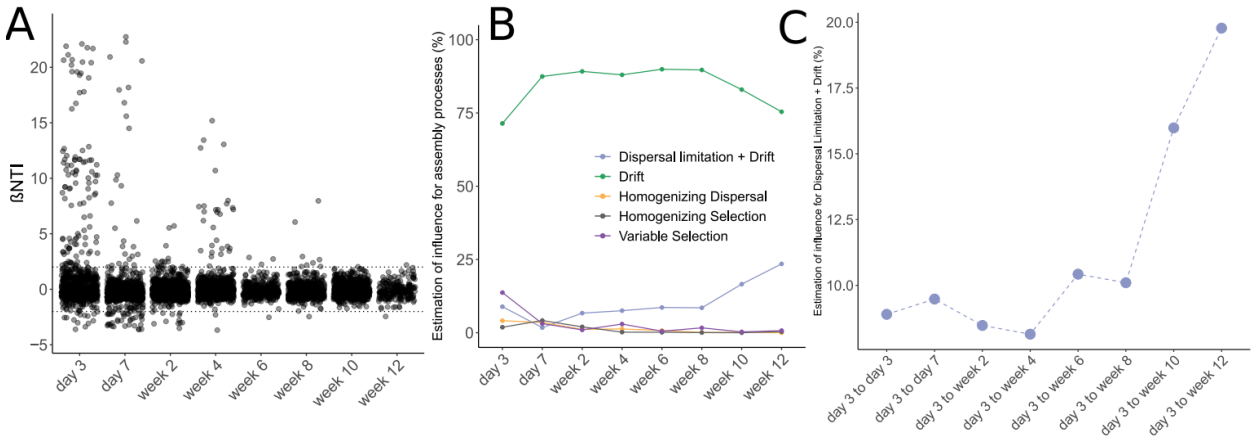

Figure 2. Influence of ecological processes on gut microbiota succession throughout time in extremely premature infants.

(A) Distribution of βNTI values for pairwise comparisons of samples between different patients within the same clinical ward. Dashed lines indicate the range of βNTI under the null hypothesis of no significant effects of selection (< |2|) (B) Contribution of individual turnover processes to observed differences in microbial community composition, resulting from pairwise comparisons of samples between different patients, sampled during the same calendar week within the same clinical ward. (C) Contribution of dispersal limitation to observed differences in microbial community composition, resulting from pairwise comparisons of samples between different patients, sampled during the same calendar week between differing clinical wards.

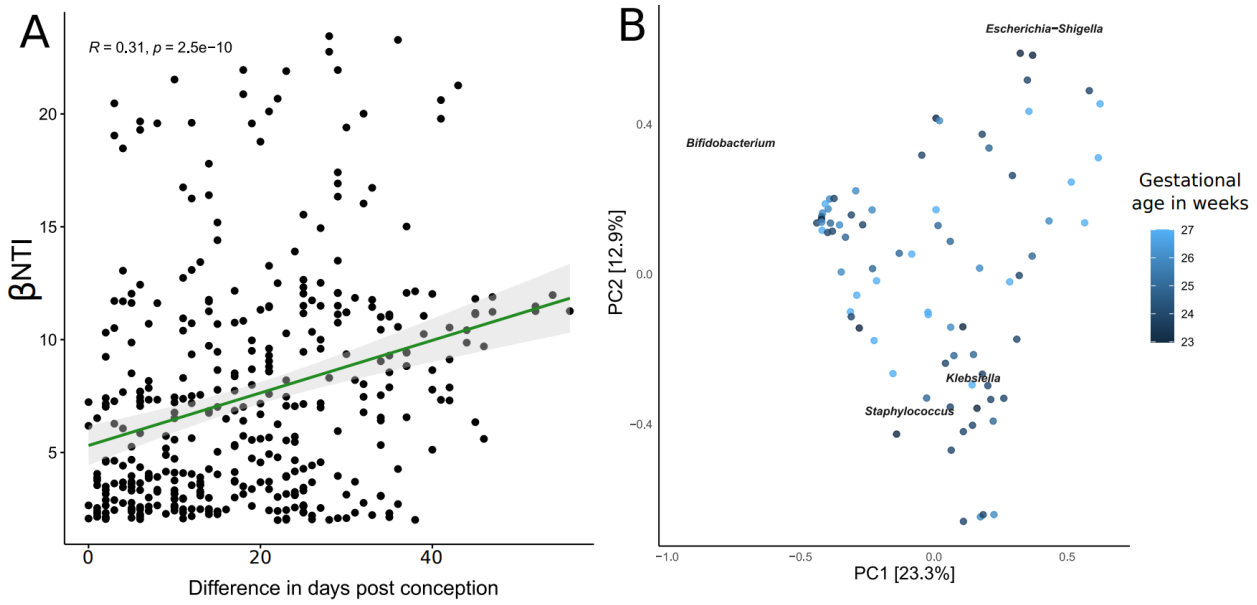

Figure 3. The underlying mechanisms of initial gut microbiota assembly in extremely premature infants.

(A) Distribution of βNTI > 2 values for pairwise comparisons of samples between different patients within NICU-1 during the first week post-delivery, regressed against differences in days post conception. Regression line (green) with confidence interval (grey) illustrates the association between βNTI > 2 and increasing differences between post-conceptional age. (B) Principal Component Analysis (PCoA) on fecal samples obtained during the first week post-delivery. Dark blue color indicates very low gestational age at birth (minimum: 23 weeks), and light blue color indicates higher gestational age at birth (maximum: 27 weeks).

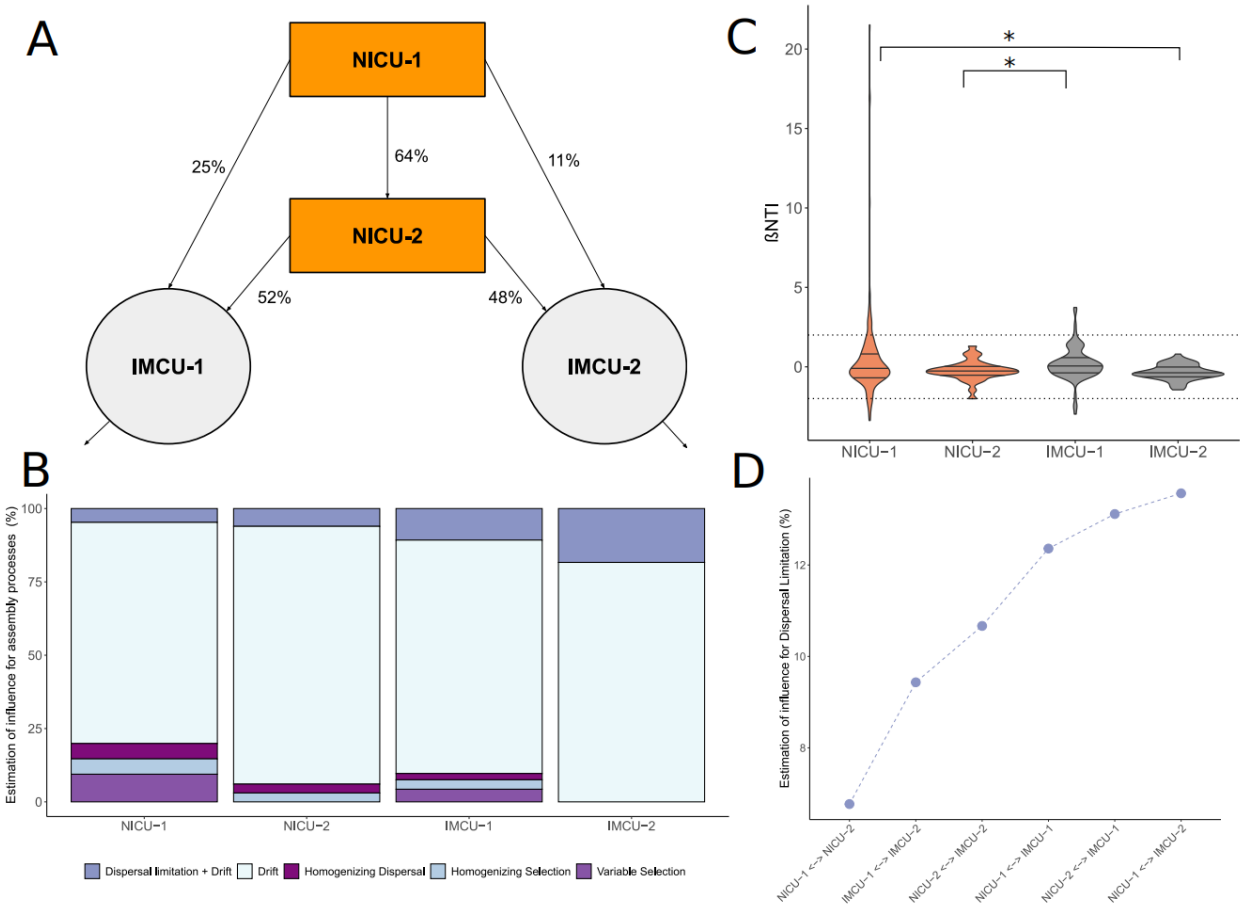

Figure 4. Influence of ecological processes on gut microbiota in neonatal wards.

(A) Schematic illustration of transfer of premature infants between neonatal wards. (B) Contribution of individual turnover processes to observed differences in microbial community composition, resulting from pairwise comparisons of samples between different patients, sampled during the same calendar week within the same clinical ward. (C) Distribution of βNTI values for pairwise comparisons of samples between different patients within the same clinical ward. Dashed lines indicate the range of βNTI under the null expectation of no significant effects of selection (< |2|). (D) Contribution of dispersal limitation to observed differences in microbial community composition, resulting from pairwise comparisons of samples between different patients, sampled during the same calendar week between differing clinical wards. Asterisks represent p values: *p < 0.05, **p < 0.01, ***p < 0.001.

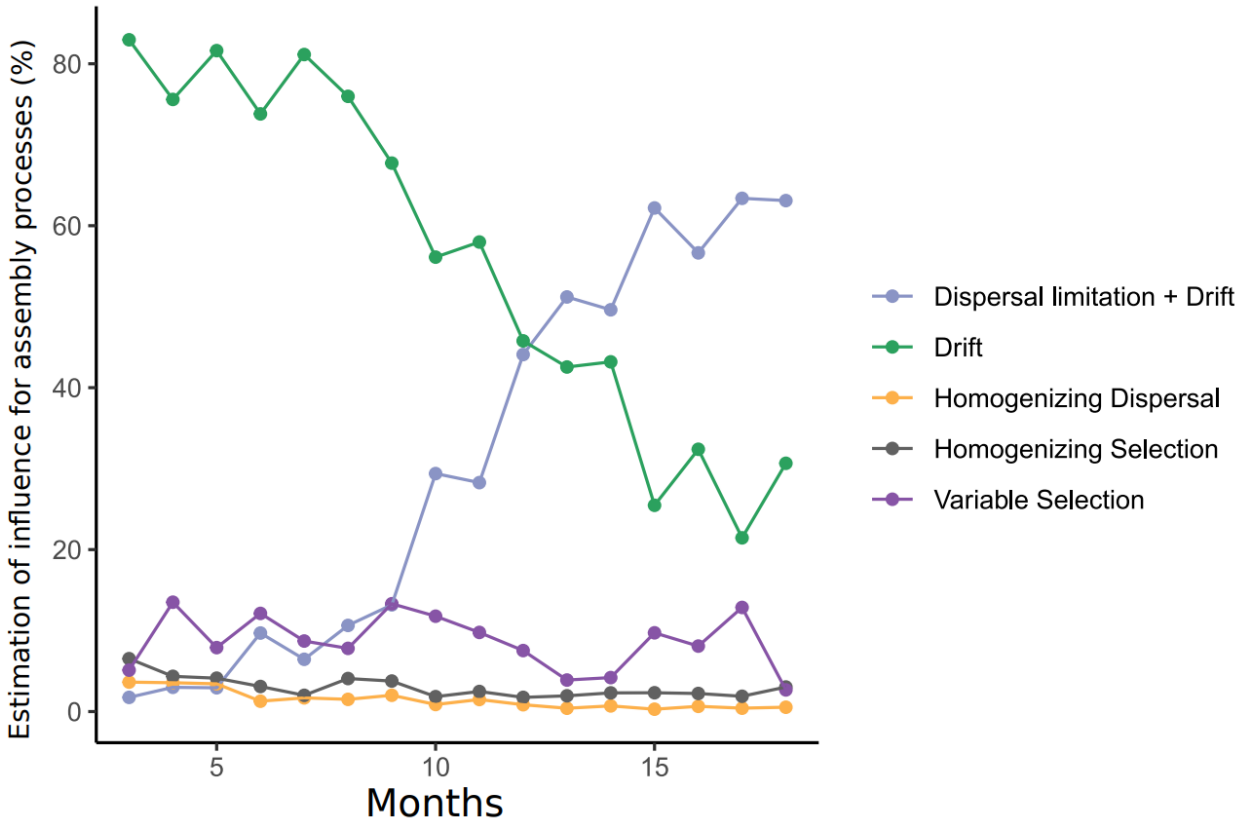

Figure 5. Influence of ecological processes on gut microbiota succession throughout time in healthy term-born infants.

Contribution of individual turnover processes to observed differences in microbial community composition, resulting from pairwise comparisons of samples between different term-born infants, sampled during the same month post-delivery.

Supplemental Information

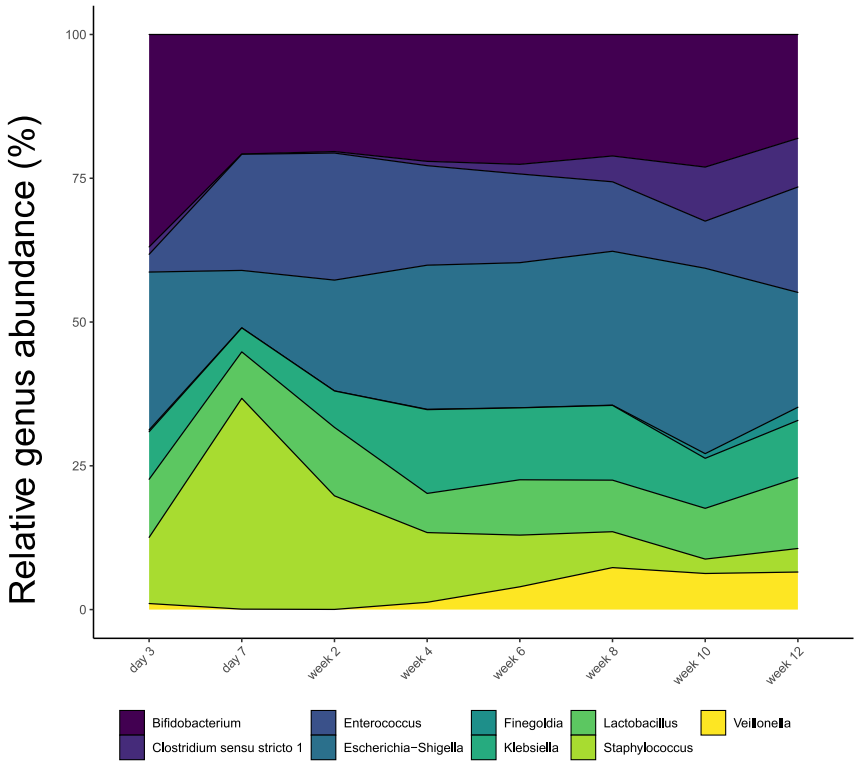

Figure S1. Relative abundance data: gut microbiota in extremely premature infants.

Relative abundances of the core genera in premature infants throughout hospitalization.

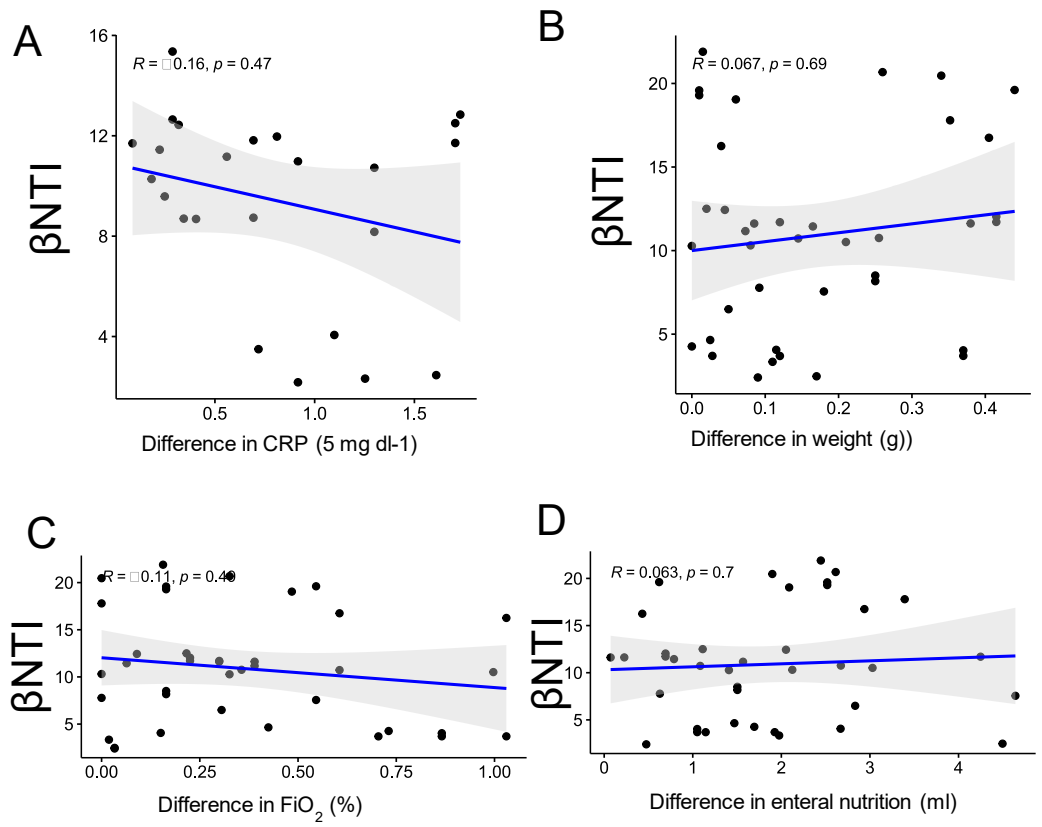

Figure S2. Mechanisms that do not underlie initial gut microbiota assembly in extremely premature infants.

Distribution of βNTI > 2 values for pairwise comparisons of samples between different patients within NICU-1 during the first week post-delivery, regressed against differences in (A) C-reactive protein levels (CRP, mg dl^{-1}). (B) Weight (g). (C) Fraction of inspired oxygen (FiO_2). (D) Amount of enteral supply (ml). Regression line (blue) with confidence interval (grey) illustrates the association between βNTI > 2 and increasing differences of referred variables.

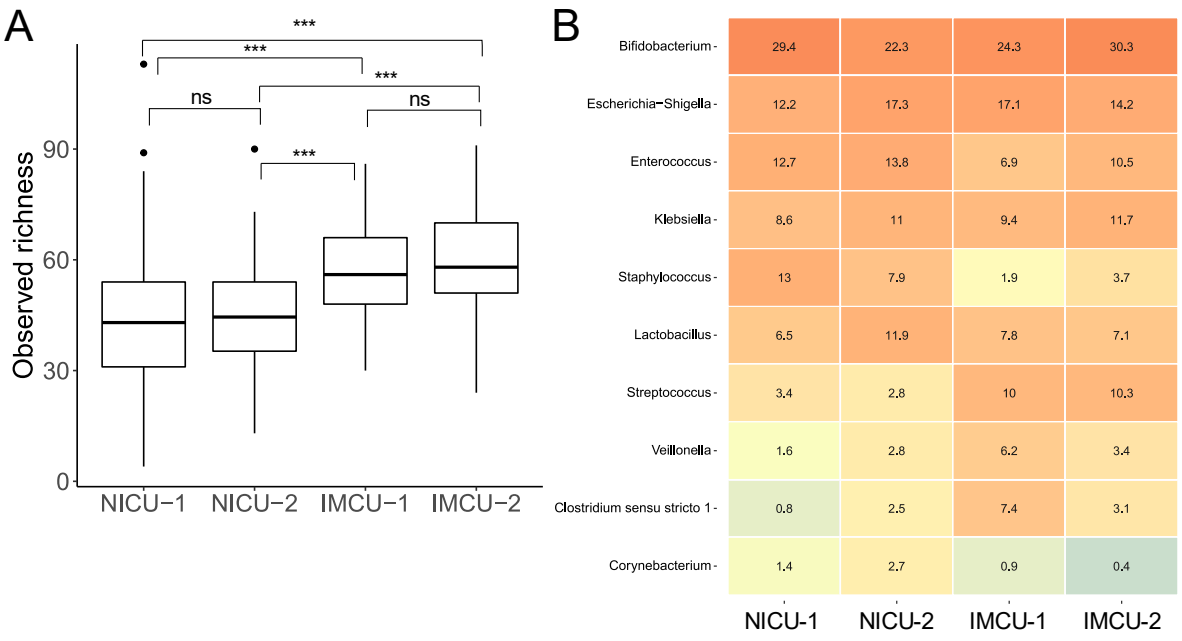

Figure S3. Neonatal wards and their respective premature infant gut microbiota.

(A) Shannon diversity within different neonatal wards. (B) Contribution (%) of specific bacterial general to the observed microbiota at respective neonatal wards. Asterisks represent p values: *p <0.05, **p < 0.01, ***p < 0.001, ns p > 0.05.

Conclusion

This thesis contributed to characterizing the gut microbiota-immune-brain axis development in extremely premature infants. The results define markers of aberrant development which underlie the pathophysiology of brain injury in these neonates, and reveal promising targets for the development of novel intervention strategies.

Neurophysiological maturation, as measured via electrocortical activity, follows a consisted trend in premature infants. Initially, discontinuous voltage (DV) is the dominant amplitude-integrated electroencephalographical (aEEG) background-pattern, followed by a period of neurophysiological maturation in which continuous voltage (CV) increases, approximately two weeks post-delivery, and eventually plateaus by term-equivalent age. However, infants with brain injury have a delayed onset of maturation and elevated amounts of fluctuations in cranial oxygen supply during maturation. The observed transient suppression of electro-cortical activation, and increased instability in cranial oxygen saturation are both predictive for severe brain damage at term equivalent age, as assessed via cranial magnetic resonance imaging (cMRI).

T cells are an important link between the gut microbiome and the brain, but their ontogenesis during early-life and their association with brain damage remained poorly understood. We described four main T cell populations in peripheral blood of premature infants and find that CD4+ T cells are the most abundant throughout hospitalization, followed by CD8+ T cells, then T Regulatory cells, and $\gamma\delta$ T cells as the smallest population. Notably, we find a strong correlation of severe brain damage with elevated $\gamma\delta$ T cell levels shortly post-delivery, seemingly driven by an initial pro-inflammatory polarization and a subsequent depletion of neuroprotective agents during neurophysiological maturation.

Overall, the gut microbiota was dominated by 10 abundant and prevalent genera, namely *Bifidobacterium, Escherichia-Shigella, Enterococcus, Lactobacillus, Staphylococcus, Streptococcus, Klebsiella, Clostridium sensu stricto 1, Veillonella,* and *Finegoldia.* We observed that strictly anaerobic bacteria (*Clostridia*, *Finegoldia*, and *Veillonella*) occurred sparsely early post-delivery and increased in abundance in later periods. In general, we find that the shift to complete anoxia manifests approximately one month post-delivery, as indicated by the highest levels of measured formate in feces, followed by a gradual increase of the anaerobic fermentation products propionate and butyrate.

We identified *Klebsiella* overgrowth in the gut as highly predictive for brain damage, especially due to elevated numbers of *Klebsiella* spp. during neurophysiological maturation. *Klebsiella* overgrowth was furthermore key for driving the assembly of a distinctive and remarkably stable microbiome cluster that associated with severe brain injury, and was exclusively observed in infants with pathologies. Therefore, we conclude that *Klebsiella* spp. are involved in the dysregulation of the gut microbiota-immune-brain axis and may exacerbate perinatal white matter injury. Our findings are summarized in Figure 3, highlighting indicators of aberrant gut microbiota-immune-brain axis development.

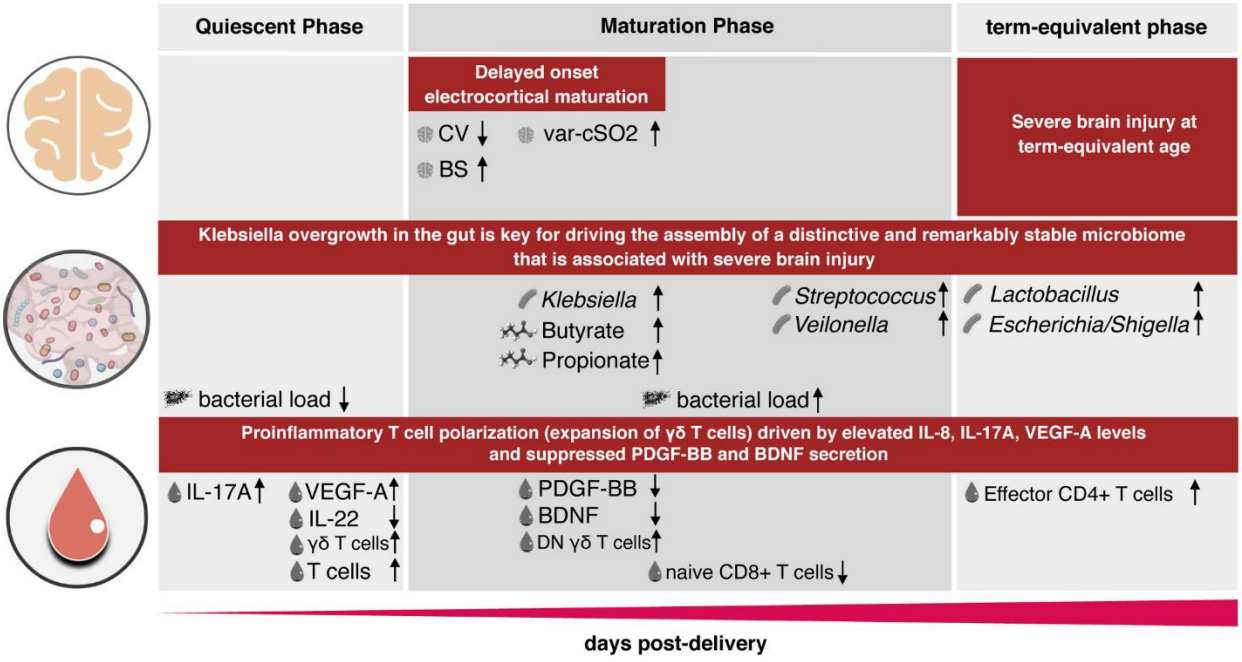

Figure 3. The gut-microbiota-immune-brain axis of extremely premature infants and biomarkers of brain injury.

Illustrative summary of significant differences in gut-microbiota-immune-brain axis development between infants with and without severe brain injuries. Arrows indicate either a significant up or down regulation that is associated with severe brain injury.

The factors that drive the assembly of diverse premature infant gut microbiota remain elusive. We find that these microbiota have very low richness and complexity in general, are initially rather unstable, but gain stability throughout hospitalization. However, the dynamics in succession post-delivery are highly variable between infants. We observed that this progression is mainly driven by stochasticity, whereby microbiota diversify over randomness in microbial death and birth rates, thereby driving inter-individual diversification, however, with persistent exchange with their environment. Once infants reach term-equivalent age, dispersal limitation begins to increase, suggesting that from this moment on the established microbiota begins to

buffer from arrival of novel microorganisms, yet the established microbiota continue to diversify inter-individually, predominantly due to stochasticity.

Perspectives

The complexity of the developing human gut ecosystem has brought together scientist from diverse research areas over the last two decades. Advancements of this scientific area are not only challenging due to the interdisciplinary nature of the field, but are furthermore complicated due to the uniqueness of microbial, immunological, and neurological fingerprints in each individual. The present thesis provides a holistic overview of the orchestrated dynamics between microbiota, immune, and neurophysiological profiles of 60 extremely premature infants, and highlights potential mechanisms of aberrant interplay, which underlie the pathogenesis of brain injury. Furthermore, this thesis addresses the principles responsible for unique development of microbes colonizing the gut, providing a conceptual framework for the origin of individuality in the gut microbiota of humans. While it broadens our understanding of gut microbiota-immune-brain axis development in neonates, it also raises novel questions and suggests potential avenues of future studies.

We found that *Klebsiella* overgrowth in the gastrointestinal tract is highly predictive for brain damage. Interestingly, we observed that *Klebsiella*-dominated gut communities were prevalent four to eight weeks post-delivery (Chapter 1: Figure 3). This aligns with recent findings from Rao et al., 2021, who additionally report that the belated occurrence of *Klebsiella* spp. is in commensal relation to the early occurrence of *Staphylococcus* spp., whereby *Klebsiella* profit from *Staphylococcus*, yet not conversely. It remains to be solved which molecular mechanisms allow the formation of such an interaction, as they potentially represent early stepping stones for the establishment of a pathological *Klebsiella*-dominated microbial community state.

Furthermore, *Klebsiella* overgrowth correlates with a preceding pro-inflammatory T cell response early post-delivery, which was characterized by elevated levels of interleukin 17a (IL-17a), vascular endothelial growth factor subtype A (VEGF-A), and $\gamma\delta$-T cells in peripheral blood. Given

the assumption of uterine sterility, we speculate that γδ-T cells were responsible for initiating a pro-inflammatory cascade via IL-17a secretion as theoretically they should be the only functionally competent cell line of the mucosal adaptive immune system so early post-delivery. However, it remains to be solved which cell types actually initiate aberrant pro-inflammatory conditions as observed during the pathogenesis of brain injury. This will hopefully be achieved in the near future by employing gnotobiotic model systems mimicking the gut microbiota-immune-brain axis. Therein, pro-inflammatory activation of T cells could be followed and explained by intracellular staining of pro-inflammatory cytokines (e.g. IL-17a) in response to selected environmental cues (e.g. presence of *Klebsiella*).

We also found that infants with brain injury have a suppressed onset of electrocortical maturation and lack the neuroprotectants platelet-derived growth factor BB (PDGF-BB) and brain derived neurotrophic factor (BDNF) during the phase of neurophysiological maturation. It should be asked in future research whether a supplementation of neuroprotectants during the phase of neurophysiological maturation could rescue infants from aggravations of brain injuries.

In Chapter 1 – Figure 5 several microbial, neurophysiological, and immunological features of brain injury were identified. Some of these features precede brain injury and could be regarded as biomarkers for early recognition of poor neurophysiological outcomes. However, several factors were not discussed in the present thesis, although they might express equal predictive value. For instance, the abundance of other fermentation end-products should be examined carefully. Ethanol in particular could be of great interest, as it was shown that Klebsiella can produce high amounts of it (Wei et al., 2018). Furthermore, secondary bile acids are produced via bacteria in the gut and were shown to have strong immunomodulatory potential (Campbell et al., 2020), but very little is known of these effects in the premature infant gut.

Furthermore, pro and prebiotics should remain in focus for future research. Overall, supplementation of probiotics has shown to reduce sepsis and NEC rates, but fails to completely eradicate their occurrence (Van Best et al., 2020). It could be assumed that the probiotic strain fails to colonize the GIT in many cases, but we know very little about the mechanisms underlying probiotic colonization success in premature infants. The assembly and succession of early life human gut microbiota is a highly dynamic process, given the recently observed rapid turnover of microbiota (Chen and Garud, 2021). We are still in need of a study that employs at least daily stool sampling in a large cohort of premature infants, so that we can begin to fully understand microbial interactions and dynamics.

Once this is achieved, we should aim towards understanding which deterministic influences are effective in manipulating the stochastic succession of GIT microbiota, in ways that ensure colonization success of specific microbiota that aid homeostatic development of mucosal immunity and shield from intrusion of pathogens. However, the field of gut microbiota-immune-brain interactions is not only complex but also large, and plenty of details remain to be discovered. I believe that we should rigorously deconstruct what we know on the one hand, but also turn to nature and copy from it on our quest for finding novel therapeutics, but also for science. Marsupials are well known for delivering underdeveloped young, that subsequently reside in mothers' pouches until reaching a certain age (Renfree and Shaw, 1996). It would be interesting for science, and of clinical value, to study marsupial pouch and offspring microbiota. Even from an evolutionary perspective, it would be helpful to understand how the assembly and succession of microbiota differs as compared to other mammals, due to potential differences in fundamental immunological mechanisms.

References

1. Albertsson, Anna-Maj, et al. "γδ T cells contribute to injury in the developing brain." The American journal of pathology 188.3 (2018): 757-767.
2. Alcon-Giner, Cristina, et al. "Microbiota supplementation with Bifidobacterium and Lactobacillus modifies the preterm infant gut microbiota and metabolome: an observational study." Cell Reports Medicine 1.5 (2020): 100077.
3. Bale, Tracy L., et al. "Early life programming and neurodevelopmental disorders." Biological psychiatry 68.4 (2010): 314-319.
4. Benakis, Corinne, et al. "Commensal microbiota affects ischemic stroke outcome by regulating intestinal γδ T cells." Nature medicine 22.5 (2016): 516-523.
5. Bonaz, Bruno, Thomas Bazin, and Sonia Pellissier. "The vagus nerve at the interface of the microbiota-gut-brain axis." Frontiers in neuroscience 12 (2018): 49.
6. Buffet-Bataillon, Sylvie, et al. "New Insights Into Microbiota Modulation-Based Nutritional Interventions for Neurodevelopmental Outcomes in Preterm Infants." Frontiers in Microbiology 12 (2021): 1467.
7. Campbell, Clarissa, et al. "Bacterial metabolism of bile acids promotes generation of peripheral regulatory T cells." Nature 581.7809 (2020): 475-479.
8. Castellote, Cristina, et al. "Premature delivery influences the immunological composition of colostrum and transitional and mature human milk." The Journal of nutrition 141.6 (2011): 1181-1187.
9. Ceschin, Rafael, et al. "Developmental synergy between thalamic structure and interhemispheric connectivity in the visual system of preterm infants." NeuroImage: Clinical 8 (2015): 462-472.
10. Chen, Daisy W., and Nandita R. Garud. "Rapid evolution and strain turnover in the infant gut microbiome." bioRxiv (2021).
11. Cryan, John F., et al. "The microbiota-gut-brain axis." Physiological reviews (2019).
12. de Muinck, Eric J., and Pål Trosvik. "Individuality and convergence of the infant gut microbiota during the first year of life." Nature communications 9.1 (2018): 1-8.
13. De Vadder, Filipe, et al. "Microbiota-generated metabolites promote metabolic benefits via gut-brain neural circuits." Cell 156.1-2 (2014): 84-96.

14. Den Besten, Gijs, et al. "The role of short-chain fatty acids in the interplay between diet, gut microbiota, and host energy metabolism." Journal of lipid research 54.9 (2013): 2325-2340.
15. Dini-Andreote, Francisco, et al. "Disentangling mechanisms that mediate the balance between stochastic and deterministic processes in microbial succession." Proceedings of the National Academy of Sciences 112.11 (2015): E1326-E1332.
16. Ferreira, Leonardo MR. "Gammadelta T cells: innately adaptive immune cells?." International reviews of immunology 32.3 (2013): 223-248.
17. Fülling, Christine, Timothy G. Dinan, and John F. Cryan. "Gut microbe to brain signaling: what happens in vagus…." Neuron 101.6 (2019): 998-1002.
18. Garel, Catherine, et al. "Fetal cerebral cortex: normal gestational landmarks identified using prenatal MR imaging." American Journal of Neuroradiology 22.1 (2001): 184-189.
19. Gelderblom, Mathias, Priyadharshini Arunachalam, and Tim Magnus. "γδ T cells as early sensors of tissue damage and mediators of secondary neurodegeneration." Frontiers in cellular neuroscience 8 (2014): 368.
20. Goehler, Lisa E., et al. "Activation in vagal afferents and central autonomic pathways: early responses to intestinal infection with Campylobacter jejuni." Brain, behavior, and immunity 19.4 (2005): 334-344.
21. Guarner, Francisco, and Juan-R. Malagelada. "Gut flora in health and disease." The Lancet 361.9356 (2003): 512-519.
22. Hansen, Mark Berner. "The enteric nervous system I: organisation and classification." Pharmacology & toxicology 92.3 (2003): 105-113.
23. Hatfield, Linda A. "Neonatal pain: What's age got to do with it?." Surgical neurology international 5.Suppl 13 (2014): S479.
24. Hickman, Suzanne E., et al. "The microglial sensome revealed by direct RNA sequencing." Nature neuroscience 16.12 (2013): 1896-1905.
25. Janzon, Anders, et al. "Interactions between the gut microbiome and mucosal immunoglobulins A, M, and G in the developing infant gut." Msystems 4.6 (2019): e00612-19.
26. Krsnik, Željka, et al. "Growth of thalamocortical fibers to the somatosensory cortex in the human fetal brain." Frontiers in neuroscience 11 (2017): 233.

27. Litvak, Yael, Mariana X. Byndloss, and Andreas J. Bäumler. "Colonocyte metabolism shapes the gut microbiota." Science 362.6418 (2018).
28. Lombardo, Michael V., et al. "Maternal immune activation dysregulation of the fetal brain transcriptome and relevance to the pathophysiology of autism spectrum disorder." Molecular psychiatry 23.4 (2018): 1001-1013.
29. Madan, Juliette C., et al. "Gut microbial colonisation in premature neonates predicts neonatal sepsis." Archives of Disease in Childhood-Fetal and Neonatal Edition 97.6 (2012): F456-F462.
30. Matcovitch-Natan, Orit, et al. "Microglia development follows a stepwise program to regulate brain homeostasis." Science 353.6301 (2016).
31. Matthews, Lillian G., et al. "Brain growth in the NICU: critical periods of tissue-specific expansion." Pediatric research 83.5 (2018): 976-981.
32. Mazmanian, Sarkis K., June L. Round, and Dennis L. Kasper. "A microbial symbiosis factor prevents intestinal inflammatory disease." Nature 453.7195 (2008): 620-625.
33. Mihajlovic, Jovana, et al. "Combined hormonal contraceptives are associated with minor changes in composition and diversity in gut microbiota of healthy women." Environmental Microbiology (2021).
34. Miller, Elizabeth Theresa, Richard Svanbäck, and Brendan JM Bohannan. "Microbiomes as metacommunities: understanding host-associated microbes through metacommunity ecology." Trends in Ecology & Evolution 33.12 (2018): 926-935.
35. Niño, Diego F., et al. "Cognitive impairments induced by necrotizing enterocolitis can be prevented by inhibiting microglial activation in mouse brain." Science translational medicine 10.471 (2018).
36. Olin, Axel, et al. "Stereotypic immune system development in newborn children." Cell 174.5 (2018): 1277-1292.
37. Pammi, Mohan, et al. "Intestinal dysbiosis in preterm infants preceding necrotizing enterocolitis: a systematic review and meta-analysis." Microbiome 5.1 (2017): 1-15.
38. Priyadarshini, Medha, et al. "Role of short chain fatty acid receptors in intestinal physiology and pathophysiology." Comprehensive Physiology 8.3 (2018): 1091.
39. Rao, Chitong, et al. "Multi-kingdom ecological drivers of microbiota assembly in preterm infants." Nature 591.7851 (2021): 633-638.

40. Rao, Sheila, et al. "Pathogen-mediated inhibition of anorexia promotes host survival and transmission." Cell 168.3 (2017): 503-516.
41. Renfree, Marilyn B., and Geoffrey Shaw. "Reproduction of a marsupial: from uterus to pouch." Animal Reproduction Science 42.1-4 (1996): 393-403.
42. Sarkar, Amar, et al. "The microbiome in psychology and cognitive neuroscience." Trends in cognitive sciences 22.7 (2018): 611-636.
43. Seki, David, et al. "Aberrant gut-microbiota-immune-brain axis development in premature neonates with brain damage." Cell Host & Microbe (2021).
44. Sgritta, Martina, et al. "Mechanisms underlying microbial-mediated changes in social behavior in mouse models of autism spectrum disorder." Neuron 101.2 (2019): 246-259.
45. Shah, Shrushti, et al. "Intraperitoneal Administration of Short-Chain Fatty Acids Improves Lipid Metabolism of Long–Evans Rats in a Sex-Specific Manner." Nutrients 13.3 (2021): 892.
46. Sherman, Michael P., Habib Zaghouani, and Victoria Niklas. "Gut microbiota, the immune system, and diet influence the neonatal gut–brain axis." Pediatric research 77.1 (2015): 127-135.
47. Silva, Ygor Parladore, Andressa Bernardi, and Rudimar Luiz Frozza. "The role of short-chain fatty acids from gut microbiota in gut-brain communication." Frontiers in endocrinology 11 (2020): 25.
48. Stewart, Christopher J., et al. "Temporal development of the gut microbiome in early childhood from the TEDDY study." Nature 562.7728 (2018): 583-588.
49. Stoecklein, Sophia, et al. "Variable functional connectivity architecture of the preterm human brain: impact of developmental cortical expansion and maturation." Proceedings of the National Academy of Sciences 117.2 (2020): 1201-1206.
50. Tezuka, Hiroyuki, and Toshiaki Ohteki. "Regulation of IgA production by intestinal dendritic cells and related cells." Frontiers in immunology 10 (2019): 1891.
51. Thion, Morgane Sonia, et al. "Microbiome influences prenatal and adult microglia in a sex-specific manner." Cell 172.3 (2018): 500-516.
52. Torow, N., et al. "Neonatal mucosal immunology." Mucosal immunology 10.1 (2017): 5-17.

53. van Best, Niels, et al. "Influence of probiotic supplementation on the developing Microbiota in human preterm neonates." Gut microbes 12.1 (2020): 1826747.
54. Wei, Xiao, et al. "Klebsiella pneumonia, one of potential chief culprits of non-alcoholic fatty liver disease: through generation of endogenous ethanol." bioRxiv (2018): 446765.
55. Winter, Sebastian E., et al. "Host-derived nitrate boosts growth of E. coli in the inflamed gut." science 339.6120 (2013): 708-711.
56. Wisgrill, Lukas, et al. "Outbreak of Yersiniabactin-producing Klebsiella pneumoniae in a neonatal intensive care unit." The Pediatric infectious disease journal 38.6 (2019): 638-642.
57. Zarrinpar, Amir, et al. "Antibiotic-induced microbiome depletion alters metabolic homeostasis by affecting gut signaling and colonic metabolism." Nature communications 9.1 (2018): 1-13.
58. Zwittink, Romy D., et al. "Metaproteomics reveals functional differences in intestinal microbiota development of preterm infants." Molecular & Cellular Proteomics 16.9 (2017): 1610-1620.